UNIVERSITÀ
DI PAVIA

Dipartimento di Medicina Molecolare

Unità di Immunologia e Patologia generale

A new functional *in vitro* cell-free assay to evaluate DNA repair mechanisms

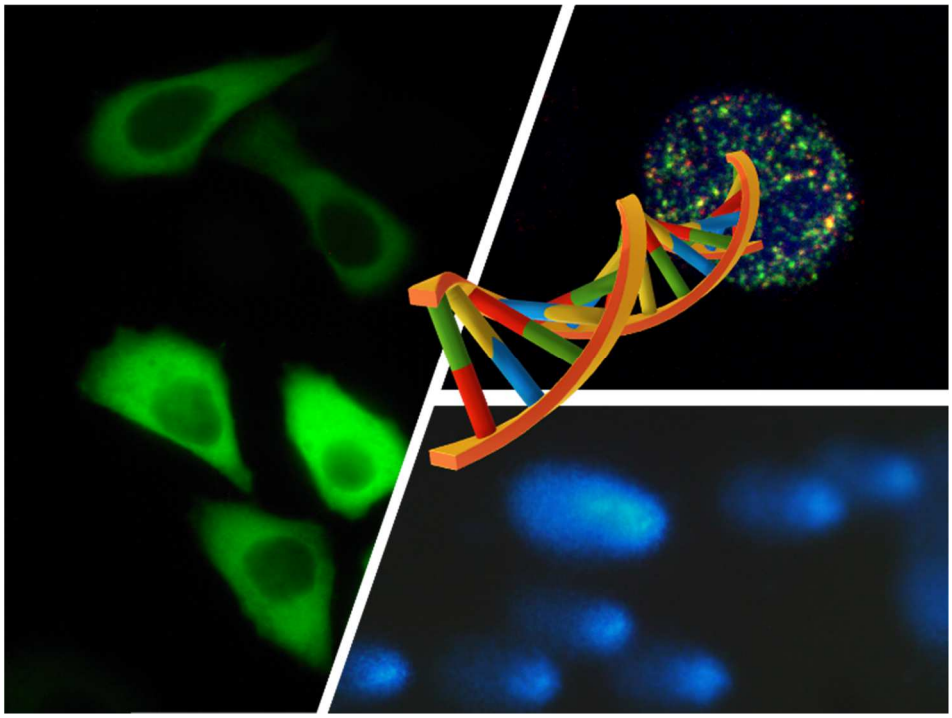

Isabella Guardamagna

Dottorato di Ricerca in
Genetica, Biologia Molecolare e Cellulare
Ciclo XXXII– A.A. 2016-2019

UNIVERSITÀ
DI PAVIA

Dipartimento di Medicina Molecolare
Unità di Immunologia e Patologia generale

A new functional *in vitro* cell-free assay to evaluate DNA repair mechanisms

Isabella Guardamagna

Supervised by Prof. Lucia Anna Stivala

Dottorato di Ricerca in
Genetica, Biologia Molecolare e Cellulare
Ciclo XXXII– A.A. 2016-2019

Abstract

DNA is exposed to endogenous and exogenous agents that are potential causes of several pathological processes; for this reason, eukaryotic cells developed many mechanisms able to control and repair lesions. One of them, Nucleotide Excision Repair (NER) is a highly versatile and complex system by which UV-photolesions, such as cyclobutane pyrimidine dimers (CPDs) or pyrimidine (6-4) pyrimidone photoproducts (6-4PPs), are recognized and removed.

A key factor, involved in the recognition of chromatin photolesions, is DDB2 (DNA Damaged binding protein 2) thanks to its ability of creating a complex together with DDB1 (UV-DDB complex). Recently, it was demonstrated that DDB2 binds directly PCNA (Proliferating Cell Nuclear Antigen) through a conserved sequence called PIP-box; the disruption of this binding in the mutated form ($DDB2^{PCNA-}$) induces a delayed DNA damage recognition but also an inefficient DNA repair activation.

To better clarify this delay, it was developed a new functional *in vitro* cell-free system in which repair activity, in isolated nuclei, was evaluated. Its responsiveness was also evaluated with different type of DNA lesions, activating different DNA repair processes, increasing further its applicability.

Moreover, the involvement of DDB1 was studied as possible actor when DDB2 loses its function. In the presence of $DDB2^{PCNA-}$ protein, the DNA repair process is inefficient, nevertheless, not completely blocked. For this reason, it was hypothesized a possible ability of DDB1 to bind directly PCNA, when DDB2 is altered or ineffective.

Acknowledgements

I would like to thank my supervisor Prof. Lucia Anna Stivala for the important opportunity to work on this project and to acquire competence in cellular and molecular biology.

A special thank also to Dr. Ornella Cazzalini and Dr. Paola Perucca for all the support and teaching during these years.

I would like to thank Dr. Ennio Prosperi (CNR-IGM, Pavia), Dr. Monica Savio (DMM, University of Pavia), Dr. Tiziana Nardo (CNR-IGM, Pavia) and Dr. Maristella Maggi (DMM, Pavia) for the material and technical support provided me.

I thank also Dr Patrizia. Vaghi (Centro Grandi Strumenti, University of Pavia) for help in confocal microscopy analysis and Dr. Marco Liotta and Dr. Paola Tabarelli de Fatis for the technical assistance and support during the X irradiation at IRCCS Maugeri (Pavia).

Abbreviations

6-4 PP = pyrimidin (6-4) pyrimidone

Aph = Aphidicoline

Ara-C = Citarabine-C

BER = Base Excision Repair

BRCA = Breast Related Cancer Antigen

BrdU = Bromodeoxyuridine

BS = Blocking Solution

BSA = Bovine Serum Albumin

Cis-Pt = Cisplatinum

CPDs = pyrimidine dimers

$CRL4A^{UV\text{-}DDB}$ = DDB1-DDB2-CUL4A-RBX1 E3-ligase complex

CRLs = Cullin-RING ubiquitin ligases

DCAFs = DDB1-CUL4A-Associated Factors

DDB1 = Damaged DNA Binding protein 1

DDB2 =Damaged DNA Binding protein 2

DMEM = Dulbecco's modified Eagle Medium

DSBs = Double strand breaks

DTT = 1,4-Dithiothreitol

dUTPs = Biotin-16-dUTPs

FBS = Fetal Bovine Serum

FEN1 = Flap endonuclease 1 enzyme

GO = 8-oxo-7,8-dihydroguanine

HR = Homologous Recombination

ICLs = Interstrand cross-link

IPTG = Isopropyl β-D-1-thiogalactopyranoside

IR = Ionizing Radiation

$KBrO_3$ = Potassium bromate

LB = Lower buffer

LWP = Low Melting Point Agar

MFI = Mean Fluorescence Intensity

MMR = Mismatch Repair

MNNG = 1-Methyl-3-nitro-1-nitrosoguanidine

NaBu = Sodium butyrate

NER = Nucleotide Excision Repair

NHER = Non-Homologous End-joining Recombination

O^6MeG = O^6-methylguanine

OD = Optical Density

PARP = Poly(ADP-ribose) polymerase

PBA = PBS + 1% Bovine Albumin

PBS = Phosphate-Buffered Saline

PBST =PBS + 0.2% Tween20

PCNA = Proliferating Cell Nuclear Antigen

PI = Propidium Iodide

PIP-box = PCNA interacting protein-box

PMSF = Phenylmethylsulfonyl fluoride

Rbx1 = RING-box1 protein

ROS = Reactive Oxygen Species

RT = Room Temperature

SDS = Sodium dodecyl sulfate

SuNaSp =Sucrose Sodium Spermine Spermidine Buffer

TLS = Traslational Synthesis Polymerase

UB = Upper Buffer

UV = Ultraviolet Radiation

XP = Xeroderma pigmentosum

XRCC1 = X-ray repair cross protein-complementing protein 1

Contents

1. Introduction

1.1 DNA damage

DNA is the biological molecule engaged in perpetuation of live, even if it is intrinsically susceptible to chemical modification by endogenous or exogenous agents. Among the endogenous agents we find, for example, the reactive oxygen species (ROS) produced during cellular metabolism that can cause oxidations to the nitrogenous bases (Bjelland S., Seeberg E., 2003) and single strand DNA breaks (Giloni L. *et al*. 1981); another endogenous source of damage is represented by errors in the replication and repair of DNA that lead to the incorporation of wrong bases, insertions and deletions (Bridges B.A., 2005; McCulloch S.D., Kunkel T.A., 2008). Exogenous agents, on the other hand, can be distinguished in physical and chemical agents; among the physical agents we find ultraviolet radiation (UV) and ionizing radiation (IR). UV radiation is divided into three classes based on the wavelength range: UV-C (190-290 nm), UV-B (290-320 nm) and UV-A (320-400 nm). The UV-C and UV-B radiations act directly on the DNA causing the formation of photoproducts and the most frequent are constituted by pyrimidine dimers (CPDs), in which two adjacent pyrimidines bound with covalent bonds forming a ring structure, and the pyrimidin (6-4) pyrimidone (6-4 photoproduct, 6-4PP) derived from the covalent bond between the C^6 of a pyrimidine and the C^4 of the adjacent pyrimidine. These photoproducts cause a distortion of DNA helix that can lead to replication problems. The UV-A radiation acts indirectly on the DNA through the excitation of molecules, endogenous and exogenous, called photosensitizers that absorb the energy transmitted by UV radiation and amplify it with the formation of free radicals that cause oxidative damage to the DNA (Epe B. 1991). IR, such as X- and γ-rays, can damage DNA by direct deposition of energy, but also indirectly, through the ionization of water molecules and the formation of hydroxyl radicals that attack DNA. DNA damage caused by ionizing radiation includes base modifications, single-strand breaks or double-stranded DNA (Hutchison F. 1985). Among the chemical agents damaging DNA, there are the alkylating factors, such as nitrogenous mustards,

methylnitronitrosoguanidine (MNNG) and nitrosoureas, which form adducts to the N and O atoms of the nitrogenous bases, causing mismatches, cross-links between DNA filament and fragmentation during the repair mechanism; then there are oxidizing agents, such as potassium bromate ($KBrO_3$), which mainly determine the oxidation of guanine, forming 8-oxo-7,8-dihydroguanine and 8-hydroxyguanine (Ballmaier D., Epe B., 1995). Among the chemical agents, chemotherapeutic drugs, such as cis-platinum (cis-Pt), can cause cross-linking between DNA and proteins or inter-/intra-strand cross links (Payet D*. et al*., 1993), resulting in functional modifications, such as, blocking of DNA replication and transcription (Noll D.M. *et al.,* 2006); or chromosomal mutations and aberrations such as, base modifications that can lead to incorrect pairing inducing transitions and transversions (Del Mundo I.M.A. *et al.,* 2019). The consequence of DNA alterations is different depending on whether it occurs in a somatic or in a germline cell: the former can undergo death, or it can become a cell with genomic instability and accumulation of other mutations facing a possible tumor transformation. The alterations in the germ cell, on the other hand, can be transmitted to the progeny and fixed as mutations (Del Mundo I.M.A. *et al.,* 2019). To prevent the deleterious effects of DNA alterations, cells activate checkpoints to allow repair of damaged DNA. If the damage cannot be repaired, cells are eliminated by apoptosis or enter a non-replicative state called senescence (Chipuk J.E., Green D.R., 2006; Collado M. *et al.* 2007). For this reason, cells developed several molecular pathways extremally regulated to repair DNA damage, and also to control and remove errors caused by DNA polymerase activated during DNA replication or DNA repair mechanisms. Five major repair pathways exist and are activated in different cell-cycle phases: nucleotide excision repair (NER), base excision repair (BER), mismatch repair (MMR), homologous recombination (HR) and non-homologous end joining (NHEJ). Moreover, some DNA damages are tolerated by translational synthesis polymerase (TLS) that bypass the damage and continue the DNA replication program, fixing mutations. In some cases, cells can activate cell cycle checkpoints or cell death pathways to limit the potentially deleterious consequences of DNA damage (Chatterjee N., Walker G.C., 2017).

1.2 Repair mechanisms of single strand DNA damage

When only one of the two DNA strands is damaged, the damaged part can be excised, and the other strand can be used as a template to guide the correction of the damaged strand. Systems that repair single strand DNA damage include MMR, BER and NER.

1.2.1 Mismatch repair (MMR)

The damages commonly repaired by the MMR are caused by incorrect pairing that may occur due to errors in the DNA replication process (Kunkel T.A. 2009) and following oxidation or alkylation of the nitrogenous bases (Chatterjee N., Walker G.C., 2017). Among the agents capable of determining alkylation of the bases we find the monofunctional MNNG alkylating agent which can lead to the formation of 7-methylguanine and 3-methyladenine which are excreted by specific glycosylases (BER) (Aquilina G. *et al.,* 1988); furthermore, it can lead to the formation of O^6-methylguanine, which can be repaired directly or it can cause incorrect pairing (Syro L.V. *et al*., 2018). Alkylating agents, such as MNNG, can add their alkyl group to the oxygen atom at position 6 of guanine, generating O^6-methylguanine (O^6MeG) (Lukash L.L. *et al*. 1991). If O^6-MeG is not repaired, during the replication an erroneous pairing O^6MeG: T or an O^6MeG: C is obtained (Chen H.T. *et al.,* 2000). In a second replication cycle, the O^6MeG: T pairing will become an A: T transition, instead the O^6MeG: C pairing will again be replicated as an O^6MeG: C pairing or it will become an incorrect O^6MeG: T pairing (Marginson G.P., Santibanez-Koref M.F., 2002). O^6MeG: T and O^6MeG: C pairing can be recognized and repaired using the repair mechanism for incorrect pairing or MMR (Syro L.V. *et al*. 2018). An important factor involved in MMR system is MSH2 protein, which creates heterodimers with either MSH6 or MSH3. MSH2/6 (also called MutSα) recognizes base mismatches and alkylation adducts, whereas MSH2/3 (called MutSβ) recognizes insertion/deletion loops. The later steps in MMR involve MLH1-PMS2 heterodimer recruitment, excision of the newly synthesized DNA by Exo1, and re-synthesis of the excised DNA by polymerase δ or η (Jascur T. *et al*. 2011) (**Figure 1**).

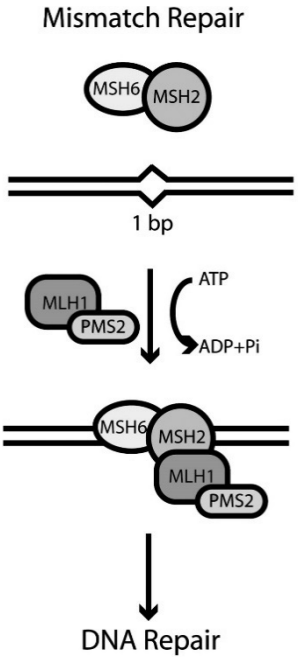

Figure 1: Schematic representation of MMR (Modified from Scherer S.J. *et al.,* 2005).

1.2.2 Base Excision repair (BER)

BER is a mechanism for repairing small lesions to nitrogenous bases that do not cause significant distortion of the double helix. These lesions include oxidation, alkylation, hydrolysis, deamination and single-strand DNA breaks (Hoeijmakers I.I.H. 2001). Guanine is the base of DNA most exposed to oxidation reactions induced by agents such as reactive oxygen species and $KBrO_3$. These oxidizing factors generate 8-oxo-7,8-dihydroguanine (GO) which is in dynamic equilibrium with its minor tautomer 8-hydroxyguanine (Yang Y.H. *et al.* 2002). GO in DNA can assume both an anti and syn conformation compared to 2'-deoxyribose and, if it is not repaired, during replication it can be paired with adenine or with cytosine (Wang Y. *et al.* 2007), leading to point mutations (Nakabeppu Y. *et al.* 2007).

BER can activate two different sub-pathways, each characterised by the total number of nucleotides that are substituted on the damaged DNA strand; the short-patch BER repairs a single nucleotide lesions, while the long-patch BER replaces two or more nucleotides (Liu Y. *et al.* 2007) (**Figure 2**). BER mechanism starts with the action of DNA glycosylase. There are different types of DNA glycosylases, each specific for a specific type of altered base (Stivers J.T., Jiang Y.L., 2003). In the short-patch BER, the DNA polymerase β inserts the missing base (Sobol R.H. *et al.* 1996; Prasad R. *et al*. 2010) and the cut is sealed by DNA ligase I or III which forms a complex with the X-ray repair cross protein-complementing protein 1 (XRCC1) (Gao Y. *et al.* 2011). XRCC1 is a protein that does not have an enzyme activity, but it acts as a support for BER (Caldecott K.W. 2008). In the long-patch BER, a DNA polymerase (β, δ, ε) is recruited on the empty space obtained from base deletion and continues to synthesize the DNA while the DNA downstream is removed, creating a flap on the DNA (Dianov G.L. *et al.* 1999). The Flap endonuclease 1 enzyme (FEN1) removes this flap (12-13 nucleotides), leaving a cut in the DNA (Almeida K.H., Sobol R.W., 2007) that is sealed by the DNA ligase I helped by PCNA. The choice between short-patch BER or long-patch BER depends on several factors such as the type of lesion, the stage of the cell cycle and the differentiation stage (Fortini P., Dogliotti E., 2007).

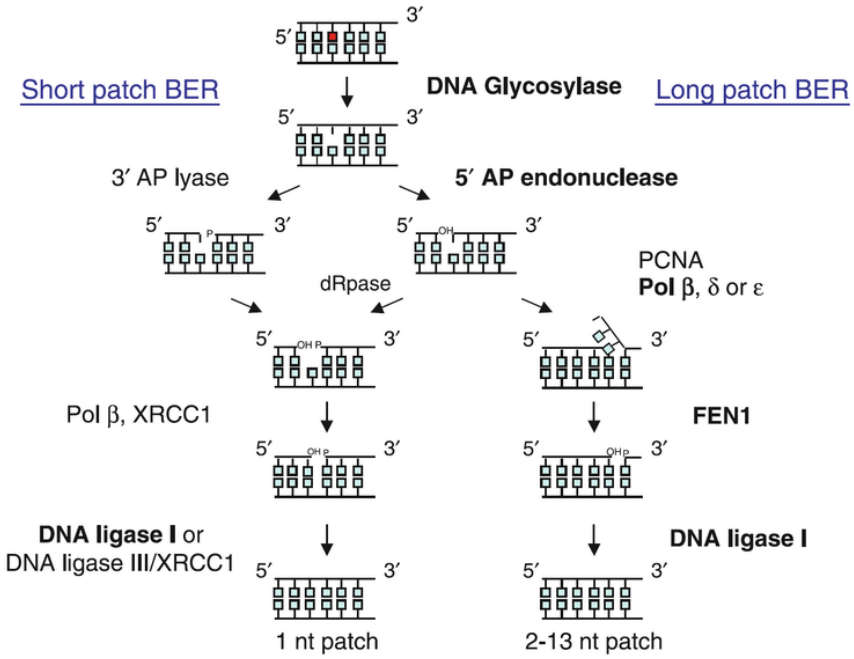

Figure 2: Schematic representation of BER (Charles Richard J.L. *et al.,* 2012).

1.2.3 Nucleotide Excision repair (NER)

NER is involved in the repair of damage caused by ultraviolet (UV) radiation, normally present in sunlight, which causes the formation of pyrimidine dimers (CPDs) and 6-4 photoproducts (6-4PP) (Chatterjee N., Walker G.C., 2017). In all eukaryotes, NER is divided into two sub-pathways called Global Genome NER (GG-NER) and Transcription-Coupled Repair (TCR-NER). The two sub-pathways are distinguished in the initial phases of the process and then converge into a single common mechanism. In GG-NER the XPC-hHR23B complex identifies regions on the entire genome in which the pairing between the two strands of DNA is altered (Masutani C. *et al.,* 1994). In the TCR-NER, on the other hand, lesions in the transcribed regions cause a blockage of the RNA-polymerases that must be removed from the DNA to allow the repair of the damages. This event requires two specific proteins of the TCR-NER, called CSA and CSB (Fousteri M. *et al.,* 2006).

The steps downstream to the damage recognition of the GG-NER and TC-NER are essentially identical: the multiprotein TFIIH complex, which contains two polypeptides called XPB and XPD with helicase activity, opens the DNA for a section of about 30 nucleotides around the lesion. The XPA protein confirms the presence of the lesion by binding to it, otherwise all the reaction ends at this stage. The DNA region opened by the action of helicase is stabilized by binding to the RPA protein, which is also a factor involved in DNA replication and which has a high binding affinity for single-stranded DNA. XPG and ERCC1/XPF are two NER-specific endonucleases that cut the DNA strand containing the lesion into 3' and 5', respectively, generating a fragment of about 30 nucleotides that will then be eliminated. An abasic portion of 30 nucleotides was thus generated with a 3'OH end in the damaged filament that can be repaired by normal enzymes that replicate DNA by copying the complementary filament that has not been damaged (Marteijn *et al*., 2014) (**Figure 3**).

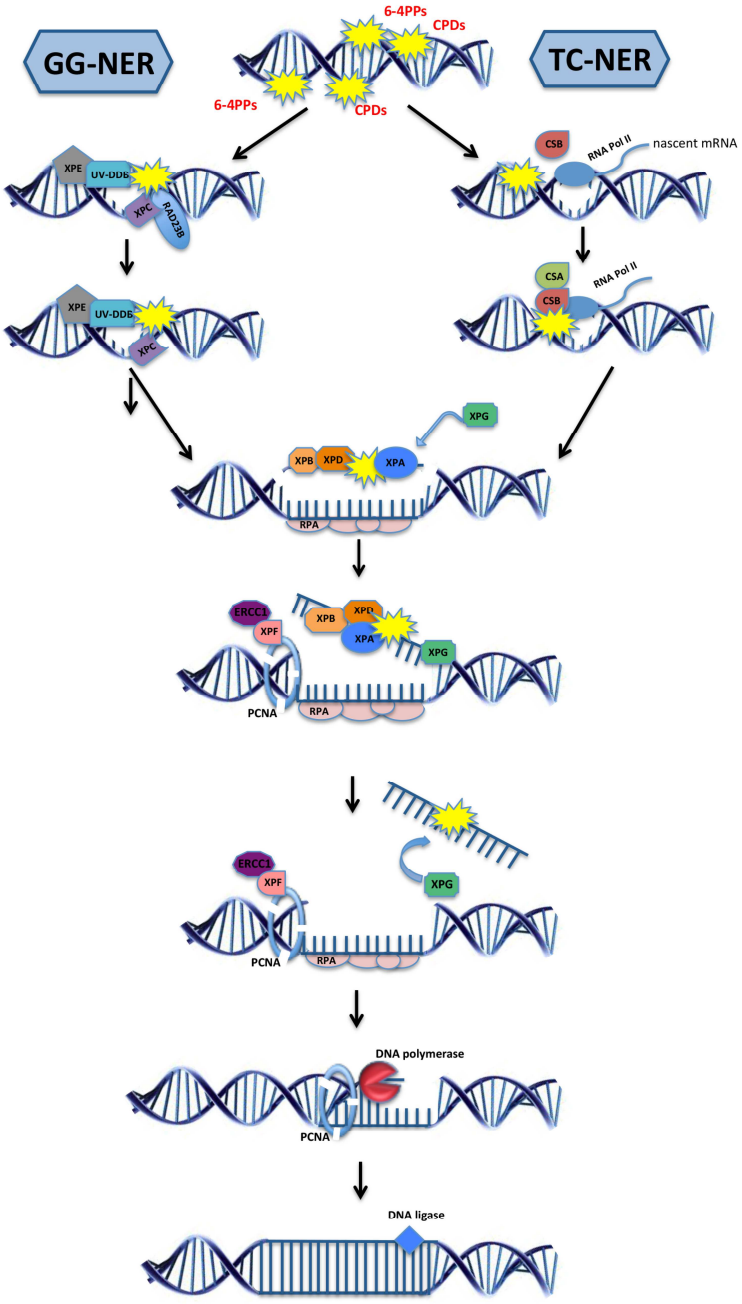

Figure 3: Schematic representation of NER mechanism (Edifizi D., Schumacher B., 2015).

1.2.4 Interstrand cross-link (ICLs) repair

The Fanconi Anemia pathway is required to repair ICLs due to crosslinking agents such as platinum compounds, nitrogen mustards, psoralens and alkylating agents, inhibiting replication and transcription (Chatterjee N., Walker G.C., 2017). A so-called anchor complex recognizes the ICL and, when activated, it recruits a core complex that is required to monoubiquitinate into a specific site protein of the FANCI/FANCD2 (ID2) heterodimer. This monoubiquitination activates nucleases, such as FANCP (SLX4) and FANCQ (XPF), and downstream repair factors that include FANCD1 (BRCA2), and FANCO (RAD51C) (Walden H., Deans A.J., 2014). ICLs repair mechanism is activated in a cell cycle-dependent manner (Kim J.M. *et al.,* 2008). In replicating cells, the presence of ICLs stalls the ongoing of replication (Raschle M. *et al*., 2008), then, XPF-ERCC1 and SNM1A induce incisions producing a gap (Wang A.T. *et al*., 2011). The leading strand with the ICLs function as template for DNA synthesis—by Translation Synthesis (TLS) polymerases POL ι, POL κ, POL ν and REV1—that proceeds up to the lesion, bypasses it, and extends beyond the lesion until it reaches the first downstream Okazaki fragment (Ho T.V. *et al*., 2011). After this step, the 3' overhang of the leftover lagging strand invades the synthesized strand in a RAD51-dependent manner (Long D.T. *et al*., 2011). Interestingly, resolution of this Homologous Recombination (HR) intermediate depends on the FANCD2-FANCI complex. NER pathway eventually removes the ICL hook that was still hanging on to the leading strand (Chatterjee N., Walker G.C., 2017). In non-replicating cells, ICLs are repaired by NER and TLS polymerases such as REV1 and POL ζ (Clauson C. *et al.,* 2013). Both GG-NER and TC-NER pathways recognize helix-distortions, although damages induced by cisplatin may escape recognition (Enoiu M. *et al*., 2012). NER factors, acting downstream to the lesion recognition, cut only the 5' side of ICLs, with further incisions possibly aided by the MutSβ complex create a ssDNA-gap (Smeaton M.B. *et al*., 2008). At the end, the error-prone TLS polymerase synthesize across the gap and with a second round NER removes the ICLs hook on the other strand (Clauson C. *et al.,* 2013) (**Figure 4**).

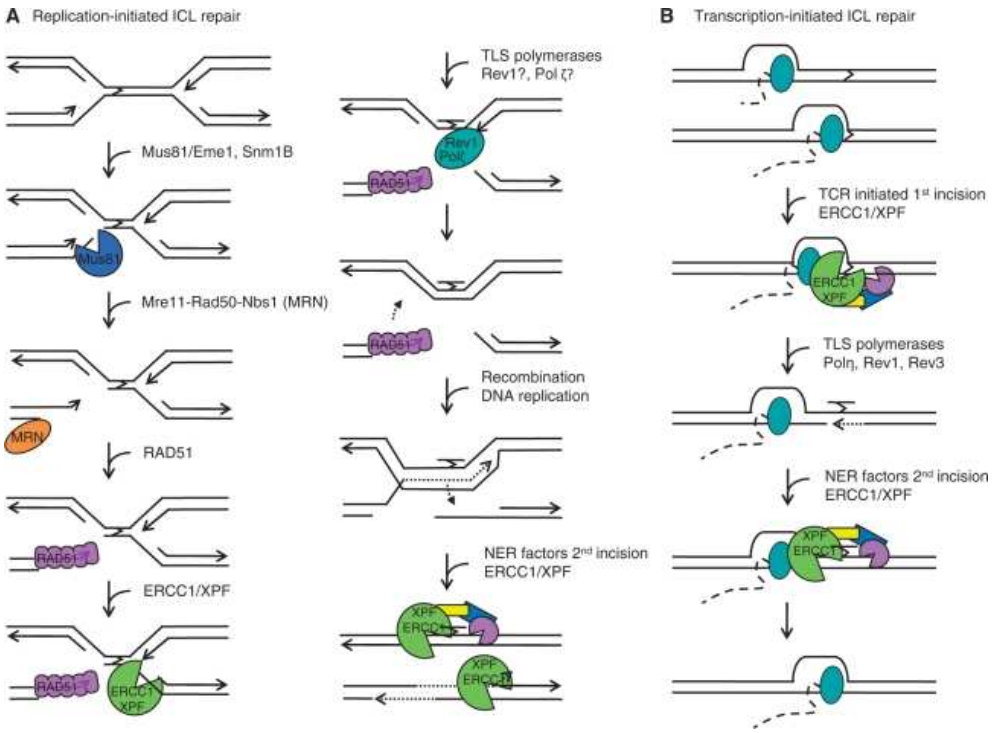

Figure 4: Model for ICL repair in mammalian cells. ICL repair can be (A) initiated either at a replication fork or (B) at a stalled RNA polymerase (Al-Minawi A.Z. *et al.,* 2009).

1.3 Repair mechanisms of double strand DNA damage

DNA double strand breaks (DSBs) are the most severe type of damage because they do not leave an intact complementary strand used as a template to repair DNA. These lesions can be induced by exogenous agents, for example anticancer chemotherapeutic drugs, including cisplatin, or ionizing radiation (IR) (Mehta A., Haber J., 2014); but also, endogenous events such as blocking of a replication fork, due to unconventional chromatin structures or collisions with transcription machinery, can lead to DSBs (Mirkin E.V., Mirkin S.M., 2007). Furthermore, if they are not properly repaired, they can lead to broken chromosomes and translocations that are associated with developmental defects, neurodegenerative diseases,

immunodeficiencies, radiosensitivity, sterility and predisposition to cancer (Jackson S.P., Bartek J., 2009). Cells can activate two pathways to repair DSBs: homologous recombination (HR) and the union of non-homologous DNA ends (NHEJ) (Hartlerode A.J., Scully R., 2009). The choice of which repair pathway to activate is cell cycle-dependent (Yun M.H., Hiom K., 2009); in G_1-phase the NHJE pathway is preferentially activated due to the absence of a sister chromatid (Ma J.L. *et al*., 2003), while in late S- and G_2-phases HR play a predominant role (Takata M. *et al.,* 1998); this choice is led by the cyclic regulation of proteins and factors involved in each specific pathway (Scully R. *et al*., 2019).

1.3.1 Homologous recombination (HR)

Homologous recombination can repair DNA double-strand breaks and cross-strand cross-links (Kondo N. *et al.,* 2010). This mechanism begins cutting the ends of double-strand breaks creating single-stranded ends, each with a 3'OH-terminal, capable of propagating in the double-stranded DNA that has the homologous sequence (Mimitou E.P., Symington L.S., 2009). These cuts occur in two steps: the first involves the Mre11-Rad50-Nbs1 complex (MNR) together with the CtBP-interacting protein (CtIP) (Sartori A.A., 2007), in the second a 5'→3' exonuclease (EXO1) is activated by the helicase Bloom's syndrome protein (BLM) (Nimonkar A.V. *et al.*, 2008). The single-stranded tail generated by this cut is bound by Replication Protein A (RPA) which is involved in the recruitment of proteins such as RAD51 (San Filippo J. *et al.,* 2008). RAD51 is an enzyme with DNA-dependent ATPase activity that forms nucleoprotein strands with DNA and is recruited on DNA double-strand breaks thanks to the Breast Related Cancer Antigen (BRCA2) protein (Yuan S.S. *et al.,* 1999). RAD51 catalyses the propagation of single-stranded DNA into homologous double-stranded DNA forming a peculiar structure called “D-loop”. Starting from the 3’ D-loop end, the reparative synthesis of DNA is propagated using the sister chromatid as a template. As a result of the propagation of the two strands of DNA in the homologous double helix and the subsequent DNA synthesis, the two double helixes are found to be covalently linked to each other via Holliday junctions. Depending

on how the Holliday junctions are resolved, the products may be non-crossover or crossover (**Figure 5**) (San Filippo J. *et al.,* 2008).

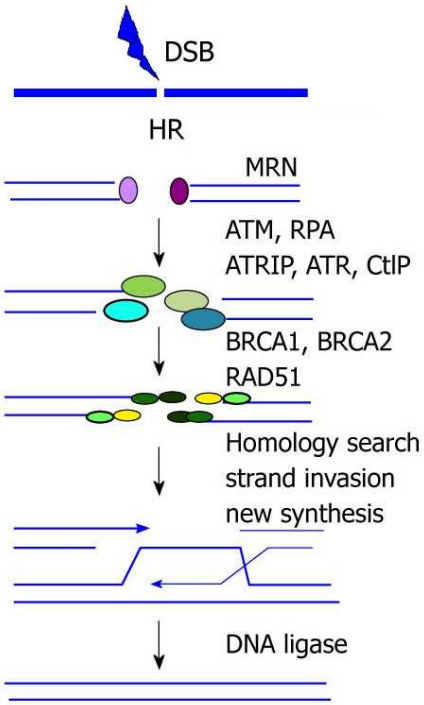

Figure 5: Schematic representation of HR mechanism (modified from Peng G., Lin S.Y., 2011).

1.3.2 Non-Homologous end joining recombination (NHEJ)

The NHEJ repairs the two breaking ends in absence of a template sequence. In this pathway, the first protein that binds the ends of damaged DNA is the Ku70/80 heterodimer. Ku interacts with the catalytic subunit of the DNA-dependent protein kinase (DNA-PKcs) and together they connect the two ends to allow repair (DeFazio L.G. *et al.*, 2002). Later, Artemis nuclease is recruited through its interaction with DNA-PKcs, and the Artemis/DNA-PKcs complex cuts the damaged DNA (Ma Y. *et al.,* 2005). The DNA ends cutting causes gaps in the DNA that are completed by polymerases

μ and λ, components of the PolX family (Ma Y., 2004). This passage can induce deletions and insertions, for this reason the NHEJ is considered more prone to errors than HR (Kass E.M., Jasin M., 2010). Finally, the two interrupted ends are reunited thanks to the action of the DNA ligase IV/XRCC4 complex (Critchlow S.E., Jackson S.P., 1998). The pathway just described is the canonical NHEJ mechanism (c-NHEJ); when the Ku protein or DNA ligase is absent (Truong L.N. *et al.,* 2013; Wang H., Xu X., 2017) or in tumors that have defects in HR (Ceccaldi R. *et al.,* 2015), may be activated the alternative NHEJ pathway (alt-NHEJ), also called Microhomology-mediated end-joining (MMEJ). The first step of the alt-NHEJ is the cutting at the ends 5'→3' to expose the micro-homologous regions, sequences 5-25 base pairs long. This cut occurs exactly in the same way described above for HR mechanism, and a possible role is played by Poly(ADP-ribose) polymerase (PARP) which acts, with a pleiotropic activity, as a platform for directly or indirectly recruitment of repair factors (Audebert M *et al*., 2004). The micro-homologous regions later bind to each other forming an intermediate that has a non-homologous 3' tail on each end of the double-strand break. These two non-homologous 3' tails are removed by the Xeroderma pigmentosum group F/protein-Excision repair cross complementing endonuclease 1 (XPF/ERCC1), then the DNA polymerase catalyzes DNA synthesis and the cuts are sealed by DNA ligase III/I. Obviously, a significant part of the original DNA sequence is removed and therefore the alt-NHEJ is a repair pathway subject to more frequent errors (Wang H., Xu X., 2017) (**Figure 6**).

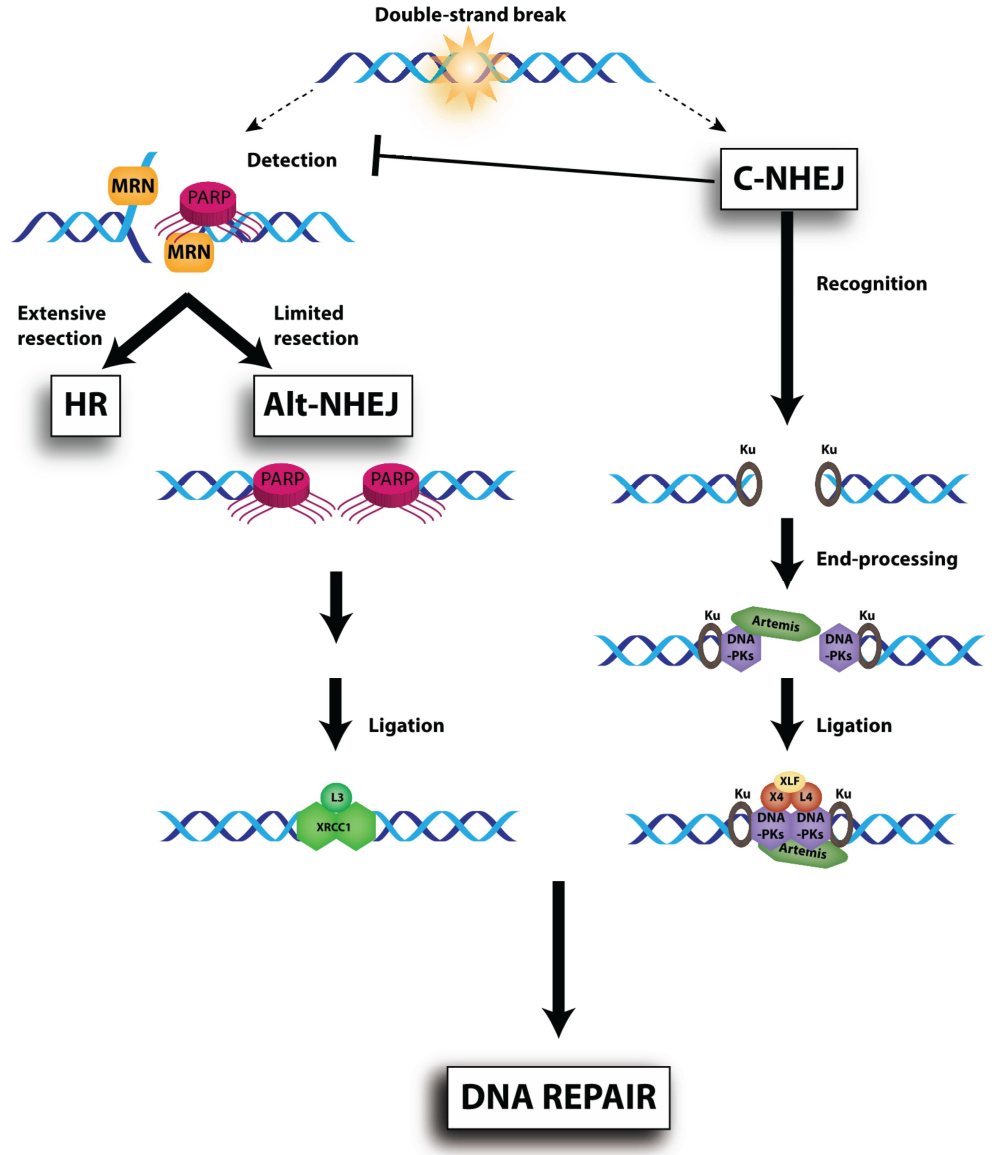

Figure 6*:* Schematic representation of repair mechanisms of double strand DNA damage (Velic D. *et al.,* 2015).

2. Review of the literature

2.1 *In vitro* assay to study nucleotide excision repair mechanism

NER and its role to remove UV lesions has always been object of investigation; the pioneers of this fields were in 1964 Howard-Flanders and Setlow, evaluating radiolabeled thymidine incorporation in genomic DNA of *E. coli (*Boyce R.P., Howard-Flanders P., 1964; Setlow R.B., Carrier W.L., 1964*);* they labelled bacteria growing them in a culture medium containing thymidine-methyl-H^3, and then exposed samples to UV irradiation. They described for the first time the CPDs removal performed by "photoactivating enzymes". The first evidence of an inefficient DNA repair mechanism observed in human fibroblasts exposed to UV irradiation was demonstrated by Cleaver in 1968 (Cleaver J.E., 1968). The fibroblasts used for these experiments, derived from patients affected by Xeroderma pigmentosum (XP), were analysed by Unscheduled DNA synthesis (UDS) technique, the first method employed to study the incorporation of [^{3}H] thymine into DNA only in the S-phase; also in this case ^{3}H-thymidine or ^{3}H-bromodeoxiuridine, added to the culture medium, highlighted a different ability of these cells, derived from patients, to activate the "repair replication", compared to normal fibroblast. The various XP groups of complementation were not yet known (Cleaver J.E., 1968). These experiments led to the identification of different XP complementation groups characterised by mutations in 8 distinct genes, from XP-A to XP-G and XP-V (variant); the latter subtype derives from mutation to the homonymous gene, also called POLH which encodes the polymerase η (Cleaver J.E., 1972; Masutani C. *et al*., 1999). Further analysis interested the characterization of individual proteins, to reconstruct *in vitro* the complex biochemical NER system (Wood R.D. *et al*., 1988; Huang J.C. *et al*., 1992); more information about this process became available when the human repair genes, XPA to XPG and ERCC1 were cloned (Legerski R., Peterson C., 1992) and various tools to study excision repair mechanism were developed (Mu D., Sancar A., 1997); in particular, the main interest was to understand the role of each protein in the processes of

recognition, excision and re-synthesis of the damaged fragment (Gillet L.C.J., Schärer O.D., 2006). To verify the sequential steps of NER, experiments with fluorescent tagged proteins, in mammalian cells, were performed, providing a quantitative depiction of the repair process (Houtsmuller A. B. *et al*., 1999; Hoogstraten D. *et al*., 2002; Rademakers S. *et al*., 2003). Recently, it was described a rapid, sensitive and quantitative assay useful to quantify NER activity in human cells, known as Oligonucleotide Retrieval Assay (ORA). This assay uses oligonucleotide constructs containing CPDs, to transfect human cells (immortalized, primary and stem-like cells), and the oligonucleotides are recovered for quantification by real-time quantitative PCR (Shen J.C. *et al*., 2014). The development and synthesis of DNA models remain a current point of interest; for this reason, it was created a novel non nucleosidic phosphoramidite reagents that contain N-[6-(9-antracenylcarbamoyl)hexanoyl]-3-amino-1,2-propandiol (nAnt) and N-[6-(5(6)-fluoresceinylcarbamoyl)hexanoyl]-3-amino-1,2-propandiol (nFlu) fractions (Evdokimov A. *et al*., 2013). Nevertheless, studies conducted on human DNA had shown that nucleosomes can determine inhibitory effects on various DNA activities (Kornberg R.D., Lorch Y., 1999; Thoma F. 1999; Tyler J.K., Kadonaga J.T., 1999), so the structural complexity of eukaryote DNA should be considered when *in vitro* DNA repair assays are used as models. Recently, methods to study repair activity with a single-molecule approach, employing fluorescent nucleotides, have been developed; for example, Zirkin S. and colleagues, developed an interesting *in vitro* system, purifying genomic DNA from damaged cells and treated it with an enzymatic cocktail composed of bacterial and bacteriophage enzymes. They observed and quantified the repair process evaluating the incorporation of fluorescent nucleotides (Zirkin S. *et al*., 2014). Generally, *in vitro* methods that study NER mechanism employ proteins purified by human cell culture (Wang Z.G. *et al*., 1991), Xenopus oocyte nuclear extract (Liu X., Smerdon M.J., 2000) or recombinant tagged protein produced by *E. coli* (Jones C.J., Wood R.D., 1993; Sijbers A.M. *et al*., 1996). More recent protein expression and purification methods employ insect cells infected with recombinant baculoviruses (Wittschieben B.Ø. *et al*., 2005); this purification protocol allows to obtain a higher expression of the target protein than *E. coli* (Gecchele E. *et al*., 2015).

2.2 Molecular mechanism of DNA damage recognition in GG-NER

As mentioned above, in GG-NER the XPC-hHR23B complex identifies altered regions on DNA (Masutani C. *et al.,* 1994) although more recent studies have demonstrated a low ability of this complex to bind nucleosomal lesions (Hara R. *et al.*, 2000; Yasuda *T. et al.,* 2005). The UV-DDB complex was identified as damage sensor factor, acting up-stream of XPC-hHR23B (Moser J. *et al.,* 2005; Sugasawa K. *et al.,* 2005), thus playing a crucial role for the *in vitro* repair mechanism on naked DNA (Mu D. *et al.,* 1995). In fact, an inefficient functionality *in vivo* of this complex induces a delayed repair kinetics (Wakasugi M*. et al.,* 2002; Cazzalini O. *et al.,* 2014).

2.2.1 Structure of UV-DDB complex

The UV-DDB complex is composed of two subunits indicated as DDB2 (or p48) and DDB1 (or p127). DDB2 is a protein encoded by the XPE gene on the short arm of chromosome 11 (11p12-p11) (Dualan R. *et al.,* 1995). The structure of DDB2 consists of five WD40 motifs and an N-terminal helix-loop-helix portion that interacts with the BPA and BPC domains of DDB1; one end of the β-helix of DDB2, opposite to the DDB1 binding site, has a hairpin structure that interacts with the minor groove of the DNA double helix; the DNA therefore interacts directly with DDB2 and not with the DDB1 protein (Sugasawa K., 2009) (**Figure 6**). The human DDB1 gene is located on the long arm of chromosome 11 (11q12-q13) and encodes a protein composed of 1140 amino acids (Tang J., Chu G., 2002). The structure of DDB1 consists of three WD40 β-helix domains (BP) called BPA, BPB, BPC and a C-terminal α-helix domain respectively. BPA and BPC are closely associated with each other (**Figure 6**), while BPB is flexibly bound to them and appears to act as an attachment site for the E3 ligase complex containing Cullin4A (Cul4A) (Angers S. *et al.,* 2006).

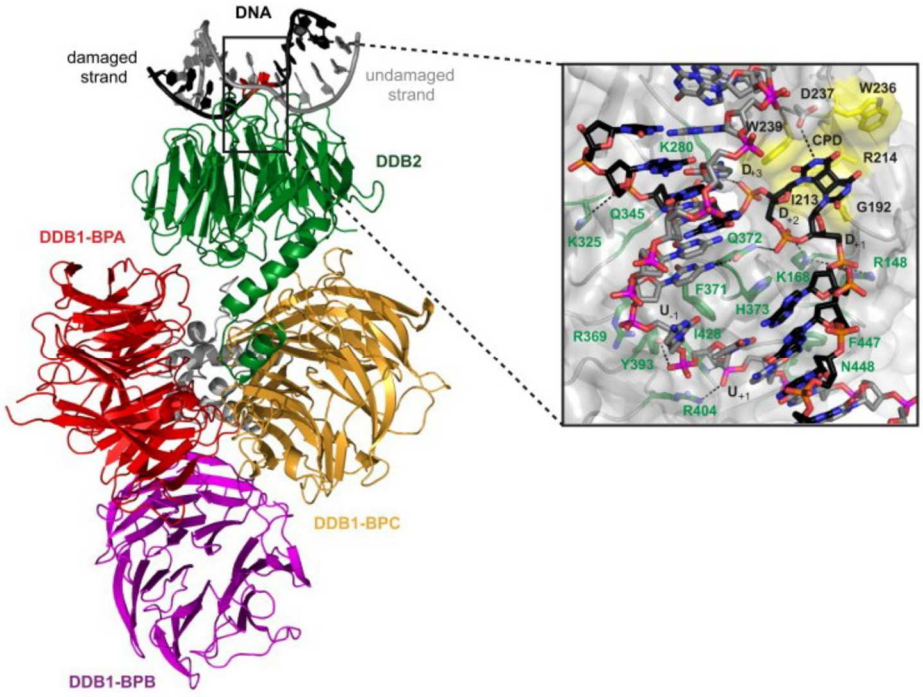

Figure 7: Representation of UV-DDB complex structure. DDB2 in green; DDB1-BPA domain in red; DDB1-BPB domain in magenta; DDB1-BPC domain in yellow; damaged/undamaged DNA helix in black/grey, respectively (Sugasawa K., 2009).

2.2.2 Functions of UV-DDB complex

The UV-DDB complex plays an important role binding proteins involved in chromatin remodeling and ubiquitination processes (Shiyanov P. et al., 1999; Nag A. et al., 2001). The ubiquitination pathway has an important function in the regulation of the initiation of NER (Takedachi A. *et al.,* 2010); DDB1 is part of the CUL4A-ubiquitin-E3-ligase mechanism, able to regulate many cellular processes, including development, transcription, replication and repair of DNA damage (Higa L.A. *et al.,* 2006). The E3 ligase family includes members called “Cullin-RING ubiquitin ligases” (CRLs) that can recruit RING-box1 (Rbx1) and E2 ligase to the C-terminal of the Cullin,

while at the N-terminal end they bind substrate proteins, such as DDB1, a protein that acts as an adapter capable of recalling substrate receptors known as DDB1-CUL4A-Associated Factors (DCAFs) (Fischer E.S. *et al.*, 2011). One of these substrate receptors is DDB2, which binds the pyrimidine dimers (CPDs) or 6-4 photoproduct (6-4PP), formed because of UV-induced DNA damage. DDB2 takes part in the DDB1-DDB2-CUL4A-RBX1 E3-ligase complex ($CRL4A^{UV\text{-}DDB}$), which has the dual function of recognizing the damage and ubiquitinate it to repair the chromatin lesion (**Figure 8**) (Hannah J., Zhou P.B., 2013).

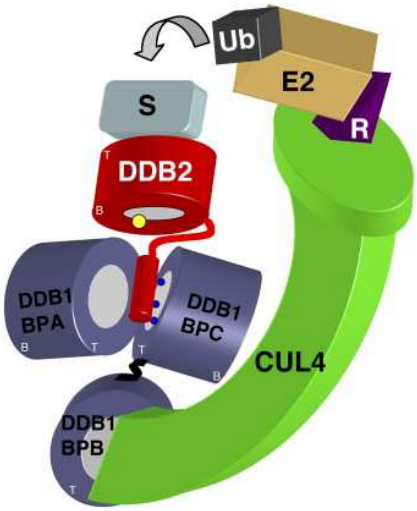

Figure 8: Schematic representation of DDB1-DDB2-CUL4A-RBX1 E3-ligase complex (Lee J., Zhou P., 2007).

The interaction between UV-DDB and Cul4A, mediated by Rbx1 protein, induces DDB2 ubiquitylation promoting its proteasomal degradation (Angers S. *et al.,* 2006); moreover, the ubiquitylation of XPC seems to enhance its binding on damaged site, inducing DDB2 release (Sugasawa K. *et al.,* 2005). Another protein important for DDB2 degradation is PCNA (**Figure 9**); in a recent study published by our laboratory, it has been demonstrated for the first time that PCNA binds directly DDB2 protein, interacting through a conserved sequence called PIP-box (PCNA interacting protein-box), which is present in all proteins interacting with PCNA such as,

for example, the cell cycle inhibitor p21 (Cazzalini O. *et al.,* 2014), pol η (Durando M. *et al.,* 2013), the clamp loader RFC-A (Montecucco A. *et al.,* 1998) or XPG (Gary R. *et al.,* 1997). Using a site-directed mutagenesis protocol, the DDB2 PIP-box sequence was disrupted producing a mutant form unable to bind PCNA ($DDB2^{PCNA-}$). The sequence analysis of DDB2 protein showed that the PIP-box region (87-94) overlaps one of the two sequences required for the interaction with DDB1 (87-98); however, the mutated amino acids do not disrupt their interaction and association in the UV-DDB complex (Cazzalini O. *et al.,* 2014). The expression of $DDB2^{PCNA-}$ protein in human cells induces not only a delayed DNA damage recognition after UV irradiation but also an inefficient DNA repair. Interestingly, $DDB2^{PCNA-}$ expression in human cells confers proliferation advantages and modifies H2AX phosphorylation (Perucca P. *et al.,* 2018).

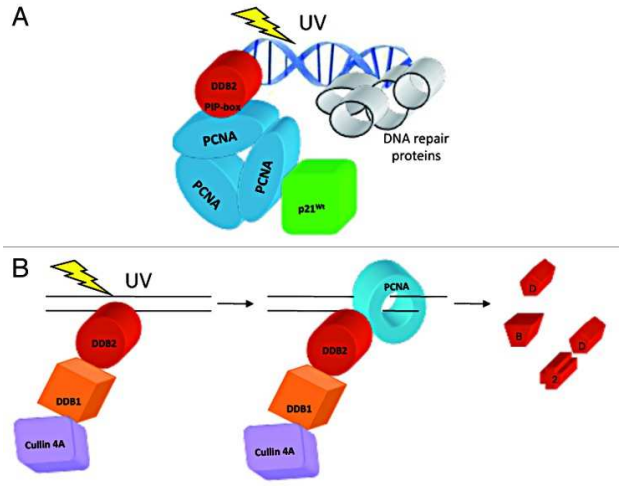

Figure 9: A) Schematic representation of DDB2 interaction with PCNA through a conserved PIP-box. (B) DBB2 is first recruited to DNA damage sites and, after the recognition step, interacts with PCNA which then promotes its proteolytic degradation (Cazzalini O. *et al.,* 2014).

3. Aims of the research

Eukaryotic cells have developed different repair mechanisms, each specific to the type of DNA-induced damage. Among these, 6-4 photoproducts (6-4 PP) and pyrimidine dimers (CDPs) are the lesions most frequently induced by UV radiation that are efficiently removed by the Nucleotide Excision Repair (NER) (Chatterjee N., Walker G.C., 2017). This process and its molecular mechanism have always been object of investigation and, using *in vitro* cell-free assays, it was possible to deeply dissect the entire pathway (Boyce R.P., Howard-Flanders P., 1964; Setlow R.B., Carrier W.L., 1964*;* Mu D., Sancar A., 1997). Many DNA repair assays reported in the present literature significant critical points, such as the use of radioisotopes (Cleaver J.E., 1968), the difficulty of producing human proteins on a large scale (Liu X., Smerdon M.J., 2000*;* Wittschieben B.Ø. *et al*., 2005), the use of plasmids as DNA templates containing the target lesions of NER; furthermore, another important point that must be considered, when studying human DNA repair, is the complexity of its structure, wrapped in nucleosomes (Kornberg R.D., Lorch Y., 1999).

Aims of the first part of this study are:

1. To develop a new *in vitro* cell-free method based on a pre-existing assay used to study DNA replication (Krude T. *et al.,* 1997). In this experimental approach, nuclei were isolated from HaCaT and HeLa cells, synchronized in the G_1-phase, to exclude replicating cells (S-phase) considered in this context as “contaminants”, and subsequently exposed to damage agents.

2. To validate this new method of investigation for studying different DNA repair mechanisms. To this end, DNA lesions were induced using chemical or physical damaging agents able to activate specific repair mechanisms. Nuclei and cytosolic extracts were obtained from HaCaT cells exposed to $KBrO_3$, MNNG, cis-Pt, UV-C and X-ray.

3. To apply this *in vitro* cell-free repair system for studying and investigating the regulation of NER mechanism, evaluating its specificity and reproducibility. The role of the human recombinant PCNA, DDB1 and DDB2 proteins and their interactions were investigated.

Recent evidence has shown an important role of DDB1 and DDB2, known as UV-DDB complex, to specifically recognize and bind UV lesions, acting as a damage sensor factor (Moser J. *et al.,* 2005; Sugasawa K. *et al.,* 2005); however, only in the last few years, it was highlighted a crucial role of the direct interaction and binding of DDB2 with PCNA, in regulating DNA damage recognition and its removal kinetic (Cazzalini O. *et al.,* 2014; Perucca P. *et al.,* 2018). This binding is mediated by a PIP-box sequence identified on DDB2 that, once mutated, disrupts their interaction and causes a delay, without implying a complete block, of the NER machinery. Moreover, DDB2 takes part in the $CRL4A^{UV\text{-}DDB}$ complex, which has the dual function of recognizing the damage and ubiquitinating repair factors to regulate the initiation of NER (Takedachi A. *et al.,* 2010; Hannah J., Zhou P.B., 2013).

Aims of the second part of this study are:

1. To investigate the involvement of DDB1, partner of DDB2 in the UV-DDB complex, as possible actor when DDB2 loses its constitutive interaction with PCNA; the hypothesis is that DDB1 may associate directly with PCNA trough a putative PIP-box sequence.

2. To disrupt the DDB1-PCNA interaction by a multisite-directed mutagenesis and verify if the mutation is deleterious for cell survival; cellular localization of the DDB1 mutated form will be evaluated, in physiological condition or after DNA damage induced by UV-C, comparing results with the wild-type one.

3. To demonstrate that the potential PIP-box sequence identified on DDB1 protein is functional to the interaction with PCNA by performing *in vitro* binding assays.

4. Materials and methods

4.1 Cell cultures and synchronization

HaCaT, HeLa and XP14BR cell lines were cultured in Dulbecco's modified Eagle's medium (DMEM [Gibco]) supplemented with 10% fetal bovine serum (FBS [Life Technologies-Gibco]), 2 mM L-glutamine (Life Technologies-Gibco), 100 U/ml penicillin, 100 µg/ml streptomycin at 37°C in a humified atmosphere with 5% CO_2.

4.2 Nuclei isolation and cytosolic extract preparation

Cells were seeded on Petri dishes 100x20 mm at a density of $1x10^6$; after two days, when the 80% of confluence was usually reached, cells were synchronized by serum starvation (0.5% FBS) for three days and treated for 24 hours using 0.5 mM L-Mimosine (Sigma). Cell cycle synchronization was verified by flow cytometry analysis of Bromodeoxyuridine (BrdU, 20 µM [Sigma-Aldrich]) added in the culture medium 1 hour before nuclei isolation.

Isolated nuclei and cytosolic extracts were prepared from untreated cells (control) and cells treated with different damaging agents:

- UV-C radiation at a dose of 10, 20 and 40 J/m^2;
- Cisplatinum (Cis-Pt, Teva Pharma) 50 µM added to cell culture medium for 1 hour;
- 1-Methyl-3-nitro-1-nitrosoguanidine (MNNG, Sigma-Aldrich) 50 µM added to cell culture medium for 30 minutes;
- Potassium bromate ($KBrO_3$, Sigma-Aldrich]) 40 µM added in PBS 1X for 15 minutes.
- X-Ray at a dose of 1 Gy/min.

4.2.1 Dounce homogenizer method

Cells, once rinsed with PBS 1X, were washed twice and incubated 10 minutes in cold hypotonic buffer (**Table 1**). At this stage, mitotic cells, more loosely attached to their substrate, were lost under hypotonic conditions followed by tapping the Petri dishes.

Reagents	Final concentrations
KOH-Hepes pH 7.8	20 mM
Potassium acetate	5 mM
$MgCl_2$	0.5 mM
DTT	1 mM

Table 1: Hypotonic buffer

After incubation in hypotonic buffer, cells still attached to the substratum were collected by a cell scraper and homogenized in a Dounce tissue grinder (Sigma) with 20-25 strokes using a loose-fitting pestle. Nuclei were pelleted at 3800 rfc for 2 minutes (Microfuge 18 centrifuge, Beckman Coulter), resuspended and washed in equal volume of SuNaSp 2X (**Table 2**) and pelleted at 3800 rcf for 2 minutes. Finally, pelleted nuclei were resuspended in SuNaSp 2X and counted with Burker chamber.

The supernatant was centrifuged at 15500 rcf for 20 minutes and the upper lipid layer was discarded.

Nuclei and cytosolic extracts were immediately frozen by dropping them as small aliquots of 10 and about 50 µl, respectively, in liquid nitrogen. The preparation of the nuclei and cytosolic extracts by Dounce was always carried out in a cold chamber.

Nuclei isolated with this method resulted functionally active and performed DNA initiation and replication *in vitro*, even if 20-25% of them showed a nuclear membrane permeabilization (Krude T., 2000).

Reagents	Final concentrations
KOH-Hepes pH 7.4	20 mM
NaCl	150 mM
Sucrose	0.5 M
Spermine	1 mM
Spermidine	0.3 mM
BSA	6%

Table 2: 2X SuNaSp buffer

4.2.2 Digitonin permeabilization method

This alternative method for nuclei isolation allows to completely preserve their membrane, which is important for the cytosol-nuclear matrix exchanges during cell metabolism. Cells were washed twice in PBS 1X, detached through Trypsin-EDTA and collected in cold complete cell medium. All steps from this point were carried out at 4°C. Cells were centrifuged at 180 rcf (Allegra 21R, Beckman Coulter) for 3 minutes. The supernatant was discarded while the pellet was washed twice with 5 ml of Digitonin permeabilization buffer (**Table 3**).

Reagents	Final concentrations
KOH-Hepes pH 7.8	50 mM
Potassium acetate	50 mM
Magnesium acetate	5 mM
DTT	2 mM
Proteases inhibitors	3 µl/100 ml

Table 3: Digitonin permeabilization buffer

Cells were centrifuged at 88 rcf (Allegra 21R, Beckman Coulter) for 5 minutes. The supernatant was removed, and the pellet resuspended in Digitonin permeabilization buffer mixed with 1 ml of Digitonin (100 µg/ml) to permeabilize the cellular membrane. The permeabilization reaction was

monitored, by fluorescence microscopy, spotting on a coverslip 2 µl of cells mixed with 2 µl of fluorescein isothiocyanate-dextran (Dextran, Sigma-Aldrich) (25 mg/ml). To permeabilize completely the cytoplasmic membrane, but not the nuclear one, Digitonin concentration was increased by 5 µg/ml increments checking the reaction with Dextran every time. To block the permeabilization reaction, 10 ml of SuNaSp-BSA buffer (**Table 4**) were added, then the cells were centrifuged at 88 rcf (Allegra 21R, Beckman Coulter) for 5 minutes, and the supernatants discarded.

Reagents	Final concentrations
KOH-Hepes pH 7.4	10 mM
NaCl	75 mM
Sucrose	0.25 M
Spermine	0.5 mM
Spermidine	0.15 mM
BSA	3%
DTT	2 mM
Protases inhibitors	3 µl/100 ml

Table 4: SuNaSp-BSA buffer

Nuclei were gently resuspended in 2X SuNaSp, ratio 1:1 v/v (**Table 2**) and were frozen by dropping 10 µl aliquots in liquid nitrogen.

4.3 The *in vitro* cell-free repair reaction

Figure 1: Schematic representation of *in vitro* cell-free repair assay

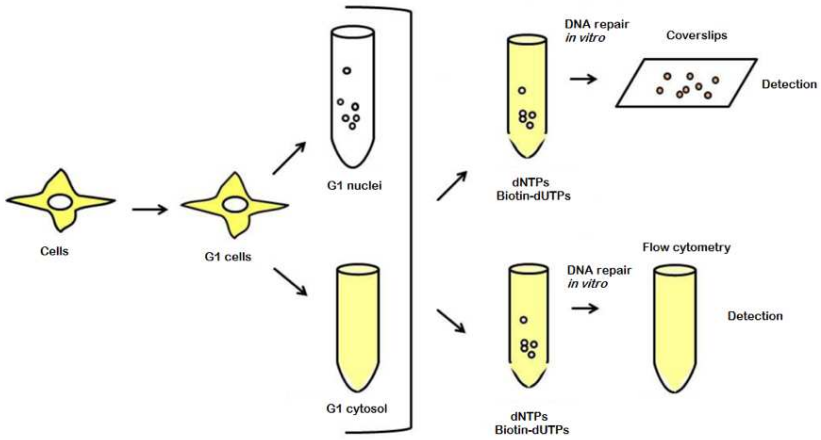

DNA repair synthesis reactions were performed in parallel to analyse results both by fluorescence microscopy and flow cytometry (**Figure 1**). Standard reaction conditions contained: 2 µl (about 2 x 10^5) of nuclei, 10 µl of cytosolic extract, and 1.53 µl of reagent mix (**Table 5**).

Reagents	Final concentrations
KOH-Hepes pH 7.8	40 mM
$MgCl_2$	7 mM
ATP	3 mM
GTP, CTP, UTP	0.1 mM (each component)
dATP, dGTP, dCTP	0.1 mM (each component)
Biotin-16-dUTPs	0.25 µM
DTT	0.5 mM
Creatine phosphate	40 mM
Phosphocreatine kinase (350 U/mg)	5 µg

Table 5: Reagent mix

Samples were prepared on ice and the reactions started incubating them at 37°C. Standard incubation time was 2 hours unless stated otherwise.

At the end of the incubation, samples were processed to reveal dUTPs incorporation into repaired DNA.

For fluorescence microscopy, nuclei were permeabilized and fixed with 0.25% Triton X-100 (Sigma) and 4% formaldehyde for 10 minutes at room temperature (RT), then stratified through 30% sucrose gradient on coverslips previously treated with Poly-L-lysine solution (Sigma) by centrifugation at 180 rcf for 5 minutes (Allegra 21R, Beckman Coulter).

For flow cytometry analysis, samples were prepared in the same experimental conditions doubling the volumes and, to stop the reactions, nuclei were fixed with 50% EtOH in physiological buffer (0.9% NaCl).

4.3.1 Fluorescence microscopy analysis

The isolated nuclei samples, fixed in 0.5% PBS-Triton X-100 and 8% paraformaldehyde (1: 1 v/v), were stratified on a sucrose gradient (30%) in scintillation vials, containing on their bottom coverslips, previously treated with Poly-L-lysine solution (Sigma-Aldrich). The samples were centrifuged at 180 rcf (Allegra 21R, Beckman Coulter) for 5 minutes, the coverslips transferred into a 24-well plate in which they were washed tree times with a Blocking Solution buffer (**Table 6, BS**).

Reagents	Quantity
BSA	1%
Triton X-100	0.04%
SDS	10%
PBS 1X	100 ml

Table 6: Blocking Solution buffer (BS)

Coverslips were then incubated with Streptavidin Alexa Fluor dye 488 (or 594) (1:350, Invitrogen) for 30 minutes at 37°C in a humified chamber, then they were washed again with BS buffer and incubated with Hoechst 33258 dye (0.5 µg/ml) for 10 minutes at RT. Coverslips were mounted in

Mowiol (Calbiochem) containing 0.25% 1,4-diazabicyclo-octane (Aldrich) as antifading agent. Images of fixed nuclei were taken with TCS SP5 II Leica confocal microscope, at 0.3 µm intervals. Nuclei were randomly acquired only to show the difference between elongation and repair DNA neo-synthesis supporting quantitative analysis performed by microscopic scoring and flow cytometry.

4.3.2 Flow cytometry analysis

The isolated nuclei samples ($2x10^6$ nuclei/sample), fixed in 50% EtOH in physiological buffer (0.9% NaCl), were transferred from 1.5 ml Eppendorf in 15 ml Falcon tubes and centrifuged at 304 rcf (Allegra 21R, Beckman Coulter) for 3 minutes.

The samples were resuspended in 1 ml of BS (**Table 6**) and centrifuged again. The supernatant was removed and each sample was resuspended in 50 µl of solution containing streptavidin-Alexa Fluor 488 (1:200) in BS. The sample used as Blank (B) was resuspended in 50 µl of BS, to have a cut-off of sample autofluorescence. After 30 minutes of incubation with streptavidin at RT, the samples were diluted in 1 ml of BS and centrifuged. The pellets were resuspended and washed in 1 ml of BS and pelleted again by centrifugation. Finally, the samples were resuspended and incubated for 30 minutes at RT with 1 ml of solution containing Propidium Iodide (**Table 7**), then stored at 4°C overnight. The next day, the samples were filtered before the flow cytometry analysis.

Reagents	Quantity
Propidium Iodide (500 µg/ml)	8.44 µl
PBS 1X	991.06 µl
Igepal CA 630	0.5 µl

Table 7: Propidium Iodide solution

4.3.3 Functionality *in vitro* cell-free repair assay validation

To validate the functionality of the method, samples prepared with UV-C irradiated nuclei were incubated with DNA synthesis inhibitors 1 mM Aphidicoline (Aph) (polymerase α and δ inhibitor) and 20 µM Citarabine -C (Ara-C) (cytosine analogue that is embedded in DNA blocking the synthesis). Each inhibitor was incubated in direct contact of the nuclei for 10 minutes on ice and, subsequently, the reaction mixture and the cytosolic extract were added. Repair synthesis reaction started when samples were incubated at 37 °C; after 2 hours of incubation, they were fixed following the protocol used for fluorescence microscopy or flow cytometry.

4.4 DNA repair efficiency of nuclei isolated from HaCaT cells exposed to different damage agents

HaCaT cells were treated with different damage agents (as reported in paragraph **4.2**) before processing them for nuclei isolation. To this end, both Dounce and Digitonin permeabilization methods were employed to compare nuclei functionality and exclude differences in their DNA damage response. Repair efficiency was evaluated analyzing samples by fluorescence microscopy and flow cytometry following the protocols reported in paragraph **4.3.1** and **4.3.2**. To clearly understand results obtained with nuclei isolated from HaCaT cells exposed to 1 Gy/min (XR nuclei), Comet assay and co-localization analyses were performed.

4.4.1 Comet assay

To understand the results obtained with nuclei isolated from HaCaT cells exposed to 1 Gy/min (XR nuclei), Comet assay and co-localization analyses were performed. Two µl of nuclei were resuspended in 150 µl of Low Melting Point Agar (LWP) and divided on two coverslips (75 µl each one), previously covered with 1% Agarose. Samples were immediately loaded in an electrophoretic cell at 4°C with an alkaline buffer (**Table 8**) for

40 minutes.

Reagents	Final concentrations
NaOH	0.3 M
EDTA	1 mM

Table 8: Alkaline buffer

The subsequent electrophoretic separation was performed at 25 V for 30 minutes at 4°C. Coverslips were washed with a Neutralizing buffer (0.4 M Tris base pH 7.5) and stained with Hoechst 33258 dye (0.5 µg/ml). Samples were observed through fluorescence Olympus BX-51 microscope (100X immersion oil lens, NA 1.25) equipped with an Olympus C4040 camera.

4.4.2 XRCC1 immunofluorescence analysis

Once XR nuclei were fixed and stratified (paragraph **4.3.1**), they were washed three times with BS buffer (**Table 6**) and then incubated for 1 hour at RT with anti-XRCC1 antibody (1: 100, Santa Cruz Biotechnology). After other three washes in BS buffer, the coverslips were incubated with anti-rabbit DyLight™ 488-conjugated (1:100, KPL) and streptavidin Alexa Fluor 594 (1:350, Invitrogen) for 30 minutes at 37°C in a humified chamber, then they were washed again with BS buffer and incubated with Hoechst 33258 dye (0.5 µg/ml) for 10 minutes at RT. Coverslips were mounted in Mowiol and images of fixed nuclei were taken with TCS SP5 II Leica confocal microscope, as previously described in the paragraph **4.3.1**.

4.5 Study of recombinant NER proteins in the *in vitro* cell-free repair assay

PCNA-His, DDB1-GST, DDB2^{Wt}-His and DDB2^{PCNA-}-His recombinant proteins were added in the synthesis reactions to study their role in the repair mechanism.

DDB2^{Wt}, DDB2^{PCNA-} and PCNA His-tag recombinant proteins were previously purified in my laboratory using commercial Ni-conjugated resin (Sigma) according to the manufacturer's instructions. Preliminary tests have been carried out either by incubating the proteins in direct contact of the UV-C nuclei for 10 minutes on ice or adding proteins to the cytosolic extract and to the reaction mixture before the addition of the UV-C nuclei. The recombinant proteins DDB2^{Wt} and DDB2^{PCNA-} were added to the scalar doses of 150 ng, 100 ng and 50 ng, DDB1 (Abnova) at 150 ng and PCNA at 400 ng.

As a negative control we prepared a sample to which BSA (1 µg) was added, not being a protein involved in DNA repair mechanisms.

4.5.1 BrdU incorporation analysis

To ascertain that the DNA repair synthesis initiates *in vitro* and to further distinguish it from DNA replication of S-phase contaminants, cells were incubated with Bromodeoxiuridine (BrdU, Sigma-Aldrich), added directly in the culture medium 1 hour before nuclei isolation. The samples were processed for flow cytometry analysis staining them as described (Stivala L.A., *et al* 1996). Cells were incubated for 30 minutes with 2 M HCl at RT, pelleted at 304 rcf (Allegra 21R, Beckman Coulter) for 3 minutes and resuspended in 0.1 M Sodium tetraborate pH 8.2 for 15 minutes. Then, they were permeabilized in PBA buffer (**Table 9**) by 1% BSA, 0.2% Tween 20 in PBS (PBA), and incubated with anti-BrdU (1:10, Becton Dickinson).

Components	Quantity
BSA	1 g
Tween 20	0.2%
1X PBS	100 ml

Table 9: PBA buffer

Cells were then washed three times with PBA and incubated 30 minutes with anti-mouse DyLight™ 488 labeled (1:100, KPL). At the end, they were washed twice in PBA and resuspended in PBS containing 10.55 µg/ml (PI) and 0.2% Igepal CA 630 (Sigma) for 30 minutes at RT.

For immunoreactions of *in vitro* synthesis, the coverslips with stratified nuclei were incubated 1 hour at RT with mouse monoclonal anti-BrdU (1:10, Amersham Pharmacia Biotech) diluted in nuclease, according to manufacturer's instructions, and anti-mouse DyLight™ 594 labeled (1:100, KPL). The coverslips were washed three time in BS buffer and incubated with Alexa Fluor 488 Streptavidin (1:350) for 30 minutes at 37°C in a humified chamber, then they were washed again with BS buffer and incubated with Hoechst 33258 dye (0.5 µg/ml) for 10 minutes at RT.

4.6 Western blot analysis

4.6.1 Total extract

HaCaT and HeLa nuclei and cytosolic extracts prepared after L-Mimosine synchronization (exposed or not to UV-C radiation) were collected and analyzed by Western blot. Nuclei were resuspended in 50 µl of PBS 1X and sonicated and, both nuclei and cytosolic extract, were quantified through Bradford method (Bradford M.M., 1976). For each sample, 30 µg of proteins were mixed with a 3X SDS-loading buffer (**Table 10**).

Reagents	Final concentrations
Tris-HCl pH 7.4	65 mM
DTT	100 mM
Glycerol	10%
SDS	1%
Bromophenol blue	0,02%

Table 10: 3X SDS-loading buffer

The electrophoresis was performed in denaturing and reducing conditions, loading samples on a 10% polyacrylamide gel (**Table 11**), employing:

- 4X Lower buffer (LB, 1.5 mM Tris-base pH 8.8 + SDS 0.4%);

- 4X Upper buffer (UB, 0.5 mM Tris-base pH 6.8 +SDS 0.4%);
- Acrylamide 30% (dilution 29:1 [Serva]);
- TEMED (Applichem);
- APS 15% (Applichem).

Plug	Quantity (µl)	Running	Quantity (µl)	Stacking	Quantity (µl)
dd H_2O	1250	**dd H_2O**	4600	**dd H_2O**	2340
LB	750	**LB**	3000	**UB**	1000
Acrylamide	1000	**Acrylamide**	4400	**Acrylamide**	660
Temed	9	**Temed**	10	**Temed**	10
APS	76	**APS**	80	**APS**	30

Table 11: 10% Polyacrylamide gel

Proteins were electrotransferred to nitrocellulose membrane through a semidry system, and membranes were blocked for 30 minutes in 5% non-fat milk in PBST buffer. DDB2 levels were detected by the anti-DDB2 antibody (1:500, Novus Biologicals) and anti-rabbit HRP conjugated (1:10000, KPL); to reveal DDB2 expression, a chemiluminescent enhancer was used (c600, Azure). Densitometric analysis was performed using the public software ImageJ (http://rbs.info.nih.gov/nih-image).

4.6.2 Chromatin bound fraction

At the end of DNA repair synthesis reaction *in vitro*, the samples were washed in 100 µl Buffer A (**Table 12**) and pelleted at 304 rcf for 1 minute at 4°C (Allegra 21R, Beckman Coulter).

Reagents	Final concentrations
Tris-HCl pH 7.4	10 mM
$MgCl_2$	2.5 mM

Table 12: Buffer A

Nuclei were lysed with 100 µl Buffer B (**Table 13**) 15 minutes on ice, then the lysate was centrifuged at 500 rcf (Microfuge 18 centrifuge, Beckman Coulter) for 5 minutes at 4°C.

Reagents	Final concentrations
EDTA	3 mM
EGTA	0.2 mM
DTT	1 mM
Igepal CA 630	1%
NaCl	0.5 M
Proteases inhibitors	3 µl/100 ml

Table 13: Buffer B

In this step, the un-bounded proteins remain in the supernatant (sol), while the chromatin bound fraction contains chromatin and the insoluble proteins (Cb).

The supernatant was mixed with 75 µl of 3X SDS-loading buffer, while the chromatin bound fraction was re-suspended in 30 µl of 3X SDS-loading buffer for polyacrylamide gel electrophoresis (PAGE), sonicated and boiled. The electrophoresis was performed in denaturing and reducing conditions, loading samples on a 12% polyacrylamide gel (**Table 14**).

Plug	Quantity (µl)	Running	Quantity (µl)	Stacking	Quantity (µl)
dd H_2O	1050	**dd H_2O**	3600	**dd H_2O**	2340
LB	750	**LB**	3000	**UB**	1000
Acrylamide	1200	**Acrylamide**	5400	**Acrylamide**	660
Temed	12	**Temed**	20	**Temed**	10
APS	40	**APS**	80	**APS**	30

Table 14: 12% Polyacrylamide gel

Proteins were electrontransferred and blocked in the same experimental condition reported in paragraph **4.6.1** and probed with the following primary antibodies: anti-6X His-tag HRP-conjugated antibody (1:2000, ThermoFisher Scientific) and anti-H3 antibody (1:20000, Millipore). The membranes were then washed in PBST, incubated for 30 minutes with appropriate HRP-conjugated secondary antibodies anti-rabbit (KPL) and revealed using enhanced chemiluminescence. Densitometric analysis was performed using the public software ImageJ (http://rbs.info.nih.gov/nih-image).

4.7 Cell transfection

HeLa cells were seeded at a density of $1.5x10^6$ on 100x20 mm Petri dishes and cultured in standard conditions; when cells arrived at 70% of confluence, they were transfected following the experimental procedure reported in **Figure 2**.

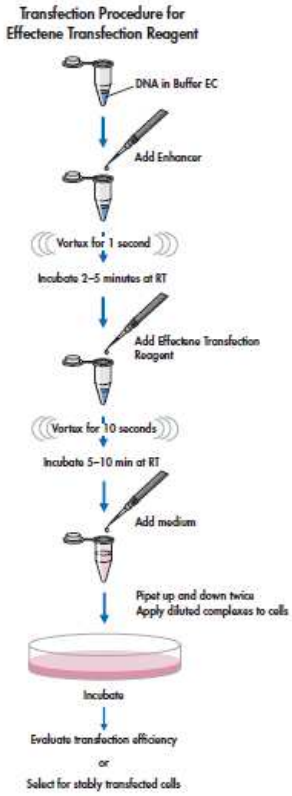

Figure 2: Effectene transfection protocol

HeLa cells were transfected with pcDNA3.1 $DDB2^{Wt}$-His or pcDNA 3.1 $DDB2^{PCNA-}$-His constructs.

The plasmid DNA was diluted in EC buffer and once the Enhancer was added, the solution was vortexed for 1 second and incubated at RT for 5 minutes. Effectene was added to the solution pipetting up and down for five

times and the mix was incubated at RT for 10 minutes. Meantime, the culture medium was removed from dishes, cells were washed once with 1X PBS before adding culture medium and the transfection mixtures (**Table 15**).

Petri dishes (mm)	Plasmid DNA (µg)	EC Buffer	Enhancer	Effectene	Volume of medium to add to cells (µl)	Volume of medium to add to mix (µl)
100x20	1	150	8	25	8900	1000

Table 15: Transfection reagent mixture

Cells were cultured for 24 hours and then collected for the immunoprecipitation assay.

4.8 Immunoprecipitation assay

HeLa cells, transfected with pcDNA3.1 $DDB2^{Wt}$-His or pcDNA 3.1 $DDB2^{PCNA-}$-His constructs, were damaged with UV-C radiation at a dose of 30 J/m^2; cells were recovered 30 minutes and 1 hour after radiation, lysed with a hypotonic buffer (**Table 16**) for 10 minutes on ice and then centrifuged at 5500 rcf (Allegra 21R, Beckman Coulter) for 1 minute at 4 °C.

Reagents	Final concentration
Tris-HCl pH 8.0	10 mM
$MgCl_2$	2.5 mM
Igepal CA 630	0.5%
DTT	1 mM
NaBu	10 mM
PMSF	1 mM
Proteases inhibitors	5 µl

Table 16: Hypotonic buffer

From supernatants (total soluble fractions), 5 µl of sample were collected for protein quantification using Bradford method and 50 µl, to which 25 µl of 3X SDS-loading buffer were added, for protein analysis by gel electrophoresis. Pellets (insoluble fractions) were washed firstly with hypotonic buffer and centrifuged at 5500 rcf (Allegra 21R, Beckman Coulter) for 1 minute at 4°C, then rinsed with isotonic buffer (**Table 17**) and centrifuged at 5500 rcf (Allegra 21R, Beckman Coulter) for 1 minute at 4°C.

Reagents	Final concentration
Tris-HCl pH 8.0	10 mM
NaCl	150 mM
PMSF	1 mM
Proteases inhibitors	5 µl

Table 17: Isotonic buffer

After centrifugation, the pellets were digested with 50 µl of 1X DNAse Buffer (**Table 18**) for 20 minutes at 4°C under stirring to prevent DNAse deposition.

Buffer A		Buffer B	
Components	**Final concentration**	**Components**	**Final concentration**
Tris-HCl pH 8.0	20 mM	**NaCl**	20 mM
MgCl2	10 mM	**PMSF**	1 mM
In Buffer B was added, firstly, 9 µl of DNAse (20 U/µl) and then Buffer A.			

Table 18: 1X DNAse buffer

After centrifugation at 12700 rcf for 1 minute at 4°C, 40 µl of the supernatant (insoluble fraction) were added to 20 µl of 3X SDS-loading buffer and collected at -20°C. Meantime, 30 µl of magnetic beads (Dynabeads™ Protein G, Invitrogen) for each sample were washed twice with 1X beads washing buffer (**Table 19**).

Components	Quantity
Citric acid	0.094 g
Sodium phosphate bibasic	0.184 g
dd H_2O	10 ml

Table 19: 2X Beads washing buffer

Magnetic beads were resuspended in 150 µl of 1X Beads washing buffer mixed with 1 µg of rabbit polyclonal anti-DDB2 antibody (Santa Cruz) and incubated for 1.5 hour on SRT1 Roller Mixer at RT. The mixture containing beads and antibody was divided between the samples of the soluble and insoluble fractions, incubated for 3 hours at 4°C (IP-fractions). For the soluble fraction, samples were quantified, and 1.5 mg/ml of proteins were incubated with magnetic beads, while the insoluble fractions were totally immunoprecipitated. After antibody incubation, samples were washed with isotonic buffer (**Table 17**) for 2 minutes at 4°C on a magnetic support (**Figure 3**) three times and resuspended in 60 µl of 3X SDS-loading buffer.

Figure 3: Magnetic support (Dynal MPC-S).

After adding the loading buffer, immunoprecipitated and input samples were boiled at 90°C for 5 minutes and loaded on denaturing and reducing gel following the same experimental condition reported in **4.6.1** paragraph. Proteins were electrotransferred to nitrocellulose, following the same experimental protocol (paragraph **4.6.1**) and probed with the

following primary antibodies: anti-DDB1 (1:1000, Genetex), anti-DDB2 (1:500, Santa Cruz), anti-PCNA (1:1000, Dako) and anti-actin (1:1000, Sigma). The membranes were then washed in PBST, incubated for 30 minutes with appropriate HRP-conjugated secondary antibodies: anti-mouse (DAKO), anti-goat and anti-rabbit (KPL) and revealed using enhanced chemiluminescence. Densitometric analysis was performed using the public software ImageJ (http://rbs.info.nih.gov/nih-image).

4.9 DDB1^{AAA}-HA construct

4.9.1 DDB1^{Wt} mutagenesis

The QuickChange Lightning Multi Site-Directed Mutagenesis protocol (Agilent Technologies), showed in **Figure 4**, was employed to mutagenize the pcDNA3-HA2-DDB1 vector (Addgene plasmid #19909; http://n2t.net/addgene:19909; RRID:Addgene_19909) (Hu J. *et al*; 2008).

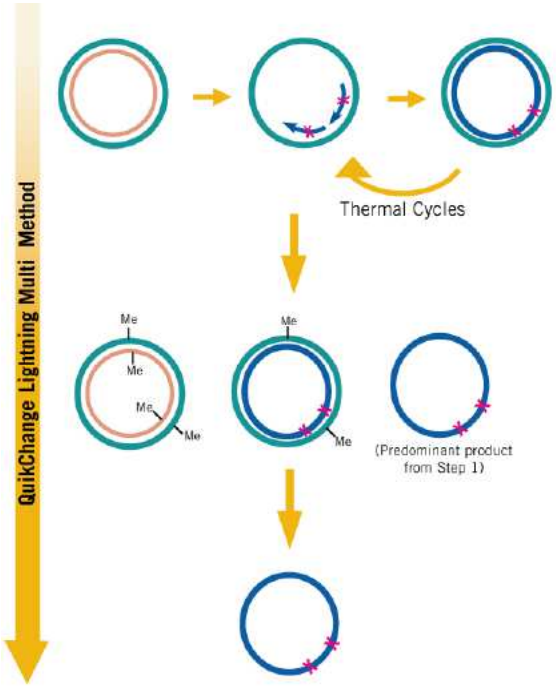

Figure 4: QuickChange Lightning Multi Site-Directed Mutagenesis protocol

The reaction protocol for template longer than 5 Kb (**Table 20**) was used because pcDNA3-HA2-DDB1 vector was 8912 bp long; the forward and revers primers designed were:

- Forward 5'-GAGCCCAAGGCCGGTCGCGCCGTGGTCGCCCAGTAT
- Reverse 5'-ATACTGGGCGACCACGGCGCGACCGGCCTTGGGCTC

Reagents	Quantity (µl)
10X QuikChange Lightning Multi reaction buffer	2.5
QuickSolution	0.75
pcDNA3-HA2-DDB1 template (100 ng)	0.5
100 mM Mutagenic primers	0.25 (each primer)
dNTP mix	1
QuikChange Lightning Multi enzyme blend	1
dd H_2O	18.75

Table 20: Mutagenesis reaction mix

Reaction was put in thermal cycler following the cycling protocol reported in **Table 21**.

Cycles	Temperature	Time
1	95°C	2 minutes
30	95°C	20 seconds
	55°C	30 seconds
	65°C	4.45 minutes
1	65°C	5 minutes

Table 21: Cycling protocol

To digest the parental ds-DNA, the amplification reaction was digested with 1 µl of Dpn I, pipetting up and down the mixture, spin down the reaction and immediately incubating it at 37°C for 5 minutes.

To transform XL 10-Gold ultracompetent cell with mutagenesis reaction, 45 µl of bacteria were aliquoted in a prechilled 14 ml Falcon polypropylene round-bottom tube and incubated on ice with 2 µl of β-mercaptoethanol mix for 10 minutes, swirling gently every 2 minutes. Then 1.5 µl of Dpn I digested-DNA were added to the ultracompetent cells, mixed and incubated 30 minutes on ice. First, tubes were heat-pulsed in a water bath at 42°C for 30 sec, secondly on ice 2 minutes. 500 µl of preheated NZY^+ broth (**Table 22**) was added and tubes were incubated at 37°C for 1 hour

with shaking at 225-250 rpm. 1 µl, 10 µl, 100 µl of XL 10-Gold ultracompetent transformed cells were plated on Luria Bertani-ampicillin (50 µg/ml) agar plates (**Table 23**) and incubated 16 hours at 37°C.

Components	Quantity
Before autoclave	
NZ amine (casein hydrolysate)	10 g
Yeast extract	5 g
NaCl	5 g
dd H_2O	1 l
After autoclave	
1 M $MgCl_2$	12.5 ml
1 M $MgSO_4$	12.5 ml
2 M Glucose	10 ml

Table 22: NZY$^+$ broth; the solution prepared before autoclave was adjust to pH 7.5 with NaOH, while the solution added after autoclave were filter-sterilized.

Components	Quantity
NaCl	10 g
Tryptone	10 g
Yeast extract	5 g
Agar	20 g
dd H_2O	1 l

Table 23: LB agar adjusted to pH 7 with 5 N NaOH before autoclave.

Since the efficiency of the mutagenesis protocol was very low, examining the troubleshooting section for "low colony number or low mutagenesis efficiency for long template (>5 Kb)", some parameters were changed in the subsequent experiments:

- QuikSolution were increased up to 1.5 µl;
- Amount of template was changed up to 200 ng;
- XL 10-Gold ultracompetent cells were transformed up to 4 µl of mutagenesis reaction.

After numerous failed attempts, the pUC57 DDB1^{AAA}-HA construct was bought by GENEWIZ®. The wild type and mutated gene sequences were aligned by CLUSTAL 2.1 (**Figure 5**).

```
CLUSTAL 2.1 multiple sequence alignment
Wild            ATGTCGTACAACTACGTGGTAACGGCCCAGAAGCCCACCGCCGTGAACGGCTGCGTGACC
AAA             ATGTCGTACAACTACGTGGTAACGGCCCAGAAGCCCACCGCCGTGAACGGCTGCGTGACC
                ************************************************************

Wild            GGACACTTTACTTCGGCCGAAGACTTAAACCTGTTGATTGCCAAAAACACGAGATTAGAG
AAA             GGACACTTTACTTCGGCCGAAGACTTAAACCTGTTGATTGCCAAAAACACGAGATTAGAG
                ************************************************************

Wild            ATCTATGTGGTCACCGCCGAGGGGCTTCGGCCCGTCAAAGAGGTGGGCATGTATGGGAAG
AAA             ATCTATGTGGTCACCGCCGAGGGGCTTCGGCCCGTCAAAGAGGTGGGCATGTATGGGAAG
                ************************************************************

Wild            ATTGCGGTCATGGAGCTTTTCAGGCCCAAGGGGGAGAGCAAGGACCTGCTGTTTATCTTG
AAA             ATTGCGGTCATGGAGCTTTTCAGGCCCAAGGGGGAGAGCAAGGACCTGCTGTTTATCTTG
                ************************************************************

Wild            ACAGCGAAGTACAATGCCTGCATCCTGGAGTATAAACAGAGTGGCGAGAGCATTGACATC
AAA             ACAGCGAAGTACAATGCCTGCATCCTGGAGTATAAACAGAGTGGCGAGAGCATTGACATC
                ************************************************************

Wild            ATTACGCGAGCCCATGGCAATGTCCAGGACCGCATTGGCCGCCCCCTCAGAGACCGGCATT
AAA             ATTACGCGAGCCCATGGCAATGTCCAGGACCGCATTGGCCGCCCCCTCAGAGACCGGCATT
                ************************************************************

Wild            ATTGGCATCATTGACCCTGAGTGCCGGATGATTGGCCTGCGTCTCTATGATGGCCTTTTC
AAA             ATTGGCATCATTGACCCTGAGTGCCGGATGATTGGCCTGCGTCTCTATGATGGCCTTTTC
                ************************************************************

Wild            AAGGTTATTCCACTAGATCGCGATAATAAAGAACTCAAGGCCTTCAACATCCGCCTGGAG
AAA             AAGGTTATTCCACTAGATCGCGATAATAAAGAACTCAAGGCCTTCAACATCCGCCTGGAG
                ************************************************************

Wild            GAGCTGCATGTCATTGATGTCAAGTTCCTATATGGTTGCCAAGCACCTACTATTTGCTTT
AAA             GAGCTGCATGTCATTGATGTCAAGTTCCTATATGGTTGCCAAGCACCTACTATTTGCTTT
                ************************************************************

Wild            GTCTACCAGGACCCTCAGGGGCGGCACGTAAAAACCTATGAGGTGTCTCTCCGAGAAAAG
AAA             GTCTACCAGGACCCTCAGGGGCGGCACGTAAAAACCTATGAGGTGTCTCTCCGAGAAAAG
                ************************************************************

Wild            GAATTCAATAAGGGCCCTTGGAAACAGGAAAATGTCGAAGCTGAAGCTTCCATGGTGATC
AAA             GAATTCAATAAGGGCCCTTGGAAACAGGAAAATGTCGAAGCTGAAGCTTCCATGGTGATC
                ************************************************************

Wild            GCAGTCCCAGAGCCCTTTGGGGGGGCCATCATCATTGGACAGGAGTCAATCACCTATCAC
AAA             GCAGTCCCAGAGCCCTTTGGGGGGGCCATCATCATTGGACAGGAGTCAATCACCTATCAC
                ************************************************************

Wild            AATGGTGACAAATACCTGGCTATTGCCCCTCCTATCATCAAGCAAAGCACGATTGTGTGC
AAA             AATGGTGACAAATACCTGGCTATTGCCCCTCCTATCATCAAGCAAAGCACGATTGTGTGC
                ************************************************************

Wild            CACAATCGAGTGGACCCTAATGGCTCAAGATACCTGCTGGGAGACATGGAAGGCCGGCTC
AAA             CACAATCGAGTGGACCCTAATGGCTCAAGATACCTGCTGGGAGACATGGAAGGCCGGCTC
                ************************************************************

Wild            TTCATGCTGCTTTTGGAGAAGGAGGAACAGATGGATGGCACCGTCACTCTCAAGGATCTC
AAA             TTCATGCTGCTTTTGGAGAAGGAGGAACAGATGGATGGCACCGTCACTCTCAAGGATCTC
                ************************************************************

Wild            CGTGTAGAACTCCTTGGAGAGACCTCTATTGCTGAGTGCTTGACATACCTTGATAATGGT
AAA             CGTGTAGAACTCCTTGGAGAGACCTCTATTGCTGAGTGCTTGACATACCTTGATAATGGT
                ************************************************************

Wild            GTTGTGTTTGTCGGGTCTCGCCTGGGTGACTCCCAGCTTGTGAAGCTCAACGTTGACAGT
AAA             GTTGTGTTTGTCGGGTCTCGCCTGGGTGACTCCCAGCTTGTGAAGCTCAACGTTGACAGT
                ************************************************************

Wild            AATGAACAAGGCTCCTATGTAGTGGCCATGGAAACCTTTACCAACTTAGGACCCATTGTC
AAA             AATGAACAAGGCTCCTATGTAGTGGCCATGGAAACCTTTACCAACTTAGGACCCATTGTC
                ************************************************************

Wild            GATATGTGCGTGGTGGACCTGGAGAGGCAGGGGCAGGGGCAGCTGGTCACTTGCTCTGGG
AAA             GATATGTGCGTGGTGGACCTGGAGAGGCAGGGGCAGGGGCAGCTGGTCACTTGCTCTGGG
                ************************************************************
```

```
Wild            GCTTTCAAGGAAGGTTCTTTGCGGATCATCCGGAATGGAATTGGAATCCACGAGCATGCC
AAA             GCTTTCAAGGAAGGTTCTTTGCGGATCATCCGGAATGGAATTGGAATCCACGAGCATGCC
                ************************************************************

Wild            AGCATTGACTTACCAGGCATCAAAGGATTATGGCCACTGCGGTCTGACCCTAATCGTGAG
AAA             AGCATTGACTTACCAGGCATCAAAGGATTATGGCCACTGCGGTCTGACCCTAATCGTGAG
                ************************************************************

Wild            ACTGATGACACTTTGGTGCTCTCTTTTGTGGGCCAGACAAGAGTTCTCATGTTAAATGGA
AAA             ACTGATGACACTTTGGTGCTCTCTTTTGTGGGCCAGACAAGAGTTCTCATGTTAAATGGA
                ************************************************************

Wild            GAGGAGGTAGAAGAAACCGAACTGATGGGTTTCGTGGATGATCAGCAGACTTTCTTCTGT
AAA             GAGGAGGTAGAAGAAACCGAACTGATGGGTTTCGTGGATGATCAGCAGACTTTCTTCTGT
                ************************************************************

Wild            GGCAACGTGGCTCATCAGCAGCTTATCCAGATCACTTCAGCATCGGTGAGGTTGGTCTCT
AAA             GGCAACGTGGCTCATCAGCAGCTTATCCAGATCACTTCAGCATCGGTGAGGTTGGTCTCT
                ************************************************************

Wild            CAAGAACCCAAAGCTCTGGTCAGTGAATGGAAGGAGCCTCAGGCCAAGAACATCAGTGTG
AAA             CAAGAACCCAAAGCTCTGGTCAGTGAATGGAAGGAGCCTCAGGCCAAGAACATCAGTGTG
                ************************************************************

Wild            GCCTCCTGCAATAGCAGCCAGGTGGTGGTGGCTGTAGGCAGGGCCCTCTACTATCTGCAG
AAA             GCCTCCTGCAATAGCAGCCAGGTGGTGGTGGCTGTAGGCAGGGCCCTCTACTATCTGCAG
                ************************************************************

Wild            ATCCATCCTCAGGAGCTCCGGCAGATCAGCCACACAGAGATGGAACATGAAGTGGCTTGC
AAA             ATCCATCCTCAGGAGCTCCGGCAGATCAGCCACACAGAGATGGAACATGAAGTGGCTTGC
                ************************************************************

Wild            TTGGACATCACCCCATTAGGAGACAGCAATGGACTGTCCCCTCTTTGTGCCATTGGCCTC
AAA             TTGGACATCACCCCATTAGGAGACAGCAATGGACTGTCCCCTCTTTGTGCCATTGGCCTC
                ************************************************************

Wild            TGGACGGACATCTCGGCTCGTATCTTGAAGTTGCCCTCTTTTGAACTACTGCACAAGGAG
AAA             TGGACGGACATCTCGGCTCGTATCTTGAAGTTGCCCTCTTTTGAACTACTGCACAAGGAG
                ************************************************************

Wild            ATGCTGGGTGGAGAGATCATTCCTCGCTCCATCCTGATGACCACCTTTGAGAGTAGCCAT
AAA             ATGCTGGGTGGAGAGATCATTCCTCGCTCCATCCTGATGACCACCTTTGAGAGTAGCCAT
                ************************************************************

Wild            TACCTCCTTTGTGCCTTGGGAGATGGAGCGCTTTTCTACTTTGGGCTCAACATTGAGACA
AAA             TACCTCCTTTGTGCCTTGGGAGATGGAGCGCTTTTCTACTTTGGGCTCAACATTGAGACA
                ************************************************************

Wild            GGTCTGTTGAGCGACCGTAAGAAGGTGACTTTGGGCACCCAGCCCACCGTATTGAGGACT
AAA             GGTCTGTTGAGCGACCGTAAGAAGGTGACTTTGGGCACCCAGCCCACCGTATTGAGGACT
                ************************************************************

Wild            TTTCGTTCTCTTTCTACCACCAACGTCTTTGCTTGTTCTGACCGCCCCACTGTCATCTAT
AAA             TTTCGTTCTCTTTCTACCACCAACGTCTTTGCTTGTTCTGACCGCCCCACTGTCATCTAT
                ************************************************************

Wild            AGCAGCAACCACAAATTGGTCTTCTCAAATGTCAACCTCAAGGAAGTGAACTACATGTGT
AAA             AGCAGCAACCACAAATTGGTCTTCTCAAATGTCAACCTCAAGGAAGTGAACTACATGTGT
                ************************************************************

Wild            CCCCTCAATTCAGATGGCTATCCTGACAGCCTGGCGCTGGCCAACAATAGCACCCTCACC
AAA             CCCCTCAATTCAGATGGCTATCCTGACAGCCTGGCGCTGGCCAACAATAGCACCCTCACC
                ************************************************************

Wild            ATTGGCACCATCGATGAGATCCAGAAGCTGCACATTCGCACAGTTCCCCTCTATGAGTCT
AAA             ATTGGCACCATCGATGAGATCCAGAAGCTGCACATTCGCACAGTTCCCCTCTATGAGTCT
                ************************************************************

Wild            CCAAGGAAGATCTGCTACCAGGAAGTGTCCCAGTGTTTCGGGGTCCTCTCCAGCCGCATT
AAA             CCAAGGAAGATCTGCTACCAGGAAGTGTCCCAGTGTTTCGGGGTCCTCTCCAGCCGCATT
                ************************************************************

Wild            GAAGTCCAAGACACGAGTGGGGGCACGACAGCCTTGAGGCCCAGCGCTAGCACCCAGGCT
AAA             GAAGTCCAAGACACGAGTGGGGGCACGACAGCCTTGAGGCCCAGCGCTAGCACCCAGGCT
                ************************************************************
```

```
Wild            CTGTCCAGCAGTGTAAGCTCCAGCAAGCTGTTCTCCAGCAGCACTGCTCCTCATGAGACC
AAA             CTGTCCAGCAGTGTAAGCTCCAGCAAGCTGTTCTCCAGCAGCACTGCTCCTCATGAGACC
                ************************************************************

Wild            TCCTTTGGAGAAGAGGTGGAGGTGCACAACCTACTTATCATTGACCAACACACCTTTGAA
AAA             TCCTTTGGAGAAGAGGTGGAGGTGCACAACCTACTTATCATTGACCAACACACCTTTGAA
                ************************************************************

Wild            GTGCTTCATGCCCACCAGTTTCTGCAGAATGAATATGCCCTCAGTCTGGTTTCCTGCAAG
AAA             GTGCTTCATGCCCACCAGTTTCTGCAGAATGAATATGCCCTCAGTCTGGTTTCCTGCAAG
                ************************************************************

Wild            CTGGGCAAAGACCCCAACACTTACTTCATTGTGGGCACAGCAATGGTGTATCCTGAAGAG
AAA             CTGGGCAAAGACCCCAACACTTACTTCATTGTGGGCACAGCAATGGTGTATCCTGAAGAG
                ************************************************************

Wild            GCAGAGCCCAAGCAGGGTCGCATTGTGGTCTTTCAGTATTCGGATGGAAAACTACAGACT
AAA             GCAGAGCCCAAGGCCGGTCGCGCCGTGGTCGCCCAGTATTCGGATGGAAAACTACAGACT
                ************   ******    ******    ****************************

Wild            GTGGCTGAAAAGGAAGTGAAAGGGGCCGTGTACTCTATGGTGGAATTTAACGGGAAGCTG
AAA             GTGGCTGAAAAGGAAGTGAAAGGGGCCGTGTACTCTATGGTGGAATTTAACGGGAAGCTG
                ************************************************************

Wild            TTAGCCAGCATCAATAGCACGGTGCGGCTCTATGAGTGGACAACAGAGAAGGAGCTGCGC
AAA             TTAGCCAGCATCAATAGCACGGTGCGGCTCTATGAGTGGACAACAGAGAAGGAGCTGCGC
                ************************************************************

Wild            ACTGAGTGCAACCACTACAACAACATCATGGCCCTCTACCTGAAGACCAAGGGCGACTTC
AAA             ACTGAGTGCAACCACTACAACAACATCATGGCCCTCTACCTGAAGACCAAGGGCGACTTC
                ************************************************************

Wild            ATCCTGGTGGGCGACCTTATGCGCTCAGTGCTGCTGCTTGCCTACAAGCCCATGGAAGGA
AAA             ATCCTGGTGGGCGACCTTATGCGCTCAGTGCTGCTGCTTGCCTACAAGCCCATGGAAGGA
                ************************************************************

Wild            AACTTTGAAGAGATTGCTCGAGACTTTAATCCCAACTGGATGAGTGCTGTGGAAATCTTG
AAA             AACTTTGAAGAGATTGCTCGAGACTTTAATCCCAACTGGATGAGTGCTGTGGAAATCTTG
                ************************************************************

Wild            GATGATGACAATTTTCTGGGGGCTGAAAATGCCTTTAACTTGTTTGTGTGTCAAAAGGAT
AAA             GATGATGACAATTTTCTGGGGGCTGAAAATGCCTTTAACTTGTTTGTGTGTCAAAAGGAT
                ************************************************************

Wild            AGCGCTGCCACCACTGACGAGGAGCGGCAGCACCTCCAGGAGGTTGGTCTTTTCCACCTG
AAA             AGCGCTGCCACCACTGACGAGGAGCGGCAGCACCTCCAGGAGGTTGGTCTTTTCCACCTG
                ************************************************************

Wild            GGCGAGTTTGTCAATGTCTTTTGCCACGGCTCTCTGGTAATGCAGAATCTGGGTGAGACT
AAA             GGCGAGTTTGTCAATGTCTTTTGCCACGGCTCTCTGGTAATGCAGAATCTGGGTGAGACT
                ************************************************************

Wild            TCCACCCCCACACAAGGCTCGGTGCTCTTCGGCACGGTCAACGGCATGATAGGGCTGGTG
AAA             TCCACCCCCACACAAGGCTCGGTGCTCTTCGGCACGGTCAACGGCATGATAGGGCTGGTG
                ************************************************************

Wild            ACCTCACTGTCAGAGAGCTGGTACAACCTCCTGCTGGACATGCAGAATCGACTCAATAAA
AAA             ACCTCACTGTCAGAGAGCTGGTACAACCTCCTGCTGGACATGCAGAATCGACTCAATAAA
                ************************************************************

Wild            GTCATCAAAAGTGTGGGGAAGATCGAGCACTCCTTCTGGAGATCCTTTCACACCGAGCGG
AAA             GTCATCAAAAGTGTGGGGAAGATCGAGCACTCCTTCTGGAGATCCTTTCACACCGAGCGG
                ************************************************************

Wild            AAGACAGAACCAGCCACAGGTTTCATCGACGGTGACTTGATTGAGAGTTTCCTGGATATT
AAA             AAGACAGAACCAGCCACAGGTTTCATCGACGGTGACTTGATTGAGAGTTTCCTGGATATT
                ************************************************************

Wild            AGCCGCCCCAAGATGCAGGAGGTGGTGGCAAACCTACAGTATGACGATGGCAGCGGTATG
AAA             AGCCGCCCCAAGATGCAGGAGGTGGTGGCAAACCTACAGTATGACGATGGCAGCGGTATG
                ************************************************************

Wild            AAGCGAGAGGCCACTGCAGACGACCTCATCAAGGTTGTGGAGGAGCTAACTCGGATCCAT
AAA             AAGCGAGAGGCCACTGCAGACGACCTCATCAAGGTTGTGGAGGAGCTAACTCGGATCCAT
                ************************************************************

Wild            ---------------------------------TAG
AAA             TCTCCCTACCCATACGATGTTCCAGATTACGCTTAG
                                                  ***
```

Figure 5: Nucleotide sequence alignment of DDB1^{Wt} and DDB1^{AAA}-HA

4.9.2 pcDNA™3.1/myc-His DDB1^{AAA}-HA cloning

pUC57 DDB1^{AAA}-HA vector was linearized by Not I restriction enzyme (Takara) at 37°C for 16 hours following the protocol reported in **Table 24.**

Reagents	Quantity (µl)
10X H Buffer	5
BSA	5
Triton X-100	5
Not I (10 U/µl)	2
pUC57-DDB1^{AAA}-HA	5
dd H_2O	28

Table 24: pUC57 DDB1^{AAA}-HA vector linearization

Linearized plasmid was loaded on a 1% agarose gel (**Table 25**) and the electrophoresis was performed in 1X TBE buffer (**Table 26**).

Reagents	Quantity
Agarose powder	0.6 g
1X TBE	60 ml
Ethidium bromide (10 mg/ml)	1.75 µl

Table 25: Agarose gel composition

Components	Quantity
0.9 M Tris-base	109 g/l
0.9 M Boric acid	56 g/l
20 mM EDTA	5.8 g/l

Table 26: 10X TBE buffer pH 8

The gel slide corresponding to the linearized plasmid was excited and purified trough QIAquick® Gel Extraction kit (Quiagen) following the manufacturer's instructions.

DDB1^{AAA}-HA gene was extract from the pUC57 vector by Kpn I

restriction enzymes (Takara) at 37°C for 16 hours following the protocol reported in **Table 27**.

Reagents	Quantity (µl)
10X L Buffer	5
Kpn I (10 U/µl)	2
pUC57-DDB1^{AAA}-HA/Not I	28
dd H_2O	15

Table 27: DDB1^{AAA}-HA gene extraction

DDB1^{AAA}-HA gene (3460 bp) was extracted, as previously described, and collected for the subsequent cloning experiments.

Also pcDNA™3.1/*myc*-His A (Invitrogen) and pET45b(+) (Novagen) vectors were digested with Kpn I and Not I; but, this two steps protocol caused a total plasmid degradation, making impossible the gel extraction after the second digestion. For this reason, a single step digestion was performed (**Table 28** and **29**) incubating the reaction at 37°C for 16 hours.

Reagents	Quantity (µl)
pcDNA™3.1/*myc*-His A (2,3 µg/µl)	3
10X Buffer K	2.5
BSA	5
Not I (10 U/µl)	1
Kpn I (10 U/µl)	1
dd H_2O	40.5

Table 28: Single step digestion of pcDNA™3.1/myc-His A

Reagents	Quantity (µl)
pET45b(+) (2,9 µg/µl)	3
10X Buffer K	2.5
BSA	5
Not I (10 U/µl)	1
Kpn I (10 U/µl)	1
dd H_2O	40.5

Table 29: Single step digestion of pET45b(+)

To transiently transfect cells, DDB1^{AAA}-HA gene was cloned into pcDNA™3.1/*myc*-His A (Invitrogen) (**Figure 6**) with DNA Ligation Kit, Mighty mix (Takara) at 25°C for 5 minutes, following the protocol in **Table 30**.

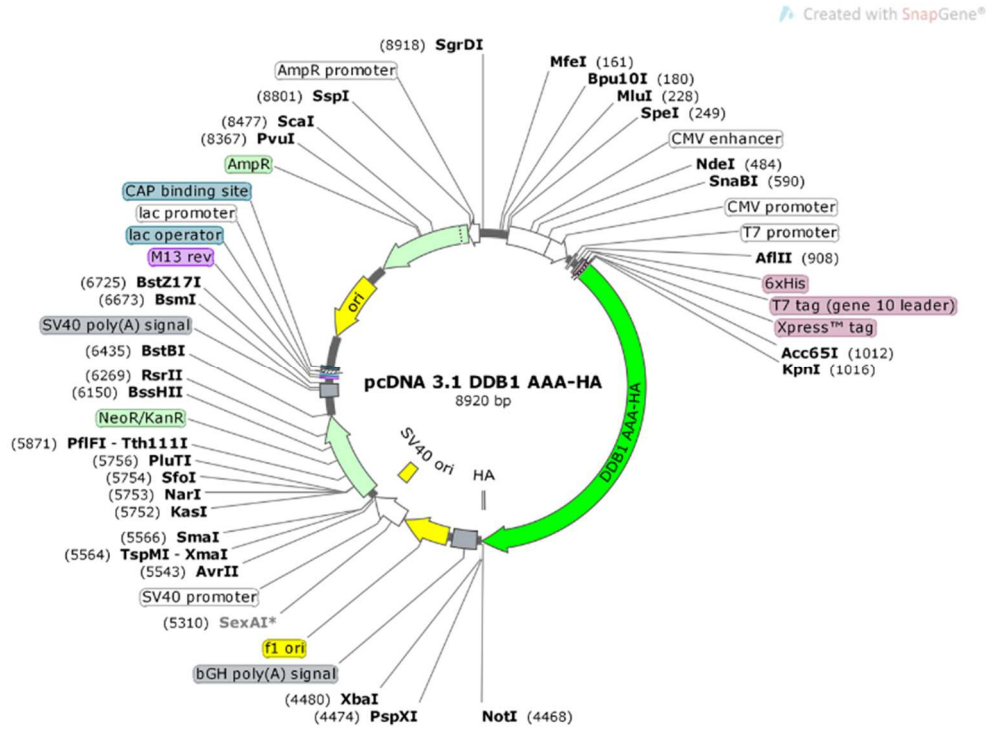

Figure 6: pcDNA™ 3.1/*myc*-His A DDB1^{AAA}-HA vector map

Reagents	Quantity (µl)
DDB1^{AAA}-HA	1.2
pcDNA™3.1/*myc*-His A Not I/Kpn I	4
2X Mighty Mix	5
Total volume	10

Table 30: Ligation protocol; ratio insert / vector 2:1.

5 µl of ligation reaction was used to transform 50 µl of One Shot® TOP10 competent cells (Invitrogen), following the specific heat-shock protocol. Competent cells were mixed by inverting with the ligation solution and incubated 30 minutes on ice. TOP10 were put into a water bath heater at 42°C for 30 seconds and then other 2 minutes on ice. 250 µl of pre-warmed S.O.C. medium was added to the cells and shaken at 225 rpm in a shaking incubator for 1 hour at 37°C. The entire culture was plated in a Tryptic Soy Agar plate (**Table 31**), selective for Ampicillin resistant bacteria, and incubated overnight at 37°C.

Components	Quantity (g/l)
Pancreatic Digest of Casein	15
Peptic digest of Soybean Meal	5
Sodium Chloride	5
Agar	15

Table 31: TSA composition

The day after, many colonies were grown and 16 colonies were pricked and let grow in a 96-well plate for 3 hours. 100 µl of each colony were inoculated in 5 ml of selective 2xYT medium and let grow overnight at 37°C in a shacking incubator at 225 rpm. 2 ml of each pre-culture were pelleted at 15500 rcf (Microfuge 18 centrifuge, Beckman Coulter), for 1 minute to isolate the plasmids by GenElute™ Plasmid Miniprep kit (Sigma) following the manufacturer's instructions. To exactly verify the construct dimension, two DNA plasmids were linearized by Kpn I at 37°C for 16 hours and then loaded on an agarose gel. To purify in a higher scale the pcDNA™3.1/myc-His DDB1^{AAA}-HA, the QUIAGEN DNA plasmid purification protocol (MIDI) was

employed following the manufacturer's instructions. The DNA was quantified at 260 nm (BMG LABTECH, Polar Star Omega) 0,97 µg/µl; the purity was also verified 1, 88 (260 nm/ 280 nm).

4.9.3 Cell transfection and co-transfection

HeLa cells were seeded at a density of $12x10^4$ on coverslip put into a 35x10 mm cultured in standard conditions; when cells arrived at 70% of confluence, they were transfected or co-transfected (**Table 32**) following the experimental procedure reported in paragraph **4.7**

Petri dishes (mm)	Plasmid DNA (µg)	EC Buffer	Enhancer	Effectene	Volume of medium to add to cells (µl)	Volume of medium to add to mix (µl)
35x10	0.4 or 0.2	100	3.2	10	1500	400

Table 32: Transfection reagent mixture

HeLa cells were transfected with pcDNA3-HA2-$DDB1^{Wt}$ or with pcDNA™ 3.1/myc-His $DDB1^{AAA}$-HA testing the optimal quantity of DNA for each sample (0.4 µg or 0.2 µg).

After 24 hours of transfection, cells were damaged with UV-C (10 J/m^2) and fixed 30 minutes after irradiation.

4.9.4 Immunofluorescence analysis

Once coverslips with transfected HeLa cells were fixed, they were washed three times with PBS 1X and then incubated 30 minutes with a Blocking Solution (1% BSA in PBT); then, they were incubated for 1 hour at RT with anti-HA antibody (1:100, Biosensis). After three washes in PBT buffer, the coverslips were incubated with anti-rabbit DyLight™ 488-conjugated (1:100, KPL) for 30 minutes, then they were washed again with

PBT and incubated with Hoechst 33258 dye (0.5 µg/ml) for 10 minutes at RT. Coverslips were mounted in Mowiol and images of fixed nuclei were taken with a Nikon Eclipse E400 fluorescence microscope equipped with a Canon Power Shot A590 IS digital camera.

4.9.5 pET45b(+) DDB1^{AAA}-HA cloning

To induce the production and purification of recombinant protein in *E.Coli*, the DDB1^{AAA}-HA gene was cloned into pET45b(+) vector (Novagen) (**Figure 7**).

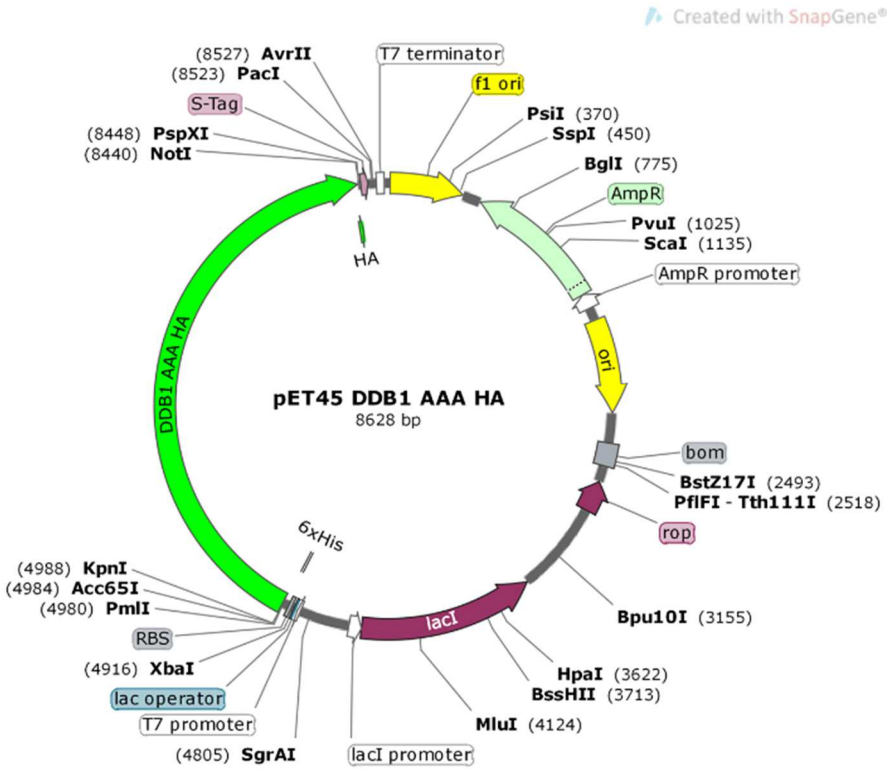

Figure 7: pET45b(+) DDB1^{AAA}-HA vector map

The experimental procedure to clone DDB1^{AAA}-HA gene into pET45b(+) vector was the same followed for the pcDNA3.1/*myc*-His A DDB1^{AAA}-HA,

previously reported in detail (paragraph **4.9.2**). The only difference was in the transformation protocol, in which BL21 ultracompetent cells were employed. 10 µl of ligation reaction were incubate 20 minutes on ice with 50 µl of BL21 competent cells. BL21 were put into a water bath heater at 42°C for 45 seconds and then other 5 minutes on ice. 150 µl of pre-warmed 2xYT medium were added to the cells and incubated at 225 rpm in shaking for 1 hour at 37°C. The entire culture was plated in a Tryptic Soy Agar plate, selective for Ampicillin resistant bacteria, and incubated overnight at 37°C.

4.9.6 Recombinant proteins purification

BL21 pET45b(+) DDB1^{AAA}-HA were growth in 10 ml selective 2xYT broth (Ampicillin 50 µg/ml) overnight; then were inoculated in 1 l monitoring the Optical Density (OD) until a final OD (A_{600} = 0.6) was obtained. Isopropyl β-D-1-thiogalactopyranoside (IPTG, 1 mM) was added to the bacterial culture for 5 hours at 25 °C, then bacteria were harvest by centrifuging at 11000 rcf (Beckman Avanti™ J-25 Centrifuge) for 12 minutes at 4°C and stored at -80°C overnight. The bacterial pellet was resuspended in 50 ml of 1X PBS with 10 mM imidazole and sonicated at 80-90% (Omni Sonic Ruptor 400) for 2 minutes, repeating it for 5 cycles. The bacterial lysate was harvest by centrifuging at 24000 rcf (Beckman Avanti™ J-25 Centrifuge) for 20 minutes at 4°C and the supernatant were centrifuged again at 40000 rcf (Beckman Avanti™ J-25 Centrifuge) for 45 minutes. The supernatant was filtered by a porous membrane (0.22 nm) and purified through nickel affinity method by a Fast Protein Liquid Chromatography. The recombinant DDB1^{AAA}-HA protein was eluted with an increasing concentration of Imidazole from 50 mM to 500 mM. 20 µl of flow through and elution samples were loaded on a 10% polyacrylamide gel to perform a Coomassie blue staining or a Western blot analysis (see paragraph **4.6.1**) with the antibodies reported in **Table 33**.

Antibodies	Dilution
Ab_I anti-DDB1 (GeneTex)	1:2000
Ab_I anti-HA (Biosensis)	1:1000
Ab_{II} anti-rabbit HRP (KPL)	1:10000

Table 33: Antibodies employed in Western blot analysis

Eluted protein was concentrated by Amicon ultra centrifugal filters units (Millipore MWCO 30 kDa) and loaded on a 10% polyacrylamide gel to perform a Coomassie blue staining. The concentrated protein was quantified by Pierce™ BCA protein Assay Kit (Thermo Scientific).

4.9.7 Coomassie blue staining

After electrophoresis, polyacrylamide gel was incubated in a staining solution (**Table 34**) for 4 hours with shaking.

Reagents	Quantity
Coomassie Brillant Blue R250	0.25 g
Glacial acetic acid	10 ml
MeOH:H_2O (1:1 v/v)	90 ml

Table 34: Coomassie staining solution

Staining solution was removed and the gel was incubated in a destaining solution (**Table 35**), changed every 30 minutes.

Reagents	Quantity
Glacial acid acetic	10%
MeOH	30%
H_2O	60%

Table 35: Coomassie destaining solution

Once gel was de-coloured, it was transferred to water and scanned.

4.9.8 *In vitro* pull-down assay

Equimolar concentrations of $DDB1^{Wt}$-GST (Abnova) or $DDB1^{AAA}$-HA were incubated with $PCNA^{Wt}$-His in 40 µl of Binding Buffer (**Table 36**) for 1 hour at 4°C.

Reagents	Quantity
Tris-HCl buffer pH 8.0	50 mM
$MgCl_2$	2.5 mM
KCl	75 mM
Glycerol	10%
DTT	1 mM
NaCl	150 mM
ImOH	10 mM
PMSF	0.2 mM

Table 36: Binding Buffer

20 µl of Protein G coupled to magnetic beads (Dynabeads, Life Technologies) were pre-incubated with 1 µg of anti-PCNA (Dako) antibody for 1 hour at 4 °C and added to each sample. Magnetic beads and recombinant proteins were kept under agitation for 2 hours, washed with a Washing buffer (**Table 37**) and eluted by 30 µl SDS-denaturing buffer. The interactions between $DDB1^{Wt}$-GST or $DDB1^{AAA}$-HA and $PCNA^{Wt}$-His were analyzed by Western blot.

Reagents	Quantity
Tris-HCl buffer pH 8.0	50 mM
$MgCl_2$	2.5 mM
KCl	75 mM
Glycerol	10%
DTT	1 mM
NaCl	300 mM
ImOH	20 mM
PMSF	0.2 mM

Table 37: Washing Buffer

Recombinant DDB1 proteins were revealed by anti-DDB1 (**Table 33**) and anti-PCNA (**Table 38**) antibodies.

Antibodies	Dilution
Ab_I anti-PCNA (Dako)	1:1000
Ab_{II} anti-mouse HRP (Sigma)	1:20000

Table 38: Antibodies employed in Western blot analysis

4.10 Statistical analysis

Results are expressed as mean ± standard deviation. Statistical significance was calculated using the Student *t*-test.

5. Results

5.1 HeLa and HaCaT synchronization

HaCaT cells (spontaneously immortalized human keratinocytes) and HeLa (cervical cancer cell line) were used as experimental models to set up the human *in vitro* cell-free repair assay. Three-days serum starved cells were synchronized in G_1-phase through a 24 hours treatment with L-Mimosine. A bi-parametric analysis of cells immuno-stained with BrdU antibody (measuring DNA synthesis) and Propidium iodide (PI, for the DNA content), was performed by flow cytometry (Partec Pass II/Attune NxT, ThermoFisher). Both cell lines were efficiently synchronised (**Figure 1**), although a better clustering in G_1-phase was detected in HaCaT samples compared with HeLa cells.

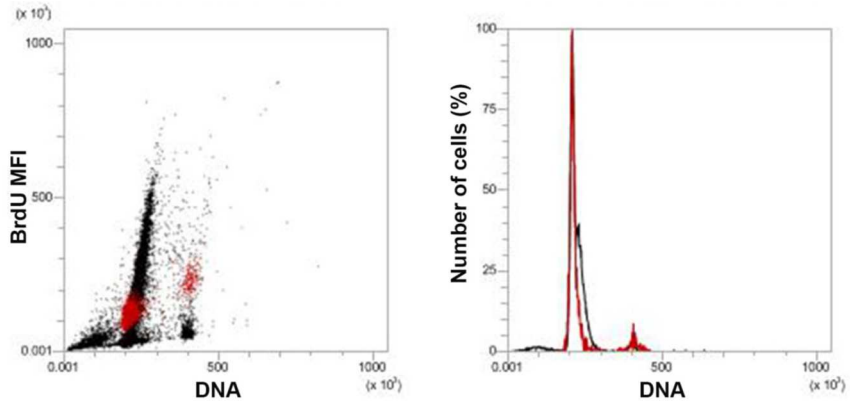

Figure 1: Cell cycle synchronization as evaluated by BrdU incorporation (20 µM) in HeLa (black dots) and HaCaT (red dots) cells for 1 hour before cell fixation (right panel) and the classical DNA profile (black for HeLa and red for HaCaT cells) as obtained by PI staining (left panel).

To obtain a homogeneous G_1-synchronised population of nuclei with the corresponding cytosolic extracts for the *in vitro* cell-free experiments, control cells and cells irradiated with UV-C to activate NER pathway were immediately processed after irradiation, as described in the paragraph **4.2**.

5.2 *In vitro* DNA repair assay in HeLa and HaCaT isolated nuclei

Firstly, we investigated whether G_1 nuclei, isolated from control and UV-C irradiated HaCaT and HeLa cells, may neo-synthetize DNA by detection of dUTPs incorporation. Incubation of HaCaT nuclei from control or irradiated cells in the corresponding cytosolic extracts highlighted a difference between DNA replication pattern, observed only in control nuclei, and a repair pattern detected in UV-C irradiated nuclei (Figure 2A). Scoring by fluorescence microscopy, 9% of DNA replication synthesis was found in control nuclei, whereas 94% of DNA repair synthesis characterized UV-C irradiated sample (**Figure 2B**); similarly, HeLa nuclei from control or irradiated cells showed about 23% and 84% dUTPs incorporation *in vitro,* respectively (**Figure 3**).

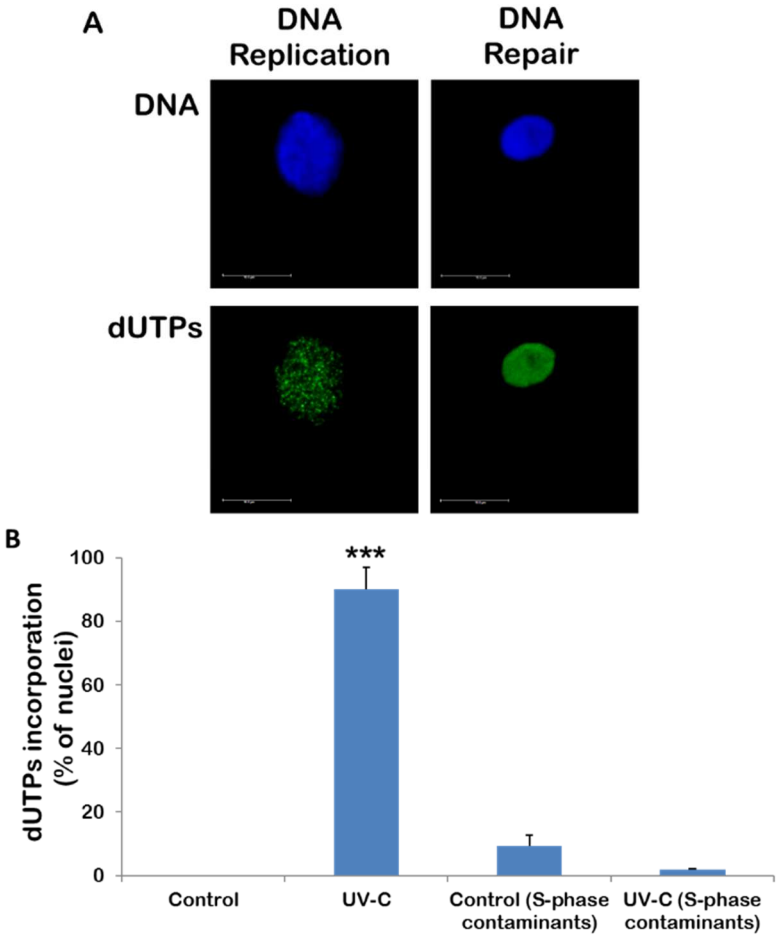

Figure 2: dUTPs *in vitro* incorporation in nuclei isolated from irradiated (UVC) and not (Control) HaCaT cells. A) Representative images of *in vitro* DNA neo-synthesis after 2 hours of incubation in standard conditions as visualized by streptavidin Alexa Fluor dye 488 (dUTPs, green) and Hoechst 33258 dye (DNA, blue). B) Visual scoring of nuclei for DNA replicative and repair synthesis, expressed as positive percentage (% of nuclei). Student's *t*-test ***p<0.001 versus control samples.

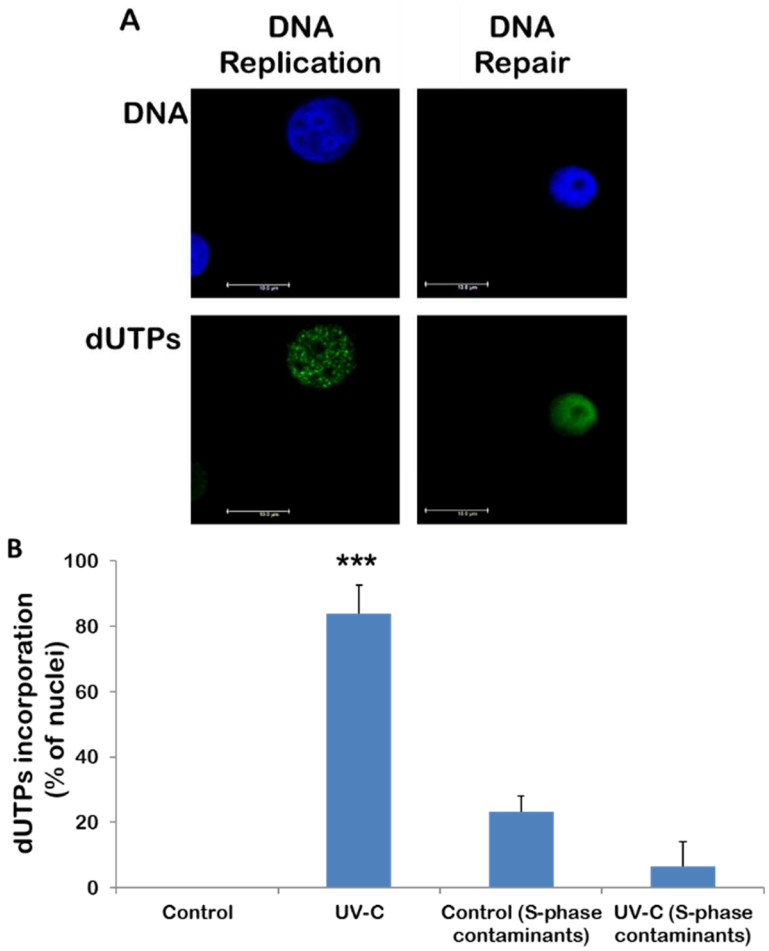

Figure 3: dUTPs *in vitro* incorporation in nuclei isolated from irradiated (UVC) and not (Control) HeLa cells. A) Representative images of *in vitro* DNA neo-synthesis after 2 hours of incubation in standard conditions as visualized by streptavidin Alexa Fluor dye 488 (dUTPs, green) and Hoechst 33258 dye (DNA, blue). B) Visual scoring of nuclei for DNA replicative and repair synthesis, expressed as positive percentage (% of nuclei). Student's *t*-test ***p<0.001 versus control samples.

To check that DNA repair synthesis really initiates *in vitro* (and not in cells) and to further distinguish it from DNA replication, cells were incubated with BrdU, added directly in the culture medium 1 hour before nuclei isolation; the cells escaped from L-Mimosine synchronization continue their cell cycle and incorporate BrdU during the S-phase. Performing the *in vitro* cell-free assay, S-phase nuclei incorporating dUTPs presented a typical DNA replicative pattern, that is exactly colocalized to that of BrdU staining, confirming the ability of S-phase nuclei to efficiently elongate DNA *in vitro* (**Figure 4**).

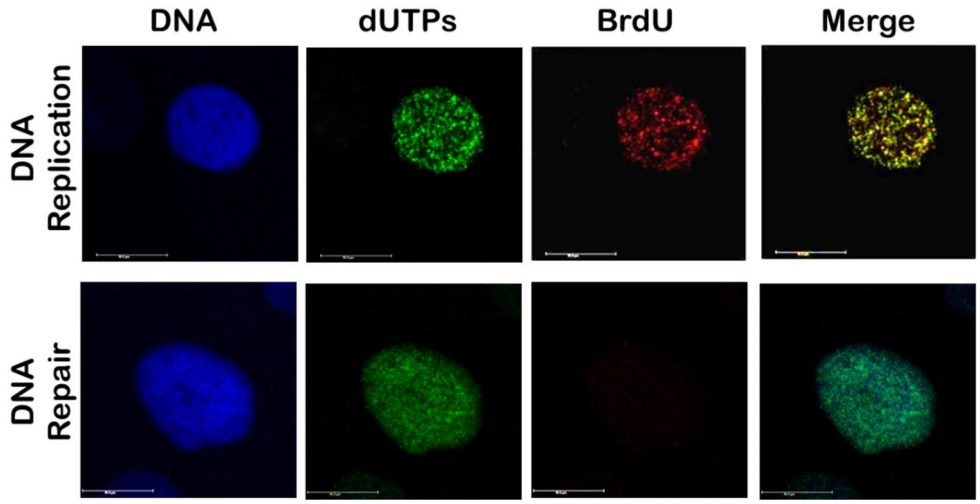

Figure 4: Confocal microscopy images of nuclei after 2 hours of incubation in the cell-free *in vitro* system. BrdU incorporated *in vivo* in HaCaT replicating cells (red fluorescence), dUTPs incorporated *in vitro* in both DNA replicative and repairing synthesis of HaCaT nuclei (green fluorescence) and DNA marked with Hoechst 33258 dye (blue).

In contrast, nuclei positive for DNA repair synthesis were not labelled by BrdU, thus demonstrating that DNA repair efficiently starts *in vitro,* and present a pattern distinct from DNA replicating nuclei. These data allow to consider the *in vitro* cell-free assay a functional method to study not only the complex mechanisms of DNA replication, but also the repair one.

Analyses by flow cytometry confirm the results obtained by fluorescence microscopy, quantifying the mean intensity of dUTPs

fluorescence (MFI), being the MFI significantly higher in the UV-C sample than in the control not irradiated (**Figure 5**).

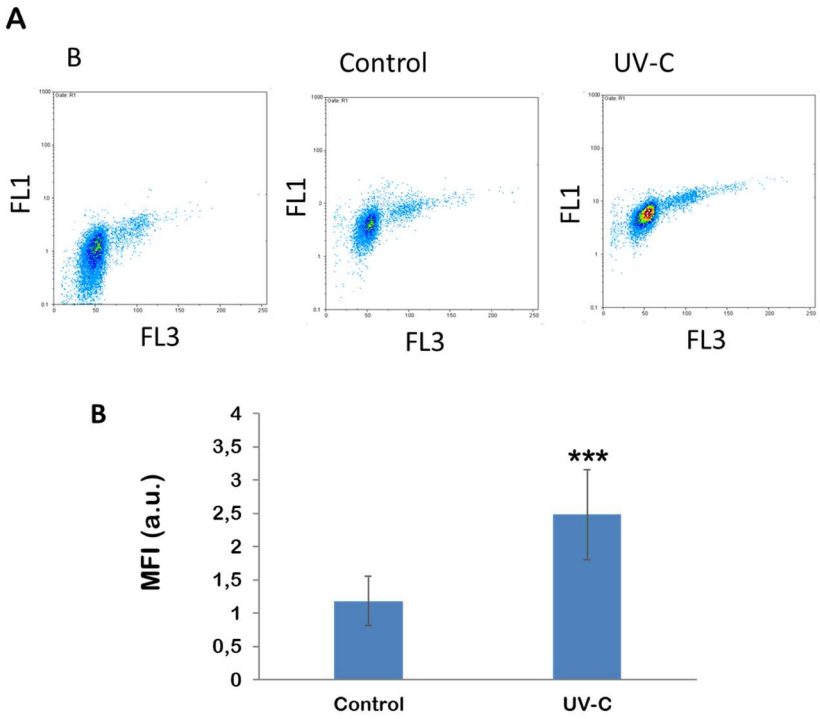

Figure 5: A) Biparametric analysis of DNA repair synthesis *in vitro* by flow cytometry of nuclei marked with streptavidin Alexa Fluor dye 488 (dUTPs, green fluorescence, FL1), and with PI (DNA, red fluorescence, FL3). B) Flow cytometry quantification of DNA repair synthesis expressed as arbitrary units of the mean fluorescence intensity (MFI a.u.). Student's *t*-test ***p<0.001.

5.2.1 Time- and dose-dependent response of *in vitro* DNA repair synthesis in nuclei isolated from UV-C treated HaCaT cells

To verify whether UV-C isolated nuclei trigger DNA repair synthesis in a time-dependent manner, they were incubated with the reagent mix (paragraph **4.3**) and fixed at different time points. At each time point, nuclei showed an evident ability to incorporate dUTPs, as observable by visual

scoring in fluorescence microscopy (**Figure 6A**); however, a different fluorescent signal intensity was detectable in samples and for this reason the quantification analysis by flow cytometry was appropriate (**Figure 6B**). As expected, the incorporation of dUTPs significantly increase with the time, achieving at 2 hours after incubation the highest signal. For this reason, we considered this time point the optimal incubation time for subsequent experiments.

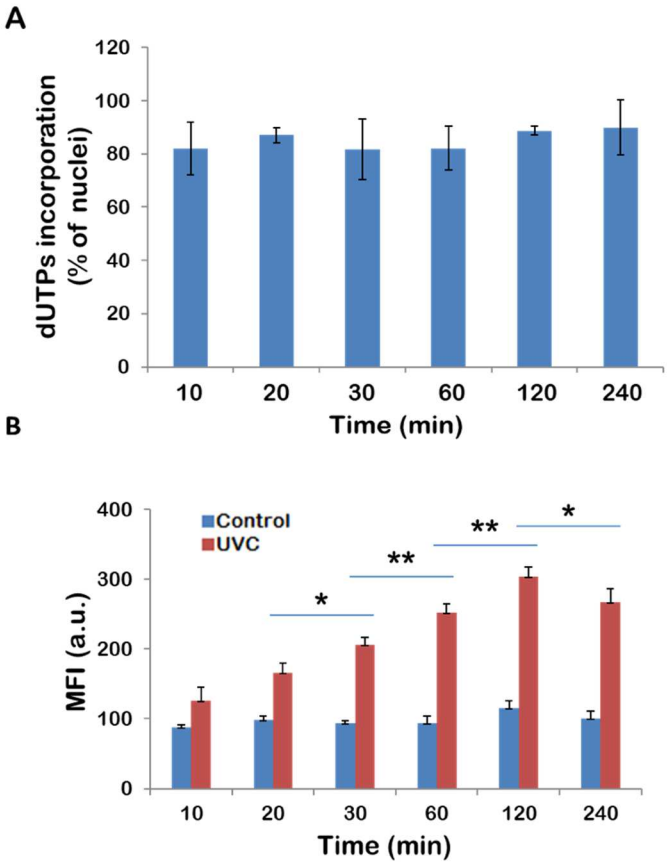

Figure 6: Time-dependent response of *in vitro* DNA repair synthesis in nuclei isolated from UV-C treated HaCaT cells. A) Visual scoring expressed as positive percentage of nuclei incorporating dUTPs (%). B) Flow cytometry quantification of DNA repair synthesis expressed as arbitrary units of the mean fluorescence intensity (MFI a.u.) Student's *t*-test *p<0.05, **p<0.01.

In addition, the dose-dependent response in the *in vitro* DNA repair assay was also analysed in nuclei isolated from HaCaT cells exposed to 10, 20 and 40 J/m^2 of UV-C fixed after 2 hours of incubation. The repair synthesis was clearly detectable already at 10 J/m^2 (**Figure 7A**), in fact, most of nuclei (80-95%) appeared dUTPs-marked positive by visual scoring of the coverslips, but they showed a lower intensity at 10 J/m^2 compared to 40 J/m^2. Quantification of fluorescence by flow cytometry showed a dose-dependent increase of dUTPs incorporation (**Figure 7B**), highlighting a linear regression (R^2 = 0,9631). The highest signal was at 40 J/m^2 and to better highlight the repair activity, this last dose was used in all the next experiments.

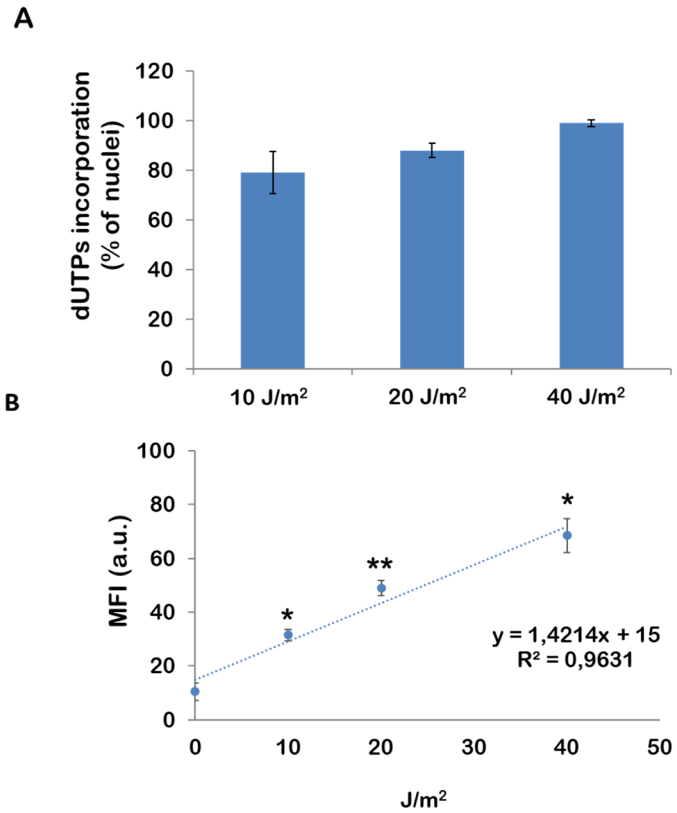

Figure 7: Dose-dependent response of *in vitro* DNA repair synthesis in nuclei isolated from UV-C treated HaCaT cells. A) Visual scoring expressed as positive percentage (%). B) Flow cytometry quantification of DNA repair synthesis expressed as arbitrary units of the mean fluorescence intensity (MFI a.u.) Student's *t*-test *p<0.05, **p<0.01.

5.2.2 *In vitro* DNA repair synthesis specificity in nuclei isolated from UV-C treated HaCaT cells

To check the specificity of this *in vitro* assay, we performed experiments introducing in the system two well-known inhibitors of DNA synthesis: Aph or/and Ara-C. The ability of these molecules to inhibit DNA neo-synthesis activity at damaged site was demonstrated as a decrease in about 30 and 12% of fluorescence intensity when Aph and Ara-C are administered singly, respectively, while their combined used increase the percentage up to 57% (**Figure 8**).

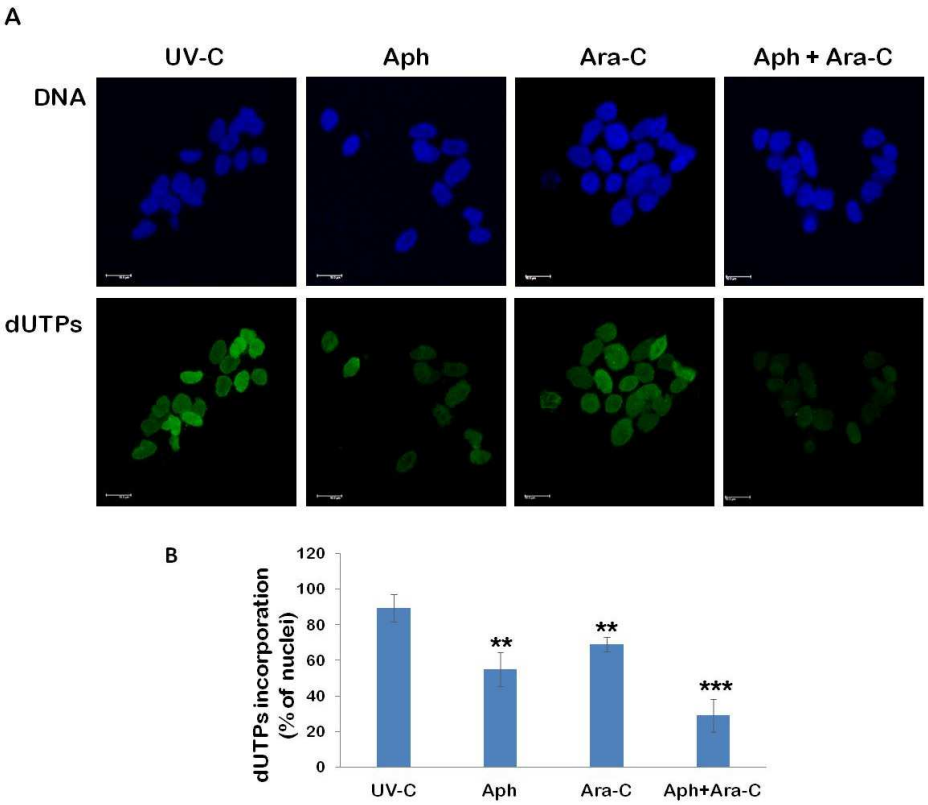

Figure 8: A) Representative images of UV-C nuclei incubated in standard conditions and marked with streptavidin Alexa Fluor dye 488 (dUTPs, green) and Hoechst 33258 dye (DNA, blue). B) Visual scoring of DNA repair synthesis of nuclei expressed as positive percentage (% of nuclei). Student's *t*-test **p<0.001 and ***p<0.001.

These data are also confirmed analysing the images by ImageJ software, quantifying the mean fluorescence intensity and visualising it through 3D plots (**Figure 9**).

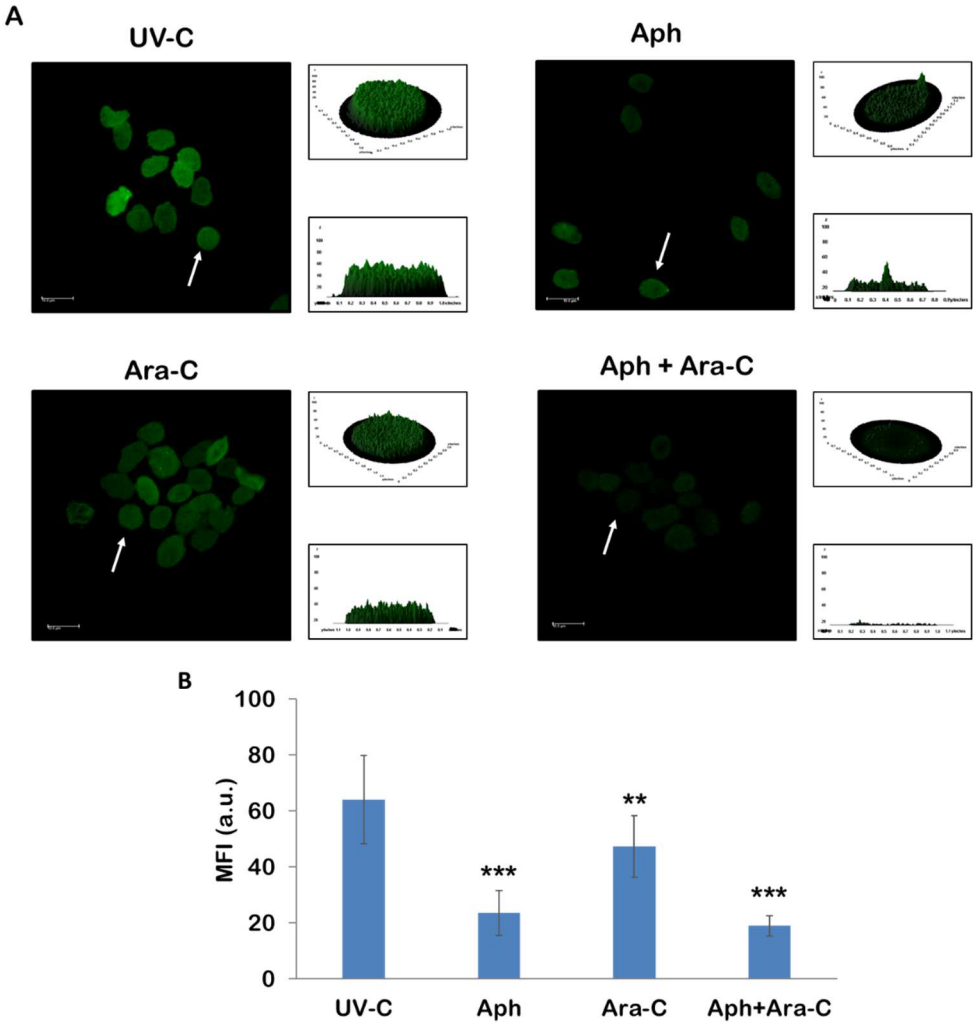

Figure 9: A) 3D plot of a representative UV-C nuclei (indicated with white arrows) incubated with Aph and/or Ara-C and marked with streptavidin Alexa Fluor dye 488 (dUTPs, green). B) ImageJ analysis of repair synthesis expressed as arbitrary units of the mean fluorescence intensity (MFI a.u.). Student's *t*-test **p<0.001 and ***p<0.001 versus UV-C samples.

The quantification of at least 20 nuclei, showed a very similar trend compared with the visual scoring by fluorescence microscope. These results were supported by the MFI signal, as quantified also by flow cytometry experiments; indeed, MFI was further reduced by 70, 39 and 78%, in Aph, or Ara-C, or both treatments, respectively, when compared to UV-C irradiated nuclei (**Figure 10**).

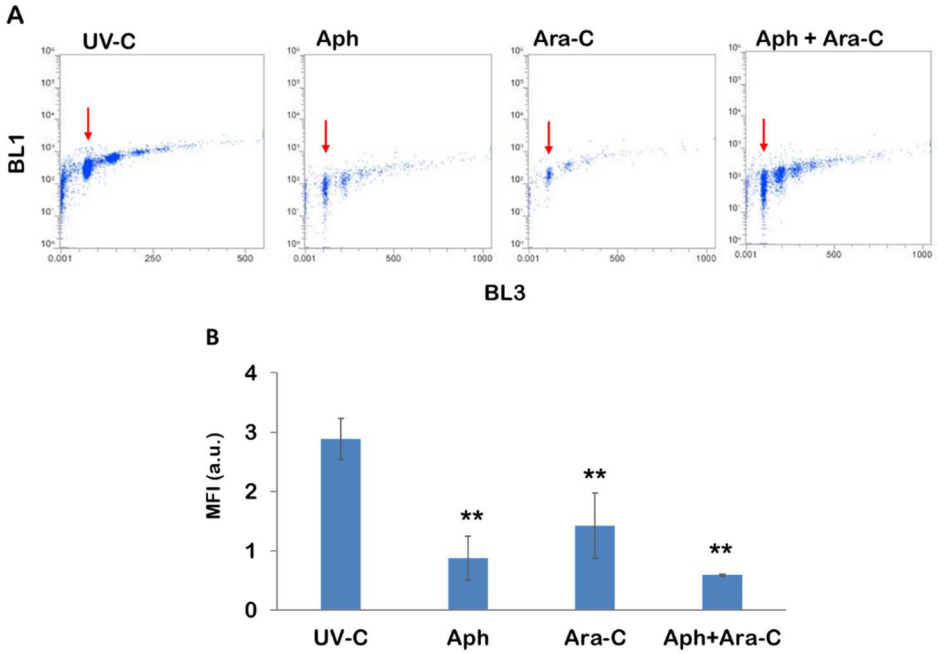

Figure 10: A) Biparametric analysis of DNA repair synthesis by flow cytometry of samples marked with streptavidin Alexa Fluor dye 488 (dUTPs, green fluorescence, FL1) and with PI (DNA, red fluorescence, FL3). B) Flow cytometry quantification of DNA repair synthesis of isolated nuclei in G_1-phase (red arrows) expressed as arbitrary units of the mean fluorescence intensity (MFI a.u.). Student's *t*-test **p<0.01 versus UV-C samples.

5.2.3 *In vitro* DNA repair synthesis in nuclei isolated from XP14BR cells

Another important check very useful to validate the system was to perform the *in vitro* repair assay with nuclei isolated from XP14BR cells (Chavanne F. et al., 2000). This cell line, derived from an XPC patient, is defective for the NER process. Thus, nuclei should be unable to activate DNA repair after UV-C exposure. As expected, XP14BR nuclei incubated in standard condition and analysed by fluorescent microscopy and flow cytometry did not incorporate dUTPs, showing any significant differences compared to control sample (**Figure 11**).

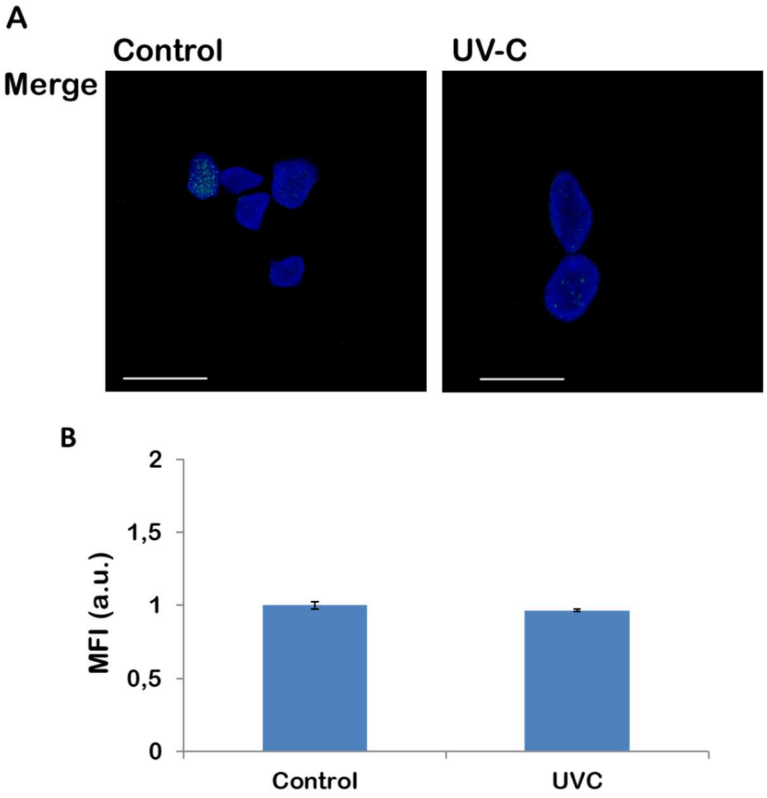

Figure 11: A) Representative images of XP14RB nuclei incubated in standard conditions and marked with streptavidin Alexa Fluor dye 488 (dUTPs, green) and Hoechst 33258 dye (DNA, blue). B) Flow cytometry quantification of DNA repair synthesis expressed as arbitrary units of the mean fluorescence intensity (MFI a.u.).

5.3 Application of *in vitro* DNA repair assay to study different repair mechanisms

To verify the ability of this cell-free system to directly detect the activation of different DNA repair processes, HaCaT cells were exposed to several damaging agents and nuclei were isolated to perform *in vitro* experiments. To this end, cells were exposed to the oxidizing agent $KBrO_3$, the alkylating MNNG, the DNA-cross-linking drug Cis-Pt or the X-irradiation (1 Gy/min). Nuclei were isolated, also, with two different methods, in order to verify the possible role of the cell membrane in the efficiency of DNA repair, being it essential in the active transport of NER cytoplasmic factors into nuclei (**Figure 12**).

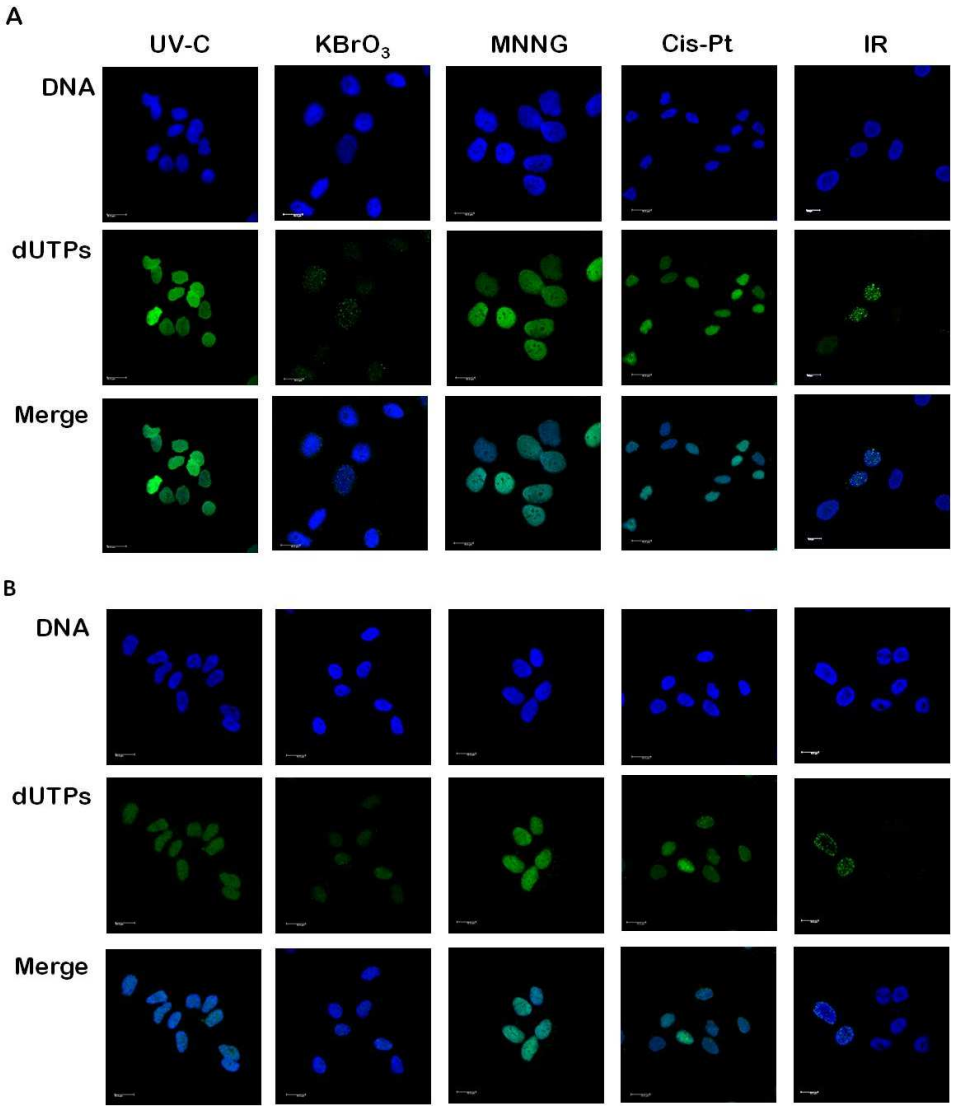

Figure 12: Representative images of nuclei incubated in standard conditions and marked with streptavidin Alexa Fluor dye 488 (dUTPs, green) and Hoechst 33258 dye (DNA, blue). A) Nuclei isolated from treated-HaCaT cell by Dounce homogenizer method; B) Nuclei isolated from treated-HaCaT cells by Digitonin permeabilization method.

Nuclei isolated from cells treated with MNNG and Cis-Pt show a significant and well detectable DNA repair response, in terms of dUTPs

incorporation. Similarly, a marked dUTPs incorporation was induced by X-irradiation, although not all nuclei were responsive (as shown in **Figure 12**); while, nuclei isolated from $KBrO_3$-treated cells, did not show an increased MFI, evaluated by flow cytometer (**Figure 13**), but analysing nuclei by confocal microscopy, many small and weak fluorescent foci appeared distributed in the chromatin of many nuclei (**Figure 14**). No significant differences were detected between nuclei isolated by the two methods regarding their DNA repair ability *in vitro*.

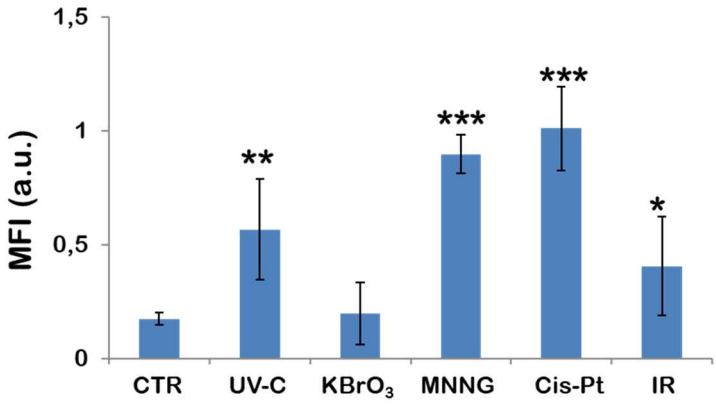

Figure 13: Flow cytometry quantification of DNA repair synthesis in nuclei isolated from HaCaT cells treated with different DNA damaging agents, expressed as arbitrary units of the mean fluorescence intensity (MFI a.u.). Student's *t*-test **p<0.001.

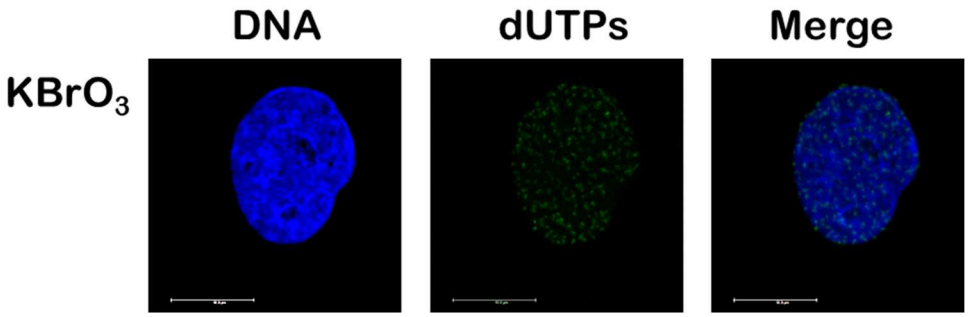

Figure 14: Representative images of a nucleus isolated from HaCaT cells treated with $KBrO_3$ at higher magnification, marked with streptavidin Alexa Fluor dye 488 (dUTPs, green) and Hoechst 33258 dye (DNA, blue).

5.3.1 DNA repair mechanism activation after Ionizing Radiation (IR) damages

The DNA repair response of nuclei isolated from HaCaT cells exposed to X-irradiation showed an increased MFI (BL1), compared with Control and UV-C samples (**Figure 15**), as better comparable in the overlay figure.

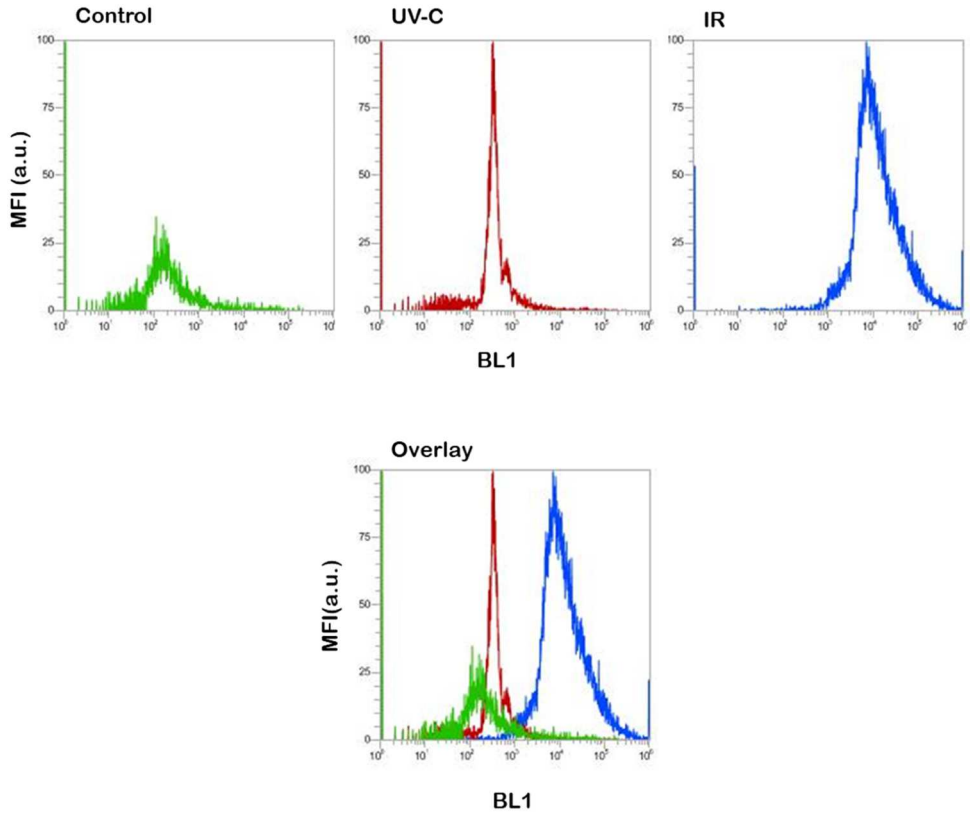

Figure 15: Monoparametric analysis by flow cytometry quantification of DNA repair synthesis expressed as arbitrary units of the mean fluorescence intensity (MFI a.u.); the green profile indicates nuclei isolated from non-treated HaCaT cells; the red one, nuclei isolated from UV-C irradiated HaCaT cells; the blue one, nuclei isolated from IR exposed HaCaT cells.

As previously mentioned, not all nuclei showed a marked DNA repair pattern as in the case of nuclei isolated from MNNG or Cis-Pt treated cells;

for this reason, nuclei isolated from IR-exposed cells, were immediately analysed by Comet assay (**Figure 16**), to verify whether all nuclei were damaged, independently from cryopreservation in liquid nitrogen.

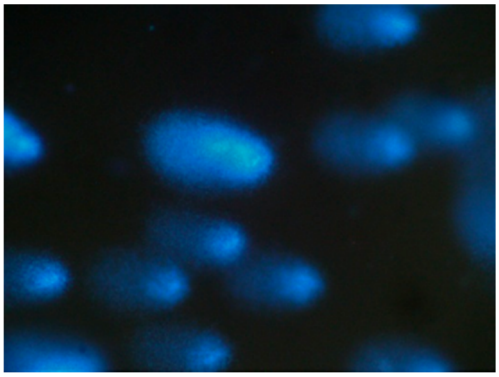

Figure 16: Nuclei isolated from IR-exposed cells analysed by Comet assay and marked by Hoechst 33258 dye (DNA, blue).

Considering that (i) IR can cause mainly single- and double-strand breaks, but also ROS generation, and (ii) nuclei were isolated from G_1-arrested cells, the DNA repair process should be dependent on NHEJ or Al-EJ, although also BER cannot be excluded. Colocalization of dUTPs with XRRC1 (X-ray repair crosscomplementing gene 1) supported the involvement of the BER sub pathways, in which XRCC1 and PARP (poly(ADP-ribose) polymerase) are among the principal players (**Figure 17**).

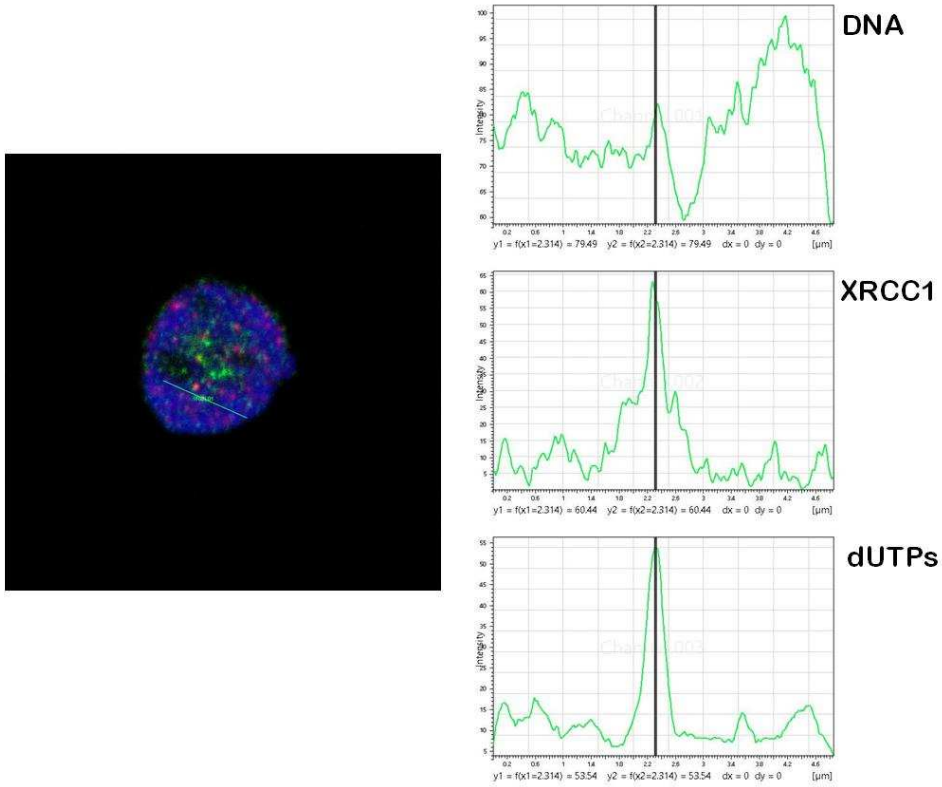

Figure 17: Colocalization of XRCC1 (green) and dUTPs (red) at the damaged DNA sites in a representative image of a nucleus isolated from HaCaT cells exposed to IR (1 Gy/min). DNA was marked with Hoechst 33258 dye (blue).

5.4 *In vitro* study of recombinant NER protein functions

A potential application of this *in vitro* repair system is to study and investigate the regulation of NER mechanism; to this end, human purified recombinant protein PCNA, DDB1 and DDB2 were used. Each protein was incubated with isolated nuclei for 10 minutes before adding the cytosolic extract from UVC-treated cells; only PCNA (400 ng) caused a significant increase in dUTPs incorporation compared to UV-C and UV-C+BSA samples, the last used as negative control. In the presence of DDB2 protein, an increased incorporation of dUTPs was observed, although the experimental

variability observed did not allow to reach a statistical significance (**Figure 18**).

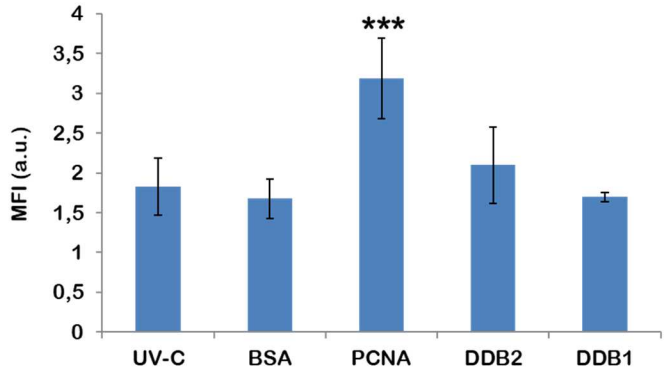

Figure 18: Flow cytometry analysis of UV-C HaCaT nuclei incubated with 400 ng of PCNA-His, 150 ng of DDB2^{Wt}-His, 150 ng of DDB1-His recombinant proteins and 1 µg of BSA as negative control. DNA repair synthesis efficiency was expressed as arbitrary units of the mean fluorescence intensity (MFI a.u.). Student's *t*-test ***p<0.001 versus UV-C samples.

Recently, in our laboratory, was deeply investigated the role of DDB2-PCNA association in DNA repair process, after UV-C irradiation; for this reason, a mutated form of DDB2 unable to correctly interact and bind PCNA was created (DDB2^{PCNA-}) (Cazzalini O. *et a*l., 2014). We explored the possible influence on DNA repair activity of DDB2^{Wt} and DDB2^{PCNA-} recombinant proteins by using this *in vitro* repair system, in nuclei isolated from UV-C irradiated HaCaT cells; as shown in Figure 16, they didn't modify the DNA repair efficiency at the all concentration used (**Figure 19**).

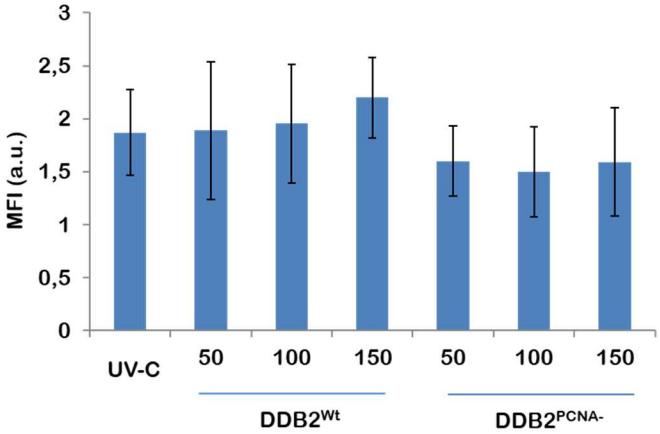

Figure 19: Flow cytometry analysis of UV-C HaCaT nuclei incubated with different concentration (as indicated) of DDB2^{Wt}-His or DDB2^{PCNA-}-His. DNA repair synthesis efficiency was expressed as arbitrary units of the mean fluorescence intensity (MFI a.u.).

To evaluate whether these results were dependent on the competition with the presence of the endogenous protein, Western blot analysis was performed in HaCaT and HeLa cell lines. The results showed a strong difference about the endogenous DDB2 levels, weakly detectable in HeLa nuclei, very abundant in HaCaT nuclei (**Figure 20**). For this reason, HeLa nuclei were chosen as model to further investigate whether DDB2 (wild-type or mutant) influences NER process *in vitro*.

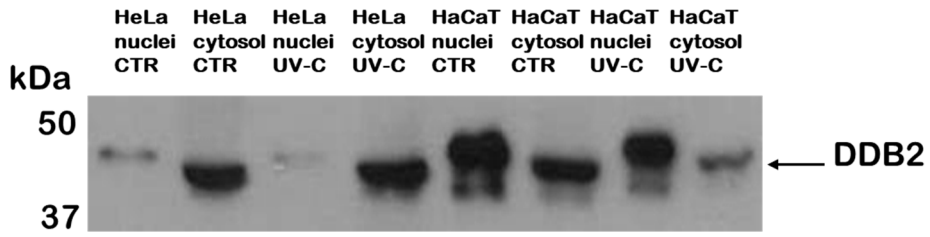

Figure 20: Western blot analysis of DDB2 endogenous levels detected in isolated nuclei and cytosolic extracts of HeLa and HaCaT, Control (CTR) or UV-C irradiated cells.

5.4.1 Study of exogenous recombinant DDB2 on DNA repair efficiency

Nuclei isolated from UV-C irradiated HeLa cells were employed to study the role of $DDB2^{Wt}$-His and $DDB2^{PCNA-}$-His recombinant proteins in the NER process activated *in vitro* in isolated UV-C nuclei. Similarly to HaCaT nuclei, addition of recombinant $DDB2^{Wt}$ protein did not affect DNA repair synthesis. However, a decrease in dUTPs incorporation of about 34% was clearly detectable in the presence of $DDB2^{PCNA-}$ mutant protein (**Figure 21**).

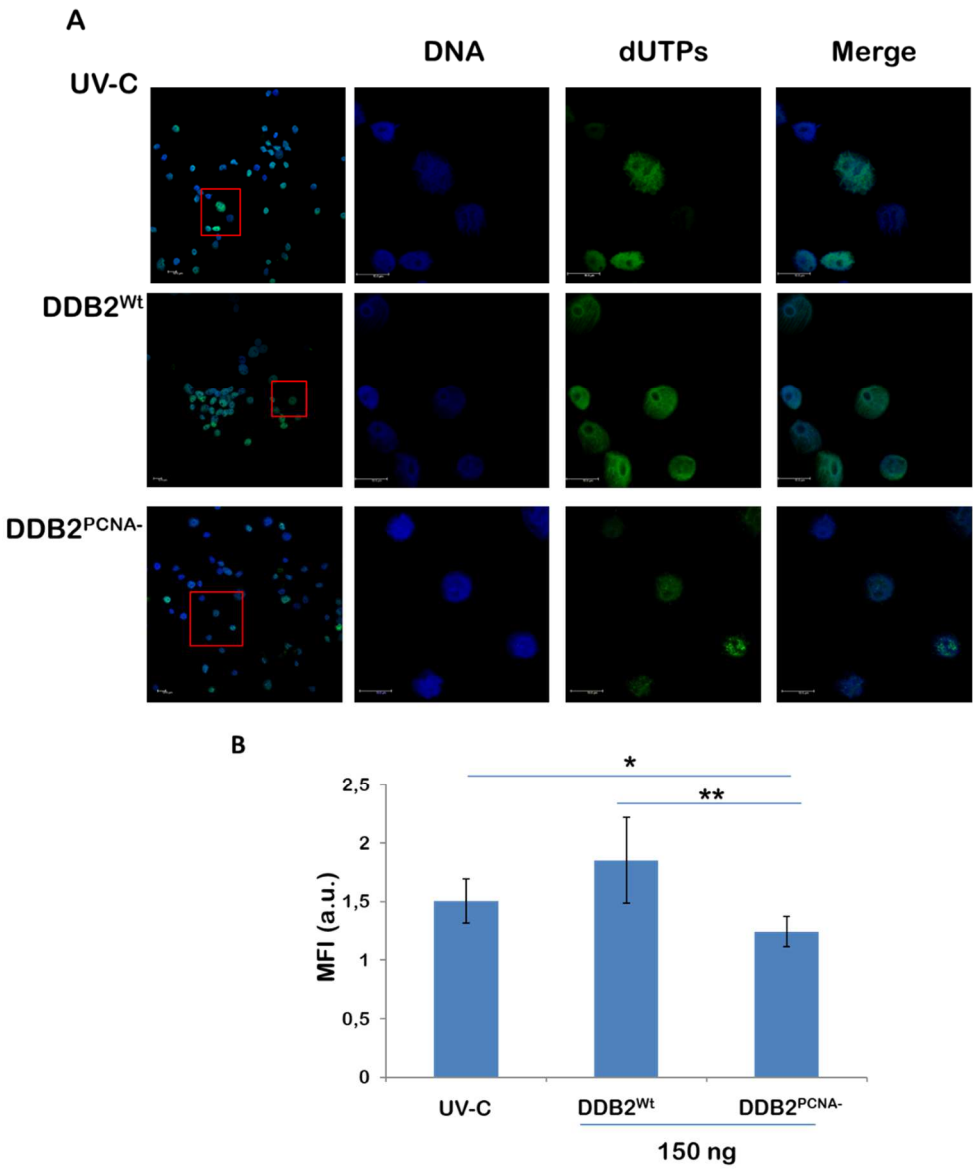

Figure 21: A) Representative images of nuclei isolated from HeLa cells damaged with UV-C incubated with DDB2^{Wt} or DDB2^{PCNA-} proteins, marked with streptavidin Alexa Fluor dye 488 (dUTPs, green) and Hoechst 33258 dye (DNA, blue). B) Flow cytometry quantification of DNA repair synthesis expressed as arbitrary units of the mean fluorescence intensity (MFI a.u.). Student's *t*-test *p<0.05, **p<0.01.

To verify DDB2-chromatin interactions after UV-C damage in the *in vitro* cell-free repair assay, recruitment of the recombinant exogenous proteins DDB2^{Wt}-His and DDB2^{PCNA-}-His to DNA repair foci was also evaluated. Results show that both DDB2 recombinant proteins can move into the nucleus and directly bind the chromatin; while, an extremely weak signal can be detectable in the soluble fraction (**Figure 22**). These experiments demonstrate that DDB2 exogenous protein is recruited *in vitro* on the damaged foci and the mutation occurred in DDB2^{PCNA-} protein does not affect its ability to bind damaged DNA.

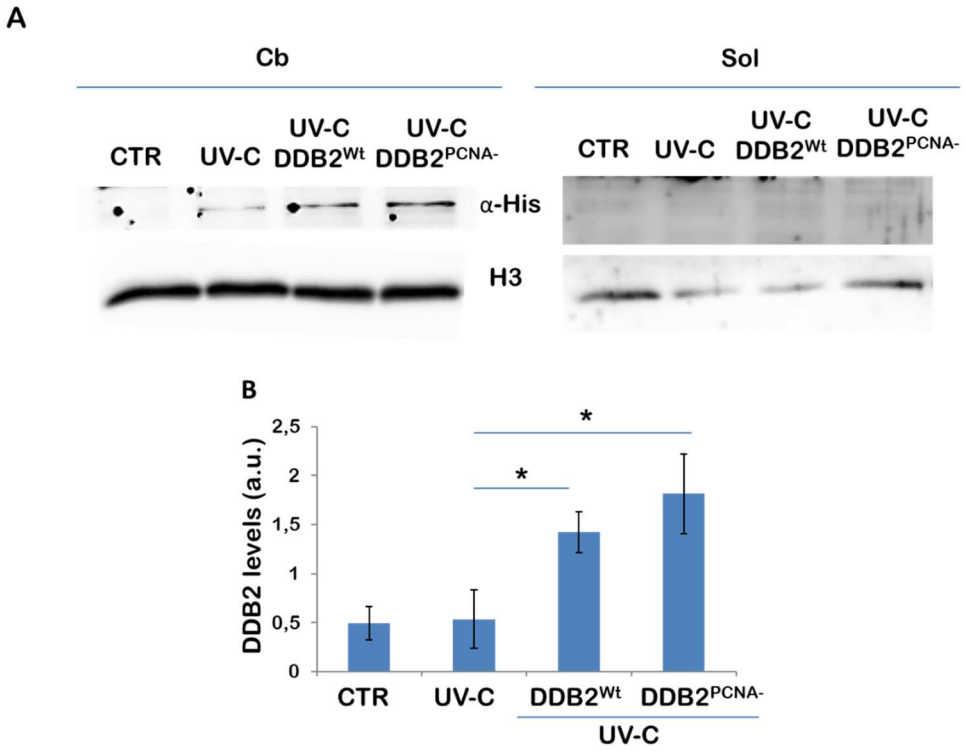

Figure 22: A) Western blot analysis of exogenous DDB2^{Wt}–His or DDB2^{PCNA-}-His proteins in chromatin bound (Cb) and soluble (Sol) fractions after *in vitro* DNA repair assay in nuclei isolated from UV-C irradiated HeLa cells. B) Cb-DDB2 analysis performed by anti-His antibody and quantified by ImageJ software expressed as arbitrary units (a.u.). Student's *t*-test *p<0.05.

5.5 Immunoprecipitation analysis of DDB2 interaction with NER factors in vivo

The interaction of DDB2 with some NER proteins was investigated to understand if DDB2 mutant protein can cause some differences in the DNA repair mechanism. To this end, immunoprecipitation of proteins recruited at DNA damaged sites was performed in HeLa cells transiently transfected with pcDNA3.1-His $DDB2^{Wt}$, kindly provided by Dr Q. Wang (Barakat B.M. *et al*., 2010), or pcDNA3.1-His $DDB2^{PCNA-}$. In **Figure 23**, soluble and chromatin bound fractions derived from irradiated HeLa cells, harvested at 0.5 and 1 hour after UV-C damage, showed the capability of the $DDB2^{PCNA-}$ protein to bind DNA until 1 hour from the irradiation. The association between $DDB2^{PCNA-}$ and DDB1 was already detectable in the chromatin fraction immediately after the irradiation, and it increased with the recovery time after DNA damage (**Figure 23 D**). As expected, no bands of PCNA were detectable in the specific lane, indicating that the protein is not able to immunoprecipitate with mutated DDB2, and confirming that the mutation introduced in the PIP-box of DDB2 is able to prevent the interaction between the two proteins (**Figure 23 D**); however, a very weak PCNA signal was detectable only at 1 hour after DNA damage in the presence of $DDB2^{PCNA-}$ protein. Taken together these results, we hypothesized a possible role of DDB1 as actor to interact and bind PCNA when DDB2 loses this function.

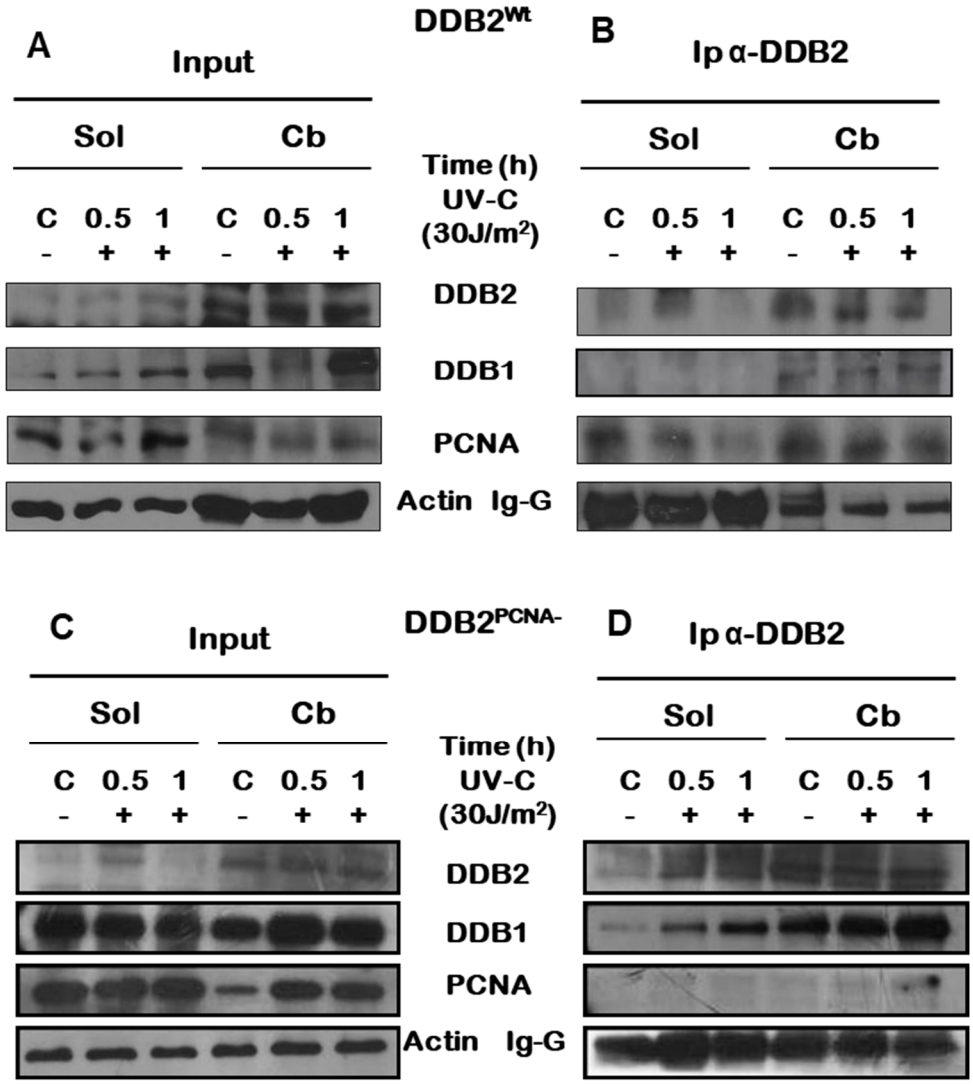

Figure 23: HeLa cells transfected with pcDNA3.1-DDB2^{Wt} (A-B) and pcDNA3.1-DDB2^{PCNA-} (C-D) plasmids were grown for 24 hours and collected 0.5 and 1 hour after UV-C irradiation (30 J/m^2). Cells were fractionated in soluble (Sol) and chromatin-bound (Cb) samples for immunoprecipitation and analysed by Western blot. (A–C) Input load: 1/30 of cell extract. (B–D) Immunoprecipitation (Ip) with anti-DDB2 antibody on fractionated cell extracts, as indicated above.

5.6 Analysis of DDB1-PCNA interaction

5.6.1 Production of pcDNA™3.1/myc-His DDB1^{AAA}-HA and pET45b(+)DDB1^{AAA}-HA plasmids

Analysing the aminoacidic sequence of DDB1 (www.uniprot.org), we have identified a putative PIP-box sequence (845-851). Performing bioinformatics studies (https://hive.biochemistry.gwu.edu/biomuta/proteinview/Q16531), the 845th aminoacid is object of a single nucleotide variant (Q>K). Moreover, this sequence is phylogenetically highly conserved and, in agreement with these findings, we have decided to mutagenize the 845th, 848th and 851st aminoacids with three Alanines (AAA) (**Figure 24**), employing The QuickChange Lightning Multi Site-Directed Mutagenesis kit (Agilent Technologies); unfortunately, no colonies were grown.

845-851 **QGRIVVF**	M. Musculus
845-851 **QGRIVVF**	B. Taurus
845-851 **QGRIVVF**	X. Tropicalis
845-851 **QGRIVVF**	G. Gallus
845-851 **QGRIIVF**	D. Rerio
845- 851 **QGRIVVF**	H. Sapiens
845- 851 **AGRAVVA**	DDB1^{AAA}

Figure 24: Identification and phylogenetic comparison of PIP-box in the DDB1 amino acidic sequence. The sequence is conserved from zebrafish to man.

For this reason, the DDB1^{AAA}-HA gene was synthesised by Genewiz and then isolated through enzymatic digestion (**Figure 25**).

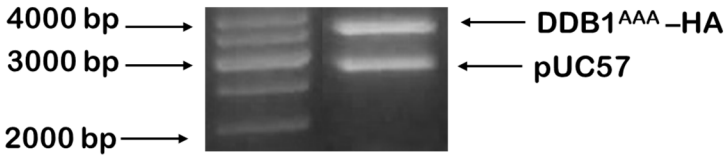

Figure 25: Kpn I/Not I digestion of pUC57 DDB1^{AAA}-HA plasmid.

To transfect cells and to perform *in vitro* assay, DDB1^{AAA}-HA gene was cloned into the pcDNA™3.1/*myc*-His A (Invitrogen) and pET45b(+) (Novagen) vectors and purified (**Figure 26**).

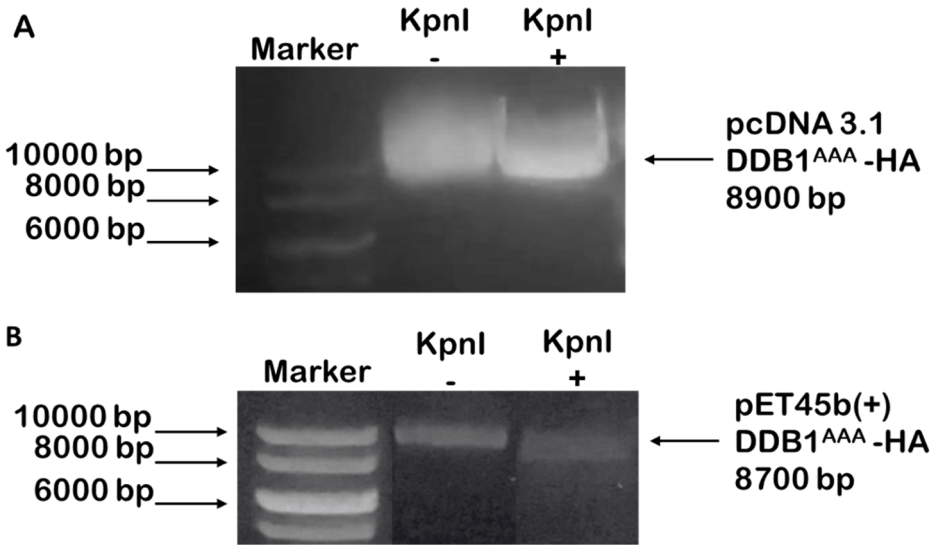

Figure 26: A) Agarose gel electrophoresis of Kpn I -/+ linearized pcDNA3.1 DDB1^{AAA}-HA plasmid; B) Agarose gel electrophoresis of Kpn I -/+ linearized pET45b(+) DDB1^{AAA} -HA plasmid.

5.6.2 Cellular transfection of pcDNA™3.1/myc-His DDB1^{AAA}-HA

To evaluate whether the mutation on DDB1 protein may alter the interaction with DDB2, thus impeding the UV-DDB complex formation and its translocation at nuclear level, HeLa cells were transiently transfected and exposed to UV-C radiation; firstly, we performed preliminary test, transfecting cells with 0.4 µg and 0.2 µg of pcDNA3-HA2-DDB1^{Wt} (DDB1^{Wt}-HA) or pcDNA™ 3.1/myc-His DDB1^{AAA}-HA (DDB1^{AAA}-HA) to find the appropriate not cytotoxic quantity of plasmid DNA able to obtain a proper protein expression level (**Figure 27)**.

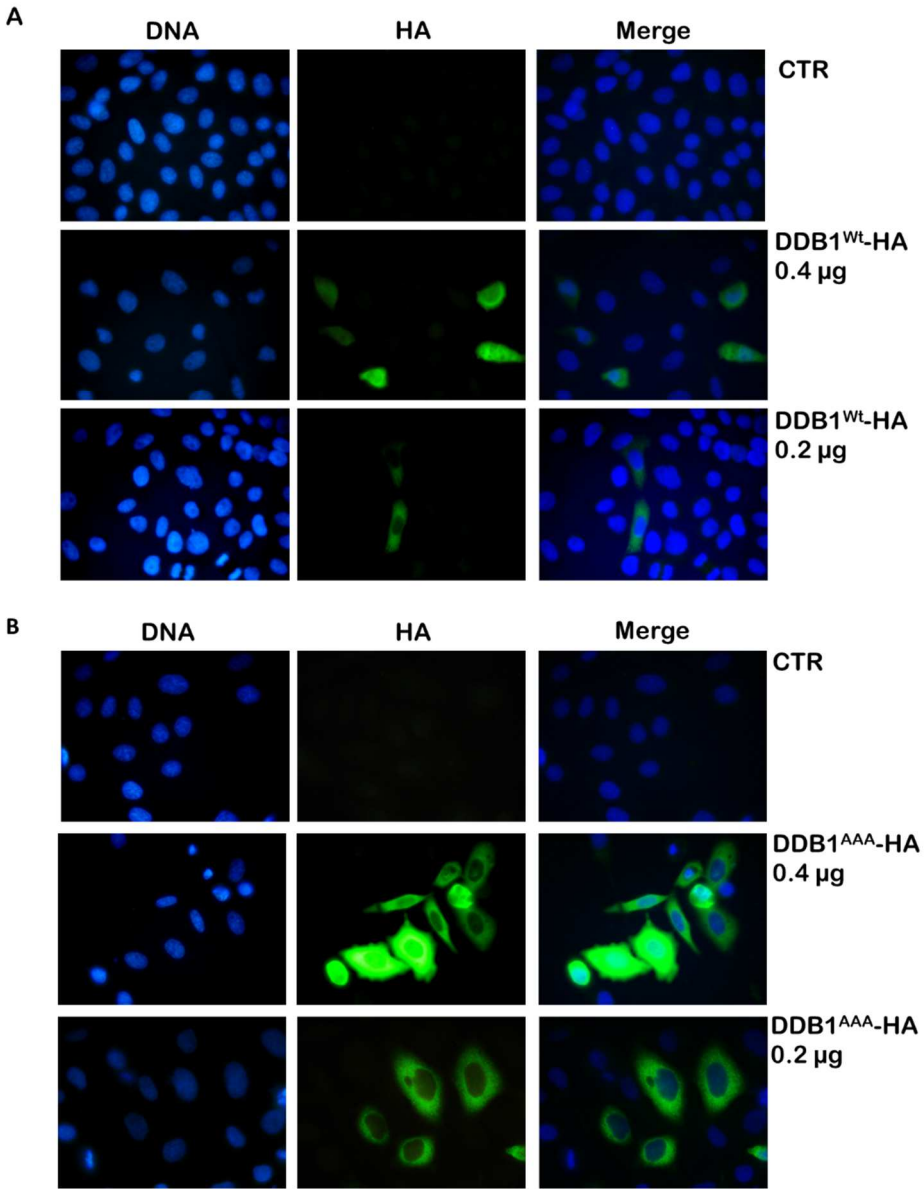

Figure 27: A) representative images of HeLa cells transiently transfected with pcDNA3-HA2-DDB1^{Wt} (DDB1^{Wt}-HA); B) representative images of HeLa cells transfected with pcDNA™ 3.1/myc-His DDB1^{AAA}-HA (DDB1^{AAA}-HA). Cells were marked with antibody anti-HA (rabbit), anti-rabbit DyeLight 488 (green) and Hoechst 33258 dye (DNA, blue).

As highlighted in the **Figure 27**, cells transfected with 0.2 µg DDB1^{Wt}-HA showed a very low protein expression, while 0.4 µg increased the number of cells expressing DDB1^{Wt}-HA without inducing any cell toxicity. On the contrary, 0.4 µg of DDB1^{AAA}-HA caused a too high protein expression with signs of suffering chromatin; for this reason, we decided to reduce the plasmid DNA to 0.2 µg for the subsequent experiments.

To evaluate the ability of DDB1^{AAA} protein to efficiently translocate into the nucleus after DNA damage, transfected cells were irradiated with UV-C at a dose of 10 J/m^2 and fixed after 30 minutes (**Figure 28**).

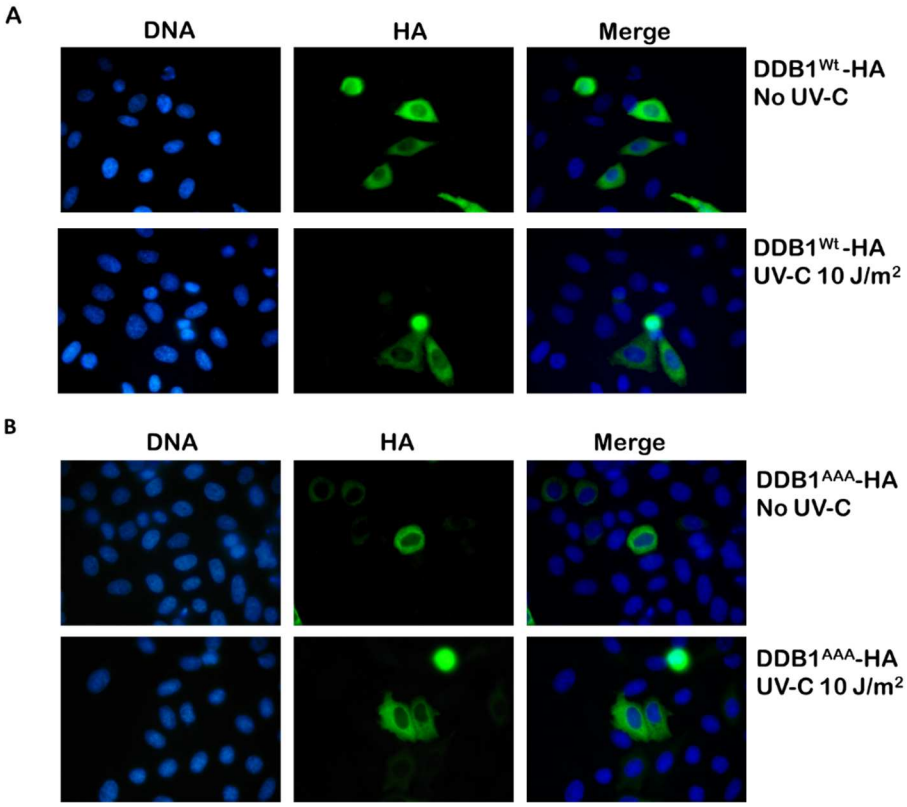

Figure 28: A) representative images of HeLa cells transfected with pcDNA3-HA2-DDB1^{Wt} (DDB1^{Wt}-HA) and exposed to UV-C radiation; B) representative images of HeLa cells transfected with pcDNA™ 3.1/myc-His DDB1^{AAA}-HA (DDB1^{AAA}-HA) and exposed to UV-C radiation. Cells were marked with antibody anti-HA (rabbit), anti-rabbit DyeLight 488 (green) and Hoechst 33258 dye (DNA, blue).

In both DDB1^{Wt} or DDB1^{AAA} transfected cells, preliminary results show that only in a very small percentage DDB1 localized at nuclear level after UV-C damage (**Figure 29**).

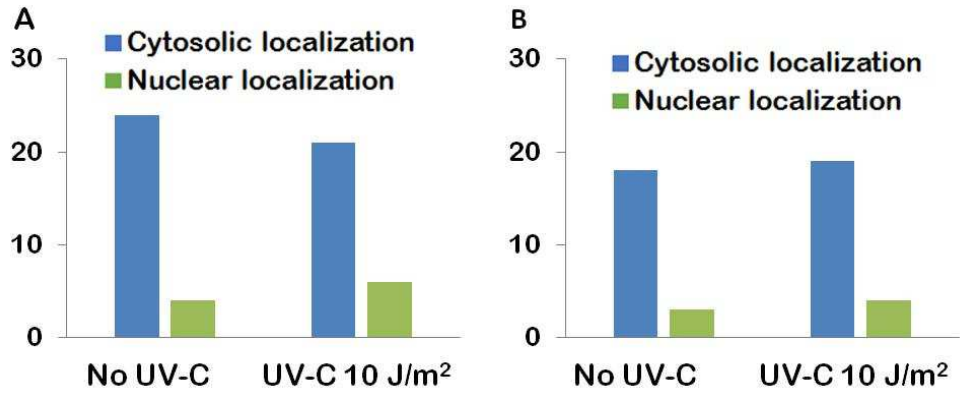

Figure 29: DDB1 localization in non-irradiated cells (No UV-C) or 30 minutes after UV-C damage (UV-C 10J/m^2). A) HeLa cells transfected with pcDNA3-HA2-DDB1^{Wt} construct; B) HeLa cells transfected with pcDNA™3.1/myc-His DDB1^{AAA}-HA construct. In blue, cytosolic localization of DDB1 and in green its nuclear localization.

5.6.3 Purification of DDB1^{AAA}-HA recombinant protein

The purification of recombinant DDB1^{AAA}-HA protein was performed through FPLC (**Figure 30**), employing Imidazole concentrations of 50, 100, 250 and 500 mM; the flow-through and the fraction number 2, 3, 5, 6 and 8 were collected and loaded on a 10% polyacrylamide gel. Recombinant protein was revealed by chemiluminescent method with anti-DDB1 (**Figure 31**) or anti-HA tag antibodies.

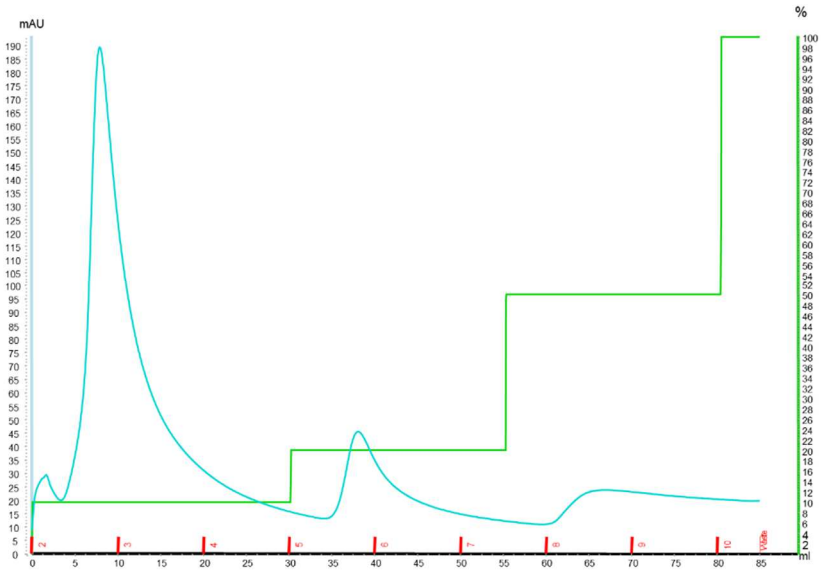

Figure 30: Purification of recombinant DDB1^{AAA}-HA protein performed through FPLC; in green: imidazole concentrations, in cyan: protein elutions.

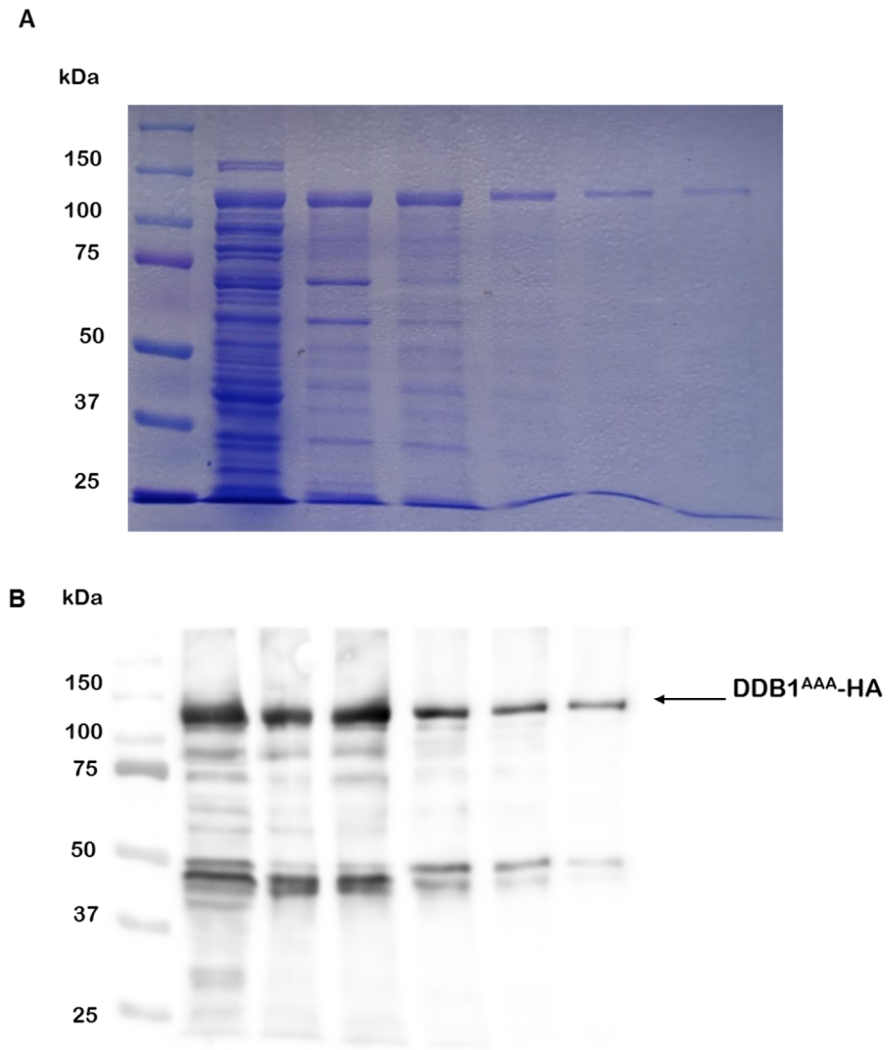

Figure 31: Flow-through and the fraction numbers 2, 3, 5, 6 and 8 were loaded on a 10% polyacrylamide gel; A) gel was stained with Coomassie Brilliant blue; B) proteins were electrotransferred on nitrocellulose membrane and revealed by anti-DDB1 antibody.

The fractions number 5, 6 and 8 were concentrated with a centrifugal filter unit (30 KDa) and quantified (2 µg/µl); 1 µg was loaded on a 10% polyacrylamide gel and revealed by Coomassie staining (**Figure 32**).

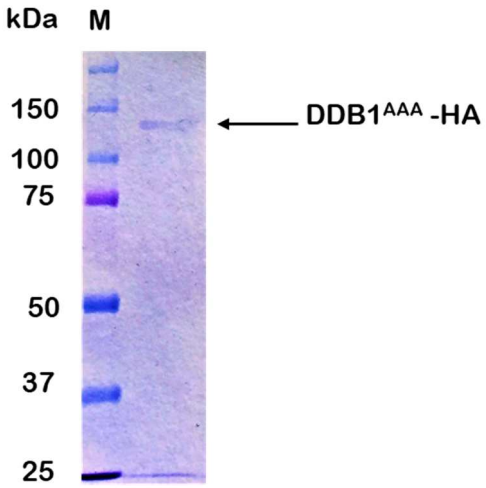

Figure 32: Concentrated DDB1^{AAA}-HA protein loaded on a 10% polyacrylamide gel and revealed by Coomassie staining.

5.6.4 *In vitro* pull-down assay

To demonstrate the functionality of the sequence identified as a potential PIP-box in DDB1, we performed an *in vitro* binding assay.

Preliminary results showed in **Figure 33** demonstrate a direct interaction between DDB1 and PCNA, both in the wild-type and mutated forms; although DDB1^{AAA} interacts with PCNA, is possible to observe a decreased signal by a densitometric analysis. Further studies may be envisaged in order to elucidate this issue.

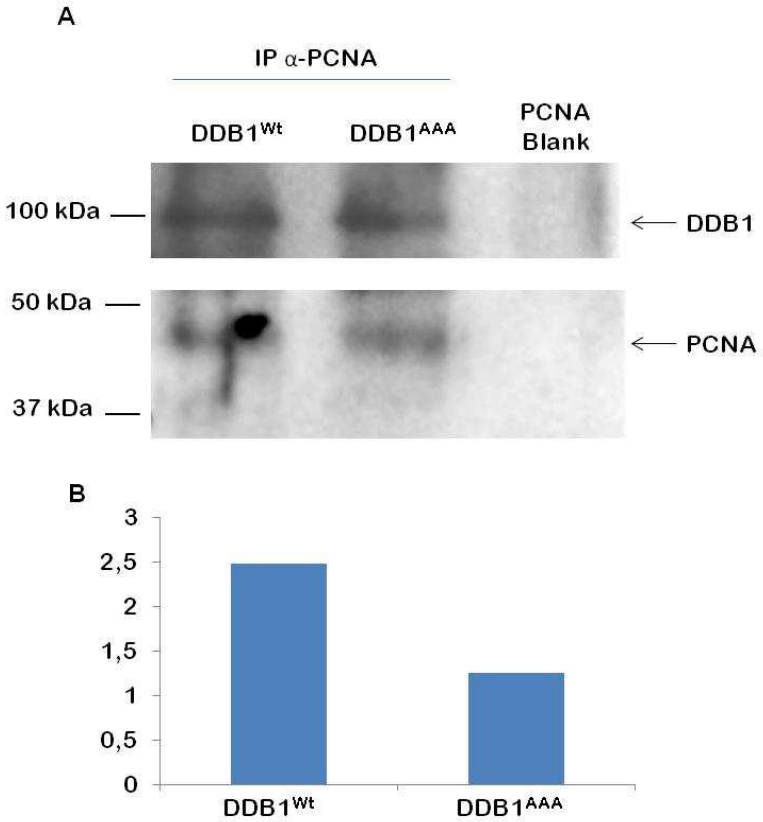

Figure 33: A) Western blot analysis of *in vitro* pull-down assay with recombinant proteins. B) Densitometry ratio analysis between DDB1^{Wt} or DDB1^{AAA} and PCNA.

6. Discussion

We decided to set up a cell-free *in vitro* assay, useful to study DNA repair machinery, with the aim to assess whether mutation disrupting DDB2-PCNA association interferes directly with DNA repair synthesis, or whether other factors/phenomena may be involved in determining NER delay after UV-induced DNA lesions. Using this method, which allows exploring the function of single NER factors, we obtained very interesting results about $DDB2^{Wt}$ and $DDB2^{PCNA-}$ activity after UV damage. Confirming results previously obtained in HEK293 cells stably transfected with pcDNA 3.1 $DDB2^{Wt}$-His or pcDNA 3.1 $DDB2^{PCNA-}$-His, we demonstrated a different repair efficiency of these two recombinant proteins with an *in vitro* system less complex but more controlled, compared to cellular models.

The *in vitro* cell-free models known in the literature and used in research laboratories to study repair mechanisms currently, employ cytosolic extracts or recombinant proteins and plasmids as DNA scaffold. Li R.Y. and colleagues developed a chemiluminescent DNA repair *in vitro* model, using plasmid DNA exposed to UV radiation (with a dose range from 5 to 450 J/m^2) and repair factors purified from HeLa cells, to demonstrate that some NER proteins required an ATP-dependent activity and the integrity of other repair factors to bind damaged DNA (Li R.Y. et al., 1998). Alternatively, to UV-exposed plasmid DNA, a vector containing a cis-syn thymine dimer, the major DNA photoproduct induced by UVB light, was constructed and incubated with HeLa or XPV cell extracts to evaluate the repair or the bypass of lesions (Ensch-Simon I. *et al.,* 1998). These models, therefore, may be not ideal to effectively explain the repair of damage to human DNA that is wrapped on nucleosomes and condensed into chromatin; some years ago, a cell-free extract derived from *Xenopus* eggs was proposed as an ideal system to elucidate the biochemical basis of cell cycle transitions, activation of DNA damage checkpoints, and DNA replication control in the presence of DNA damage generating biochemical knock-out extracts (Costanzo V., Gautier J., 2004; Roper K., Coverley D., 2012; Sannino V. *et al.,* 2017); however, some important disadvantages of

this methods are i) the generation of *Xenopus* specific depleting antibodies in high amount, correlated with ii) the too reach source of biologically active proteins and membrane components provided by egg extract, and iii) the production in large-scale of wild-type or mutated soluble proteins to be re-added to egg extracts (Garner E., Costanzo V., 2009). In addition, *Xenopus laevis* egg extract cell-free system makes use of nuclei isolated from *Xenopus* sperm and cytosolic egg extracts. To obtain sperm nuclei male animals are sacrificed, while to re-use female frogs, to obtain egg extracts, it is necessary to wait four months (Sannino V. *et al.,* 2017).

The method we developed for assessing the efficiency of DNA repair employ a pre-existing cell-free system set up for studying DNA initiation of replication (Krude T. *et al.,* 1997). To perform *in vitro* cell-free repair assay, I isolated nuclei and cytosolic extracts from human G_1 synchronized cells previously treated with damaging agents to induce chromatin alterations. Synchronization of cells in G_1-phase was necessary to eliminate cells in S-phase, whose isolated nuclei, being able to elongate their DNA *in vitro*, contribute to contaminate DNA repairing with DNA replicating nuclei. To trigger DNA repair synthesis *in vitro*, isolated nuclei were incubated with the corresponding cytosolic extracts and a reaction mixture containing biotinylated dUTPs and a phosphagen system, consisting of creatine phosphate and phosphocreatine kinase, necessary to provide energy to the synthesis mechanism (Krude T. *et al.,* 1997); in absence of this system the DNA synthesis is completely blocked (data not shown). DNA repair synthesis is monitored by dUTPs incorporation and samples can be analysed by fluorescence microscopy, flow cytometry and Western blot; in this way, DNA repair efficiency and fluorescence intensity are easily quantified through streptavidin conjugated with fluorescent molecules and, the activation of recombinant proteins to bind the damaged DNA or to interact with other repair factors are highlighted.

The nuclear envelope is considered a sort of barrier between the nucleus and cytoplasm; its important function is to maintain this compartmentation to encase the genetic material. The nuclear envelope is considered a barrier that allows proteins and molecules to move between cytosol and nuclear compartments. Regulation of several metabolic

pathways, including DNA repair, requires a trafficking of these factors across the nuclear membrane, thereby its integrity is fundamental. For this reason, nuclei have been isolated with two different methods: the Dounce homogenizer and the cell membrane permeabilization with Digitonin. The former is a mechanical isolation method which consists in breaking the cytoplasmic membrane through a pestle, thus obtaining both isolated nuclei and cytosolic extracts. However, it was documented that in about 20-25% of the isolated nuclei, the nuclear membrane can be permeabilized; nevertheless, the ability of replicative DNA synthesis in permeabilized nuclei did not appear modified (Krude T., 2000). On the contrary, the permeabilization with Digitonin is a method of chemical isolation, which consists in permeabilizing the cytoplasmic membrane leaving the cytosolic content to escape, preserving the integrity of the nuclear membrane. In our conditions, similarly to the result obtained for replicative nuclei (Krude T., 2000), nuclei isolated by both methods preserved their ability of repairing DNA.

Two different cell lines, HaCaT and HeLa, were employed to carried out the experiments, in order to verify whether results obtained were independent from the cell line. A high percentage (95-98%) of dUTPs-positive G_1 nuclei, compared to unirradiated samples, observed in both nuclei preparation, clearly indicate that this *in vitro* repair assay may be applied to different cell types. In addition, the marked dUTPs signals only in the damaged nuclei, as well as the absence of BrdU incorporation in living cells before nuclei isolation, indicate that DNA synthesis initiated *in vitro,* and only in UVC-exposed nuclei, is due to DNA repair and not to the initiation/elongation of DNA replication. This evidence is consistent with the observation that dUTPs incorporation occurs all throughout the chromatin, as a uniformly distributed signal and many very small foci, differently from those of the typical early, mid and late S-phase replication patterns (Hozák P. *et al.,* 1994; Pierzyńska-Mach A. *et al.,* 2016). Moreover, repair synthesis demonstrated a time- and dose- dependent kinetics, with a higher signal observed at 2 hours after incubation in nuclei isolated from cells exposed to 40 J/m^2. To exclude a-specific signals in damaged nuclei not related to DNA repair synthesis, two well-known inhibitors, such as Ara-C and Aph, were

added to each sample. A severe reduction of dUTPs incorporated signal, mainly when they were added together, in agreement with data in the literature (Nakao S. *et al.,* 2013), demonstrated clearly that dUTPs signal specifically correspond to DNA synthesis occurring *in vitro*. An important demonstration of this specificity of repair activity was obtained by using nuclei isolated from UVC-exposed XP14BR compared with their non irradiated counterpart; in this case we were not able to discriminate an evident repair signal from the background, supporting the inability of this cell to activate an efficient NER mechanism unless the re-introduction of XPC protein (Chavanne F. *et al.,* 2000; Arlett C.F. *et al.,* 2006).

Considering this first part of the results, the performed cell-free method has proven to be a highly versatile system, as it allows to analyze the data with more approaches (e.g. fluorescence microscopy, flow cytometry, western blot) making the observations robust and reproducible. The use of fluorescent markers (Zirkin S*. et al.,* 2014), furthermore, makes the system safer than previous methods involving radioactivity (Cleaver J.E., 1968; Mu D., Sancar A., 1997).

In addition, its responsiveness to different type of DNA lesions, activating different DNA repair processes, increases further its applicability. In our experiments, nuclei isolated from HaCaT cells, treated with some damaging agents, activate specific DNA repair pathways, which are identifiable thank to the different pattern and size of foci distribution observed in each sample. In fact, the stronger dUTPs signals have been achieved in nuclei isolated from cells treated with Cis-Pt or MNNG. Cis-Pt is a chemotherapeutic drug able to induce inter- and intra-strand cross-link; generally, this type of adducts are substrates of NER pathway, even if in non-replicating cells a smaller number of adducts (about 2%) are resistant to NER mechanism (Gillet L.C.J., Schärer O.D., 2006) and probably a co-operation between NER and TLS polymerases allows to repair also these damages (Clauson C. *et al.,* 2013; Chatterjee N., Walker G.C., 2017). On the other hand, MNNG is an alkylating agent able to induce the activation of both BER and MMR; in our experimental condition, BER is the pathway preferentially activated, and the strong signal of dUTPs suggests that DNA adducts were removed via long-patch mechanism, involving PCNA-dependent

polymerase, as was previously demonstrated (Stivala L.A. *et al.,* 1993). This observation is supported by the very low signal of DNA repair synthesis after treatment with the oxidative agent $KBrO_3$ that leads to point mutations (Nakabeppu Y. *et al.* 2006), suggesting the activation of short-patch BER mechanism. A question still unresolved and subject of future analysis concerns the data obtained from nuclei isolated after exposure of cells to ionizing radiation (X-rays); only a part (about 15-20%) of nuclei present a peculiar dUTPs pattern that not coincide with replicative BrdU signal. Nevertheless, DNA damage occurred to all nuclei, as assessed by Comet test, but the nature of damage is not already clear, because X-Rays can cause direct (DSBs) or indirect (ROS) damages. Colocalization of dUTPs sites with XRRC1 strong supports the involvement of the BER sub-pathways, in which XRCC1 and PARP (poly (ADP-ribose) polymerase) are principal players, but repair via Al-EJ or NHEJ cannot be excluded (Zhao H. *et al.,* 2019).

Taking advantages from this *in vitro* repair system, a significant tool is the possibility to study and investigate the regulation of NER mechanism, by introducing human purified recombinant proteins directly involved in this pathway. UV-C exposed HaCaT cells showed a significant positive influence in DNA repair synthesis after the introduction of recombinant PCNA protein. Focusing the attention on DDB2 protein, responsible for the recognition of UV radiation damage in the GG-NER pathway (Sugasawa K*. et al.,* 2001; Reardon JT, Sancar A., 2003), we produced and purified a mutated form of DDB2, unable to interact with PCNA ($DDB2^{PCNA-}$). The interaction between DDB2 and PCNA plays a critical role in NER, as recently demonstrated, since the expression of the $DDB2^{PCNA-}$ protein in human cells determines, not only a delay in the recognition of photoproducts, but also an inefficient damage repair (Perucca P. *et al.,* 2018); the addition of the $DDB2^{PCNA-}$ protein in nuclei isolated from UV-C irradiated HaCaT cells, a reduction of the DNA repair efficiency, even if not significant, was highlighted. In contrast, a high statistical significance was achieved in the same experimental conditions but using UV-C irradiated HeLa isolated nuclei. Therefore, it was hypothesized that the difference between the two cell lines could be due to the competition, in HaCaT, for the DNA-binding site between the endogenous and the exogenous protein added during the assay. This hypothesis was

confirmed when Western blot analysis showed very high levels of endogenous DDB2 in nuclei and cytosolic extract of HaCaT cells, unlike the HeLa. This data confirms what has already been indicated in the literature for HeLa cells that, being infected by the HPV virus encoding the E6 protein responsible for the degradation of p53 (Scheffner M. et al., 1990), in turn regulator of DDB2 expression, express low levels of the protein (Hwang B.J. *et al.,* 1999; Tang J. *et al.,* 2000). Furthermore, in irradiated HaCaT cells, DDB2 is more present in the nucleus than in non-irradiated cells; this is because DDB2 protein is produced at the cytosolic level and is then translocated to the nuclear level to recognize UV damage. This result also agrees with the role of defense of cutaneous keratinocytes against solar radiation, mediated by DDB2 in function of recognition of ultraviolet DNA damage.

We have previously demonstrated that overexpression of $DDB2^{PCNA-}$ protein in HeLa cells induces a delay in DNA damage recognition and, consequently, an inefficient DNA repair process; this mutation does not impair the interaction with DDB1 in the UV-DDB complex, while the DDB2-PCNA interaction is completely abolished; nevertheless, a very weak PCNA signal was detectable at the DNA damaged foci, at 1 hour after UV damage in the presence of $DDB2^{PCNA-}$, and only a delay of NER mechanism was found (Cazzalini O. *et al.,* 2014; Perucca P. *et al.,* 2018). Thus, a possible involvement of DDB1 in mediating DNA binding of PCNA, when DDB2 is altered or ineffective, was hypothesized. To go into this matter, we use a mutated construct of DDB1, unable to interact with PCNA. The mutation does not modify the cytoplasmic localization of $DDB1^{AAA}$-HA, both in physiological condition or after UV-C exposure, comparable with the wild-type form (Iovine B. *et al.,* 2011). This result could be influenced by the low expression of the endogenous DDB2 protein in HeLa cells, being the last protein responsible of DDB1 nuclear translocation during NER process (Alekseev S. *et al.,* 2008). Preliminary experiments suggest a direct interaction between $DDB1^{Wt}$ and $PCNA^{Wt}$, highlighting an unknown binding activity of these two proteins so far; the fact that mutated DDB1 protein binds PCNA in the *in vitro* assay, opens to the possibility of a second PIP-box on DDB1 sequence (Gilljam K.M. *et al.*, 2009; Kim D.H. *et al.,* 2010) or on un-

conventional PIP-box sequences recently identified (Prestel A. *et al.,* 2019). These experiments will have to be confirmed by further analysis and preliminary results obtained so far leave many unanswered questions.

7. Conclusions and perspectives

The new *in vitro* cell-free assay employed in this research project for assessing the efficiency of DNA repair was developed from a pre-existing cell-free system set up for studying DNA initiation of replication. The different pattern of DNA neo-synthesis and the experimental conditions employed have allowed to clearly discriminate the repair neo-synthesis from a possible initiation or elongation of replicative events. The method we developed highlights some clear advantages, compared with other cell-free assays reported in literature.

It is useful to elucidate DNA repair mechanism and protein roles directly on nuclei isolated from human cells, preserving the complex chromatin structure, but simplifying the experimental model to the nucleus.

A cell-line independent response was observed, encouraging the possibility to employ this system with both tumoral and non-tumoral cells, primary cultured cells or established cell lines.

The integrity of nuclear membrane is maintained, allowing proteins or molecules to actively translocate from cytosolic extract into the nucleus, preserving the ability of nuclei to actively synthetase DNA.

The introduction of human recombinant proteins (PCNA-His, DDB1-GST, $DDB2^{Wt}$-His and $DDB2^{PCNA-}$-His) in the DNA synthesis reactions allow to dissect and elucidate some key steps of repair pathways.

The easy quantification techniques employed to analyse the repair activity of nuclei exposed to damaging agents, using fluorescent markers, makes this method safer than previous radiolabelled tracers.

The introduction of specific inhibitors of DNA synthesis (Aph) or chain terminator (Ara-C), and the lack of DNA repair response in XPC-derived cells, clearly demonstrate the specificity of the assay, excluding the possibility of observing phenomena not directly related with repair DNA synthesis.

A critical point we have found is the competitive activity between proteins expressed constitutively by cells used and the recombinant exogenous one. For this reason, an important point not to be underestimated is the genotypic and phenotypic characteristics of cells.

We are currently trying to improve sensitivity of this cell-free system by applying biochemical knockout for future studies in order to evaluate whether and in which mechanism of DNA repair a given protein or protein complex is implicated.

Future applications of the *in vitro* repair assay will better elucidate the role of PCNA-binding activity on the UV-DDB complex; when DDB2-PCNA interaction is completely abolished, DNA repair activity is reduced but not blocked, and new preliminary evidence showed in this research indicates a possible direct interaction between DDB1 and PCNA. This hypothesis will be investigated in future experiments, together with the influence of the co-expression of the DDB1 and DDB2 proteins in their wild-type and mutated forms on NER process.

References

Alekseev S, Luijsterburg MS, Pines A, Geverts B, Mari PO, Giglia-Mari G, Lans H, Houtsmuller AB, Mullenders LH, Hoeijmakers JH, Vermeulen W. Cellular concentrations of DDB2 regulate dynamic binding of DDB1 at UV-induced DNA damage. Mol Cell Biol. 2008, 28:7402-7413.

Almeida KH, Sobol RW. A unified view of base excision repair: lesion dependent protein complexes regulated by post-translational modification. DNA Repair. 2007, 6:695-711.

Al-Minawi AZ, Lee YF, Håkansson D, Johansson F, Lundin C, Saleh-Gohari N, Schultz N, Jenssen D, Bryant HE, Meuth M, Hinz JM, Helleday T. The ERCC1/XPF endonuclease is required for completion of homologous recombination at DNA replication forks stalled by inter-strand cross-links. NAR. 2009, 37:6400-6413.

Angers S, Li T, Yi X, MacCoss MJ, Moon RT, Zheng N. Molecular architecture and assembly of the DDB1-CUL4A ubiquitin ligase machinery. Nature. 2006, 443:590-593.

Aquilina G, Frosina G, Zijno A, Di Muccio A, Dogliotti E, Abbondandolo A, Bignami M. Isolation of clones displaying enhanced resistance to methylation agents in O^6-methylguanine-DNA-methyltransferase proficient CHO cells. Carcinogenesis. 1988, 9:1217-1222.

Arlett CF, Plowman PN, Rogers PB, Parris CN, Abbaszadeh F, Green MH, McMillan TJ, Bush C, Foray N, Lehmann AR. Clinical and cellular ionizing radiation sensitivity in a patient with xeroderma pigmentosum. Br J Radiol. 2006, 79:510-517.

Audebert M, Salles B, Calsou P. Involvement of poly(ADP-ribose) polymerase-1 and XRCC1/DNA ligase III in an alternative route for DNA double-strand breaks rejoining. J Biol Chem. 2004, 279:55117-55126.

Ballmaier D, Epe B. Oxidative DNA damage induced by potassium bromate under cell-free conditions and in mammalian cells. Carcinogenesis. 1995, 16:335-342.

Barakat BM, Wang QE, Han C, Milum K, Yin DT, Zhao Q, Wani G, Arafa el-SA, El-Mahdy MA, Wani AA. Overexpression of DDB2 enhances the sensitivity of human ovarian cancer cells to cisplatin by augmenting cellular apoptosis. International Journal of Cancer. 2010, 127:977-988.

Bjelland S, Seeberg E. Mutagenicity, toxicity and repair of DNA base damage induced by oxidation. Mutat Res. 2003, 531:37-80.

Boyce RP, Howard-Flanders P. Release of ultraviolet light-induced thymine dimers from DNA in *E. coli* K-12. PNAS. 1964, 51:293–300.

Bradford MM. A rapid and sensitive method for the quantification of microgram quantities of protein utilizing the principle of protein-dye binding. Analytical Biochemistry. 1976, 72:248-255.

Bridges BA. Error prone DNA repair and translesion synthesis: focus on the replication fork. DNA Rep. 2005, 4:618-619, 634.

Caldecott KW. Single-strand break repair and genetic disease. Nat Rev Genet. 2008, 9:619-631.

Cazzalini O, Perucca P, occhi R, Sommatis S, Prosperi E, Stivala LA. DDB2 association with PCNA is required for its degradation after UV-induced DNA damage. Cell Cycle. 2014, 13:240-248.

Ceccaldi R, Liu JC, Amunugama R, Primack B, Petalcorin MI, O'Connor KW, Konstantinopoulos PA, Elledge SJ, Boulton SJ. Homologous-recombination-deficient tumors are dependent on Poltheta-mediated repair. Nature. 2015, 518:258-62.

Charles Richard JL, Shukla MS, Menoni H, Ouararhni K, Lone IN, Roulland Y, Papin C, Ben Simon E, Kundu T, Hamiche A, Angelov D, Dimitrov S. FACT Assists Base Excision Repair by Boosting the Remodeling Activity of RSC. *PLoS Genet*. 2016, 12:e1006221.

Chatterjee N, Walker GC. Mechanisms of DNA damage, repair and mutagenesis. Environ Mol Mutagen. 2017, 58:235-263.

Chavanne F, Broughton BC, Pietra D, Nardo T, Browitt A, Lehmann AR, Stefanini M. Mutations in the XPC gene in families with xeroderma pigmentosum and consequences at the cell, protein, and transcript levels. Cancer Res. 2000, 60:1974-1982.

Chen HT, Bhandoola A, Difilippantonio MJ. Response to RAG-mediated V(D)J cleavage by NBS1 and gamma-H2AX. Science. 2000, 290:1962-1964.

Chipuk JE, Green DR. Dissecting p53-dependent apoptosis. Cell Death Differ. 2006, 13:994-1002.

Clauson C, Scharer OD, Niedernhofer L. Advances in understanding the complex mechanisms of DNA interstrand cross-link repair. Cold Spring Harb Perspect Biol. 2013, 5:a012732.

Cleaver JE. Defective repair replication of DNA in xeroderma pigmentosum. Nature. 1968, 218:652-656.

Cleaver JE. Xeroderma Pigmentosum: Variants with Normal Dna Repair and Normal Sensitivity to Ultraviolet Light. Invest Dermatol. 1972, 58:124-128.

Collado M, Blasco MA, Serrano M. Cellular senescence in cancer and aging. Cell. 2007, 130:223-233.

Costanzo V, Gautier J. Xenopus cell-free extracts to study DNA damage checkpoints. Methods Mol Biol. 2004, 241:255-267.

Critchlow SE, Jackson SP. DNA end-joining: from yeast to mam. Trends Biochem Sci. 1998, 23:394-398.

DeFazio LG, Stansel RM, Griffith JD, Chu G. Synapsis of DNA ends by DNA-dependent protein kinase. EMBO J. 2002, 21:3192-3200.

Del Mundo IMA, Vasquez KM, Wang G. Modulation of DNA structure formation using small molecules. Biochim Biophys Acta Mol Cell Res. 2019, Epub ahead of print.

Dianov GL, Prasad R, Wilson SH, Bohr VA. Role of DNA polymerase beta in the excision step of long patch mammalian base excision repair. J Biol Chem. 1999, 274:13741-13743.

Dualan R, Brody T, Keeney S, Nichols AF, Admon A, Linn S. Chromosomal localization and cDNA cloning of the genes (DDB1 and DDB2) for the p127 and p48 subunits of a human damage-specific DNA binding protein. Genomics. 1995, 29:62-69.

Durando M, Tateishi S, Vaziri C. A non-catalytic role of DNA polymerase η in recruiting Rad18 and promoting PCNA monoubiquitination at stalled replication forks. NAR. 2013, 41:3079-3093.

Edifizi D, Schumacher B. Genome Instability in Development and Aging: Insights from Nucleotide Excision Repair in Humans, Mice, and Worms. Biomolecules. 2015, 5:1855-1869.

Enoiu M, Jiricny J, Scharer OD. Repair of cisplatin-induced DNA interstrand crosslinks by a replication-independent pathway involving transcription-coupled repair and translesion synthesis. NAR. 2012, 40:8953–8964.

Ensch-Simon I, Burgers PM, Taylor JS. Bypass of a site-specific cis-Syn thymine dimer in an SV40 vector during *in vitro* replication by HeLa and XPV cell-free extracts. Biochemistry. 1998, 37:8218-8226.

Epe B. Genotoxicity of singlet oxygen. Chem Biol Interact. 1991, 80:239-260.

Evdokimov A, Petruseva I, Tsidulko A, Koroleva L, Serpokrylova I, Silnikov V, Lavrik O. New synthetic substrates of mammalian nucleotide excision repair system. NAR. 2013, 41:e123.

Fischer ES, Scrima A, Böhm K, Matsumoto S, Lingaraju GM, Faty M, Yasuda T, Cavadini S, Wakasugi M, Hanaoka F, Iwai S, Gut H, Sugasawa K, Thomä NH. The Molecular Basis of CRL4DDB2/CSA Ubiquitin Ligase Architecture, Targeting, and Activation. Cell. 2011, 147:1024-1039.

Fortini P, Dogliotti E. Base damage and single-strand break repair: mechanisms and functional significance of short- and long-patch repair subpathways. DNA Repair. 2007, 6:398-409.

Fousteri M, Vermeulen W, van Zeeland AA, Mullenders LH. Cockayne syndrome A and B proteins differentially regulate recruitment of chromatin remodeling and repair factors to stalled RNA polymerase II *in vivo*. Mol Cell. 2006, 23:471-482.

Gao Y, Katyal S, Lee Y, Zhao J, Rehg JE, Russell HR, McKinnon PJ. DNA ligase III is critical for mtDNA integrity but not Xrcc1-mediated nuclear DNA repair. Nature. 2011, 471:240-244.

Garner E, Costanzo V. Studying the DNA damage response using *in vitro* model systems. DNA Repair. 2009, 8:1025-1037.

Gary R, Ludwig DL, Cornelius HL, MacInnes MA, Park MS. The DNA repair endonuclease XPG binds to proliferating cell nuclear antigen (PCNA) and shares sequence elements with the PCNA-binding regions of FEN-1 and cyclin-dependent kinase inhibitor p21. J. Biol. Chem. 1997, 272:24522-24529.

Gecchele E, Merlin M, Brozzetti A, Falorni A, Pezzotti M, Avesani L. A comparative analysis of recombinant protein expression in different biofactories: bacteria, insect cells and plant systems. JoVE. 2015, 97:52459.

Gillet LCJ, Schärer OD. Molecular mechanism of mammalian global genome nucleotide excision repair. Chem Rev. 2006, 106:253-276.

Gilljam KM, Feyzi E, Aas PA, Sousa MM, Müller R, Vågbø CB, Catterall TC, Liabakk NB, Slupphaug G, Drabløs F, Krokan HE, Otterlei M. Identification of a novel, widespread, and functionally important PCNA-binding motif. J Cell Biol. 2009; 186:645-654.

Giloni L, Takeshita M, Johnson F, Iden C, Grolloman AP. Bleomycin-induced strand scission of DNA. Mechanism of deoxyribose cleavage. JBC. 1981. 256: 8608-8615.

Hannah J, Zhou PB. The CUL4A ubiquitin ligase is a potential therapeutic target in skin cancer and other malignancies. Chin J Cancer. 2013, 32:478-482.

Hara R, Mo J, Sancar A. DNA damage in the nucleosome core is refractory to repair by human excision nuclease. Mol Cell Biol. 2000, 20:9173-9181.

Hartlerode AJ, Scully R. Mechanisms of double-strand break repair in somatic mammalian cells. Biochem J. 2009, 423:157-168.

Higa LA, Wu M, Ye T, Kobayashi R, Sun H, Zhang H. CUL4-DDB1 ubiquitin ligase interacts with multiple WD40-repeat proteins and regulates histone methylation. Nat Cell Biol. 2006, 8:277-283.

Ho TV, Guainazzi A, Derkunt SB, Enoiu M, Scharer OD. Structure-dependent bypass of DNA interstrand crosslinks by translesion synthesis polymerases. NAR. 2011, 39:7455–7464.

Hoeijmakers IIH. Genome maitenance mechanisms for preventing cancer. Nature. 2001, 411:366-374.

Hoogstraten D, Nigg AL, Heath H, Mullenders LHF, Van Driel R, Hoeijmakers JHJ, Vermeulen W, Houtsmuller AB. Rapid switching of TFIIH between RNA polymerase I and II transcription and DNA repair *in vivo*. Mol cell. 2002, 10:1163-1174.

Houtsmuller AB, Rademakers S, Nigg AL, Hoogstraten D, Hoeijmakers JHJ, Vermeulen W. Action of DNA repair endonuclease ERCC1/XPF in living cells. Science. 1999, 284:958-961.

Hozák P, Jackson DA, Cook PR. Replication factories and nuclear bodies: the ultrastructural characterization of replication sites during the cell cycle. J Cell Sci. 1994, 107:2191-2202.

Hu J, Zacharek S, He YJ, Lee H, Shumway S, Duronio RJ, Xiong Y. WD40 protein FBW5 promotes ubiquitination of tumor suppressor TSC2 by DDB1-CUL4-ROC1 ligase. Genes & Development. 2008, 22:866-871.

Huang JC, Svoboda DL, Reardon JT, Sancar A. Human nucleotide excision nuclease removes thymine dimers from DNA by incising the 22nd phosphodiester bond 5' and the 6th phosphodiester bond 3' to the photodimer. PNAS. 1992, 89:3664-3668.

Hutchison F. Chemical changes induced in DNA by ionizing radiation. Prog Nucleic Acid Res Mol Biol. 1985, 32:115-154.

Hwang BJ, Ford J, Hanawalt PC, Chu G. Expression of the p48 xeroderma pigmentosum gene is p53-dependent and is involved in global genomic repair. PNAS. 1999, 96:424-428.

Iovine B, Iannella ML, Bevilacqua MA. Damage-specific DNA binding protein 1 (DDB1): a protein with a wide range of functions. Int J Biochem Cell Biol. 2011; 43:1664-1667.

Jackson SP, Bartek J. The DNA-damage response in human biology and disease. Nature. 2009, 461:1071-1078.

Jascur T, Fotedar R, Greene S, Hotchkiss E, Boland CR. N-methyl-N'-nitro-N-nitrosoguanidine (MNNG) triggers MSH2 and Cdt2 protein-dependent degradation of the cell cycle and mismatch repair (MMR) inhibitor protein p21Waf1/Cip1. The J Biol Chem. 2011, 286:29531–29539.

Jones CJ, Wood RD. Preferential binding of the xeroderma pigmentosum group A complementing protein to damaged DNA. Biochemistry. 1993, 32:12096-12104.

Kass EM, Jasin M. Collaboration and competition between DNA double-strand break repair pathways. FEBS Letters. 2010, 584:3703-3708.

Kim DH, Budhavarapu VN, Herrera CR, Nam HW, Kim YS, Yew PR. The CRL4Cdt2 ubiquitin ligase mediates the proteolysis of cyclin-dependent kinase inhibitor Xic1 through a direct association with PCNA. Mol Cell Biol. 2010, 30:4120–4133.

Kim JM, Kee Y, Gurtan A, D'Andrea AD. Cell cycle-dependent chromatin loading of the Fanconi anemia core complex by FANCM/FAAP24. Blood. 2008, 111:5215–5222.

Kondo N, Takahashi A, Ohnishi T. DNA damage induced by alkylating agents and repair pathways. J Nucleic Acids. 2010, 2010:543531.

Kornberg RD, Lorch Y. Twenty-five years of the nucleosome, fundamental particle of the eukaryote chromosome. Cell. 1999, 98:285–294.

Krude T, Jackman M, Pines J, Laskey RA. Cyclin/Cdk-Dependent Initiation of DNA Replication in a Human Cell-Free System. Cell. 1997, 88:109-119.

Krude T. Initiation of human DNA replication *in vitro* using nuclei from cells arrested at an initiation-competent state. J Biol Chem. 2000, 275:13699-13707.

Kunkel TA. Evolving views of DNA replication (in)fidelity. Cold Spring Harb Simp Quant Biol. 2009, 74:91-101.

Lee J, Zhou P. DCAFs, the missing link of the CUL4-DDB1 ubiquitin ligase. Mol Cell. 2007, 26:775-780.

Legerski R, Peterson C. Expression cloning of a human DNA repair gene involved in xeroderma pigmentosum group C. Nature. 1992, 359:70-73.

Li RY, Calsou P, Jones CJ, Salles B. Interactions of the transcription/DNA repair factor TFIIH and XP repair proteins with DNA lesions in a cell-free repair assay. J Mol Biol. 1998, 281:211-218.

Liu X, Smerdon MJ. Nucleotide excision repair of the 5 S ribosomal RNA gene assembled into a nucleosome. J Biol Chem. 2000, 275:23729-23735.

Liu Y, Prasad R, Beard WA, Kedar PS, Hou EW, Shock DD, Wilson SH. Coordination of steps in single-nucleotide base excision repair mediated by apurinic/apyrimidinic endonuclease 1 and DNA polymerase beta. J Biol Chem. 2007, 282:13532-41.

Long DT, Raschle M, Joukov V, Walter JC. Mechanism of RAD51-dependent DNA interstrand cross-link repair. Science. 2011, 333:84–87.

Lukash LL, Boldt J, Pegg AE, Dolan ME, Maher VM, McCormick J. Effect of O6-alkylguanine-DNA alkyltransferase on the frequency and spectrum of mutations induced by N-methyl-N'-nitro-N-nitrosoguanidine in the HPRT gene of diploid human fibroblast. Mutat Res. 1991, 250:397-409.

Ma JL, Kim EM, Haber JE, Lee SE. Yeast Mre11 and Rad1 proteins define a Ku-independent mechanism to repair double-strand breaks lacking overlapping end sequences. Mol. Cell. Biol. 2003, 23:8820–8828.

Ma Y, Schwarz K, Lieber MR. The Artemis: DNA-PKcs endonuclease cleaves DNA loops, flaps, and gaps. DNA Repair. 2005, 4:845-851.

Ma Y. A biochemically defined system for mammalian nonhomologous DNA end joining. Mol Cell. 2004, 16:701-713.

Marginson GP, Santibanez-Koref MF. O6-alkylguanine-DNA alkyltransferase: role in carcinogenesis and chemotherapy. BioEssays. 2002, 24:255-266.

Marteijn JA, Lans H, Vermeulen W, Hoeijmakers JH. Understanding nucleotide excision repair and its roles in cancer and ageing. Nat Rev Mol Cell Biol. 2014, 15:465-481.

Masutani C, Kusumoto R, Yamada A, Dohmae N, Yokoi M, Yuasa M, Araki M, Iwai S, Takio K, Hanaoka F. The XPV (xeroderma pigmentosum variant) gene encodes human DNA polymerase eta. Nature. 1999, 399:700-704.

Masutani C, Sugasawa K, Yanagisawa J, Sonoyama T, Ui M, Enomoto T, Takio K, Tanaka K, van der Spek PJ, Bootsma D, Hoeijmakers JHJ, Hanaoka F. Purification and cloning of a nucleotide excision repair complex involving the xeroderma pigmentosum group C protein and a human homologue of yeast RAD23. EMBO J. 1994, 13:1831-1843.

McCulloch SD, Kunkel TA. The fidelity of DNA synthesis by eukaryotic replicative and translesion synthesis polymerasis. Cell Res. 2008, 18:148-161.

Mehta A, Haber JE. Sources of DNA double-strand breaks and models of recombinational DNA repair. Cold Spring Harb Perspect Biol. 2014, 6:a016428.

Mimitou EP, Symington LS. Nucleases and helicases take center stage in homologous recombination. Trenda Biochem Sci. 2009, 34:264-272.

Mirkin EV, Mirkin SM. Replication fork stalling at natural impediments. Microbiol Mol Biol Rev. 2007, 71: 13–35.

Montecucco A, Rossi R, Levin DS, Gary R, Park MS, Motycka TA, Ciarrocchi G, Villa A, Biamonti G, Tomkinson AE. DNA ligase I is recruited to sites of DNA replication by an interaction with proliferating cell nuclear antigen: identification of a common targeting mechanism for the assembly of replication factories. EMBO J. 1998, 17:3786-3795.

Moser J, Volker M, Kool H, Alekseev S, Vrieling H, Yasui A, van Zeeland AA, Mullenders LH. The UV-damaged DNA binding protein mediates efficient targeting of the nucleotide excision repair complex to UV-induced photo lesions DNA Rep. 2005, 4:571-582.

Mu D, Park CH, Matsunaga T, Hsu DS, Reardon JT, Sancar A. Reconstitution of human DNA repair excision nuclease in a highly defined system. J Biol Chem. 1995, 270:2415-2418.

Mu D, Sancar A. DNA excision repair assay. Prog Nucleic Acid Re. 1997, 56:63-81.

Nag A, Bondar T, Shiv S, Raychaudhuri P. The xeroderma pigmentosum group E gene product DDB2 is a specific target of cullin 4A in mammalian cells. Mol Cell Biol. 2001, 21:6738-6747.

Nakabeppu Y, Sakumi K, Sakamoto K, Tsuchimoto D, Tsuzuki T, Nakatsu Y. Mutagenesis and carcinogenesis caused by the oxidation of nucleic acids. Biol Chem. 2006, 387:373-379.

Nakao S, Zhang S, Vaara M, Syväoja JE, Lee MY, Tsurimoto T, Karran P, Oda S. Efficient long DNA gap-filling in a mammalian cell-free system: A potential new *in vitro* DNA replication assay. Biochimie. 2013, 95:320-328.

Nimonkar AV, Ozsoy AZ, Genschel J, Modrich P, Kowalczykowski SC. Human exonuclease 1 and BLM helicase interact to resect DNA and initiate DNA repair. PNAS. 2008, 105:16906-16911.

Noll DM, Mason TM, Miller PS. Formation and repair of interstrand cross-links in DNA. Chem Rev. 2006, 106:277-301.

Payet D, Gaucheron F, Sip M, Leng M. Instability of the monofunctional adducts in cis-[Pt(NH3)2(N7-N-methyl-2-diazapyrenium)Cl](2+)-modified DNA: rates of cross-linking reactions in cis-platinum-modified DNA. NAR. 1993, 21: 5846-5851.

Peng G, Lin SY. Exploiting the homologous recombination DNA repair network for targeted cancer therapy. World J Clin Oncol. 2011, 2:73-79.

Perucca P, Mocchi R, Guardamagna I, Bassi E, Sommatis S, Nardo T, Prosperi E, Stivala LA, Cazzalini O. A damaged DNA bindin protein 2 mutation disrupting interaction with proliferating-cell nuclear antigen affects DNA repair and confers proliferation advantage. BBA. 2018, 1865:898-907.

Pierzyńska-Mach A, Szczurek A, Cella Zanacchi F, Pennacchietti F, Drukała J, Diaspro A, Cremer C, Darzynkiewicz Z, Dobrucki JW. Subnuclear localization, rates and effectiveness of UVC-induced unscheduled DNA synthesis visualized by fluorescence widefield, confocal and super-resolution microscopy. Cell Cycle. 2016, 15:1156-1167.

Prasad R, Shock DD, Beard WA, Wilson SH. Substrate channeling in mammalian base excision repair pathways: passing the baton. J Biol Chem. 2010, 285:40479-40488.

Prestel A, Wichmann N, Martins JM, Marabini R, Kassem N, Broendum SS, Otterlei M, Nielsen O, Ms MW, Ploug M, Boomsma W, Kragelund BB. The PCNA interaction motifs revisited: thinking outside the PIP-box. Mol. Life Sci. 2019, Epub ahead of print.

Rademakers S, Volker M, Hoogstraten D, Nigg AL, Mone MJ, van Zeeland AA, Hoeijmakers JHJ, Houtsmuller AB, Vermeulen W. Xeroderma pigmentosum group A protein loads as a separate factor onto DNA lesions. Mol Cell Biol. 2003, 23:5755-5767.

Raschle M, Knipscheer P, Enoiu M, Angelov T, Sun J, Griffith JD, Ellenberger TE, Scharer OD, Walter JC. Mechanism of replication-coupled DNA interstrand crosslink repair. Cell. 2008, 134:969–980.

Reardon JT, Sancar A. Recognition and repair of the cyclobutane thimine dimer, a major cause of skin cancers, by the human excision nuclease. Genes Dev. 2003, 17:2539-2551.

Roper K, Coverley D. Reconstitution of the cellular response to DNA damage *in vitro* using damage-activated extracts from mammalian cells. Exp Cell Res. 2012, 318:527-538.

San Filippo J, Sung P, Klein H. Mechanism of eukaryotic homologous recombination. Annu Rev Biochem. 2008, 77:229-257.

Sannino V, Pezzimenti F, Bertora S, Costanzo V. Xenopus laevis as Model System to Study DNA Damage Response and Replication Fork Stability. Methods Enzymol. 2017, 591:211-232.

Sartori AA. Human CtIP promotes DNA end resection. Nature. 2007, 450:509-514.

Scheffner M, Werness BA, Huibregtse JM, Levine AJ, Howley PM. The E6 oncoprotein encoded by human papillomavirus types 16 and 18 promotes the degradation of p53. Cell. 1990, 63:1129-1136.

Scherer SJ, Avdievich E, Edelmann W. Functional consequences of DNA mismatch repair missense mutations in murine models and their impact on cancer predisposition. Biochem Soc Trans. 2005, 33:689-693.

Scully R, Panday A, Elango R, Willis NA. DNA double-strand break repair-pathway choice in somatic mammalian cells. Nat Rev Mol Cell Biol. 2019, 20:698-714.

Setlow RB, Carrier WL. The disappearance of thymine dimers from DNA: an error-correcting mechanism. PNAS. 1964, 51:226–231.

Shen JC, Fox EJ, Ahn EH, Loeb LA. A rapid assay for measuring nucleotide excision repair by oligonucleotide retrieval. Sci Rep. 2014, 8:4894.

Shiyanov P, Nag A, Raychaudhuri P. Cullin 4A associates with the UV-damaged DNA-binding protein DDB. J Biol Chem. 1999,274:35309-35312.

Sijbers AM, de Laat WL, Ariza RR, Biggerstaff M, Wei YF, Moggs JG, Carter KC, Shell BK, Evans E, de Jong MC, Rademakers S, de Rooij J, Jaspers NG, Hoeijmakers JH, Wood RD. Xeroderma pigmentosum group F caused by a defect in a structure-specific DNA repair endonuclease.Cell. 1996, 86:811-822.

Smeaton MB, Hlavin EM, McGregor Mason T, Noronha AM, Wilds CJ, Miller PS. Distortion-dependent unhooking of interstrand cross-links in mammalian cell extracts. Biochemistry. 2008, 47:9920–9930.

Sobol RH, Horton JK, Kuhn R, Gu H, Singhal RK, Prasad R, Rajewski K, Wilson SH. Requirement of mammalian DNA polymerase beta in bese excision repair. Nature. 1996, 379:183-186.

Stivala LA, Prosperi E, Rossi R, Bianchi L. Involvement of proliferating cell nuclear antigen in DNA repair after damage induced by genotoxic agents in human fibroblasts. Carcinogenesis. 1993, 14:2569-2573.

Stivala LA, Savio M, Cazzalini O, Pizzala R, Rehak L, Bianchi L, Vannini V, Prosperi E. Effect of beta-carotene on cell cycle progression on human fibroblast. Carcinogenesis. 1996, 17:2395-2401.

Stivers JT, Jiang YL. A Mechanistic Perspective on the Chemistry of DNA Repair Glycosylases. Chem Rev. 2003, 103:2729-2759.

Sugasawa K, Okamoto T, Shimizu Y, Masutani C, Iwai S, Hanaoka F. A multistep damage recognition mechanism for global genomic nucleotide excision repair. Genes Dev. 2001, 15:507-521.

Sugasawa K, Okuda Y, Saijo M, Nishi R, Matsuda N, Chu G, Mori T, Iwai S, Tanaka K, Tanaka K, Hanaoka F. UV-induced ubiquitylation of XPC protein mediated by UV-DDB-ubiquitin ligase complex. Cell. 2005, 121:387-400.

Sugasawa K. UV-DDB: a molecular machine linking DNA repair with ubiquitination. DNA Rep. 2009, 8:969-972.

Syro LV, Camargo M, Serna CA, Rotondo F, Ortiz LD, Kovacs K. Temozolomide and pituitary tumors: current understranding, unresolved issues, and future direction. Frontiers in Endocrinology. 2018, 9:318.

Takata M, Sasaki MS, Sonoda E, Morrison C, Hashimoto M, Utsumi H, Yamaguchi-Iwai Y, Shinohara A, Takeda S. Homologous recombination and non-homologous end-joining pathways of DNA double-strand break repair have overlapping roles in the maintenance of chromosomal integrity in vertebrate cells. *EMBO J*. 1998, 17:5497-508.

Takedachi A, Saijo M, Tanaka Ke. DDB2 complex-mediated ubiquitylation around DNA damage is oppositely regulated by XPC and Ku and contributes to the recruitment of XPA. Mol Cell Biol. 2010, 30:2708–2723.

Tang J, Chu G. Xeroderma pigmentosum complementation group E and UV-damaged DNA-binding protein. DNA Rep. 2002, 1:601-616.

Tang J, Hwang B, Ford J, Hanawalt P, Chu G. Xeroderma pigmentosum p48 gene in humans enhances global genomic repair and suppresses UV-induced mutagenesis. Mol Cell. 2000, 5:737-744.

Thoma F. Light and dark in chromatin repair: repair of UV-induced DNA lesions by photolyase and nucleotide excision repair. EMBO J. 1999, 18:6585–6598.

Truong LN, Li Y, Wu X. Microhomology-mediated end-joining and homologus recombination share the initial end resection step to repair DNA double-strand breaks in mammalian cells. PNAS. 2013, 110: 7720-7725.

Tyler JK, Kadonaga JT. The “dark side” of chromatin remodeling: repressive effects on transcription. Cell. 1999, 99:443–446.

Velic D, Couturier AM, Ferreira MT, Rodrigue A, Poirier GG, Fleury F, Masson JY. DNA Damage Signalling and Repair Inhibitors: The Long-Sought-After Achilles' Heel of Cancer. Biomolecules. 2015, 5:3204–3259.

Wakasugi M, Kawashima A, Morioka H, Linn S, Sancar A, Mori T, Nikaido O, Matsunaga T. DDB accumulates at DNA damage sites immediately after UV irradiation and directly stimulates nucleotide excision repair. J Biol Chem. 2002, 277:1637-1640.

Walden H, Deans AJ. The Fanconi Anemia DNA Repair Pathway: Structural and Functional Insights into a Complex Disorder. Annu Rev Biophys. 2014, 43:257-278.

Wang AT, Sengerova B, Cattell E, Inagawa T, Hartley JM, Kiakos K, Burgess-Brown NA, Swift LP, Enzlin JH, Schofield CJ, Gileadi O, Hartley JA, McHugh PJ. Human SNM1A and XPF-ERCC1 collaborate to initiate DNA interstrand cross-link repair. Genes Dev. 2011, 25:1859–1870.

Wang H, Xu X. Microhomology-mediated end-joining: new players join the team. Cell Biosci. 2017, 7:6.

Wang Y, Reddy S, Beard WA, Wilson SH, Schlick T. Differing conformational pathways before and after chemistry for insertion of dATP versus dCTP opposite 8-oxoG in DNA polymerase beta. Biophys J. 2007, 92:3063-3070.

Wang ZG, Wu XH, Friedberg EC. Nucleotide excision repair of DNA by human cell extract is suppressed in reconstituted nucleosome. J Biol Chem. 1991, 266:22472-22478.

Wittschieben BØ, Iwai S, Wood RD. DDB1-DDB2 (xeroderma pigmentosum group E) protein complex recognizes a cyclobutane pyrimidine dimer, mismatches, apurinic/apyrimidinic sites, and compound lesions in DNA. J Biol Chem. 2005, 280:39982-39989.

Wood RD, Robins P, Lindahl T. Complementation of the xeroderma pigmentosum DNA repair defect in cell-free extracts. Cell. 1988, 53:97-106.

Yang YH, Goddard WA, Noyes KT, Sowers LC, Hwang S, Chung DS. First principles calculations of the tautomers and pKa values of 8-oxoguanine: implications for mutagenicity and repair. Chem Res Toxicol. 2002, 15:1023-1035.

Yasuda T, Sugasawa K, Shimizu Y, Iwai S, Shiomi T, Hanaoka F. Nucleosomal structure of undamaged DNA regions suppresses the non-specific DNA binding of the XPC complex. DNA Rep. 2005, 4:389-395.

Yuan SS, Lee SY, Ghen G, Song M, Tomlinson GE, Lee EY. BRCA2 is required for ionizing radiation-induced assembly of Rad51 complex *in vivo*. Cancer Res. 1999, 59:3547-3551.

Yun MH, Hiom K. CtIP-BRCA1 modulates the choice of DNA double-strand-break repair pathway throughout the cell cycle. Nature. 2009, 459:460–463.

Zhao H, Zhuang Y, Li R, Liu Y, Mei Z, He Z, Zhou F, Zhou Y. Effects of different doses of X-ray irradiation on cell apoptosis, cell cycle, DNA damage repair and glycolysis in HeLa cells. Oncol Lett. 2019, 17:42–54.

Zirkin S, Fishman S, Sharim H, Michaeli Y, Don J, Ebestein Y. Lighting up individual DNA damage sites by *in vitro* repair synthesis. JACS. 2014, 136:7771-7776.

List of original manuscripts

Perucca P, Mocchi R, Guardamagna I, Bassi E, Sommatis S, Nardo T, Prosperi E, Stivala LA, Cazzalini O. *"A DDB2 mutation disrupting interaction with PCNA affects DNA repair and confers proliferation advantage"*. BBA; (2018); 1865(6):898-907.

Bassi E, Perucca P, Guardamagna I, Prosperi E, Stivala LA, Cazzalini O. *"Exploring new potential role of DDB2 by Host Cell Reactivation assay in human tumorigenic cells".* BMC Cancer; (2019); 1013.

Guardamagna I, Bassi E, Savio M, Perucca P, Cazzalini O, Prosperi E, Stivala LA. "*A functional in vitro cell-free system for studying DNA repair in isolated nucle*i". Under review (November 2019).

BBA - Molecular Cell Research 1865 (2018) 898–907

Contents lists available at ScienceDirect

BBA - Molecular Cell Research

journal homepage: www.elsevier.com/locate/bbamcr

A damaged DNA binding protein 2 mutation disrupting interaction with proliferating-cell nuclear antigen affects DNA repair and confers proliferation advantage

Paola Perucca[a,1], Roberto Mocchi[a,1,2], Isabella Guardamagna[a], Elisabetta Bassi[a], Sabrina Sommatis[a,2], Tiziana Nardo[b], Ennio Prosperi[b,*], Lucia Anna Stivala[a,*], Ornella Cazzalini[a,*]

[a] Dipartimento di Medicina Molecolare, Unità di Immunologia e Patologia generale, Università degli Studi di Pavia, Pavia, Italy
[b] Istituto di Genetica Molecolare (IGM) del CNR, Pavia, Italy

ARTICLE INFO

Keywords:
DDB2
PCNA
NER
Genome instability
UV damage

ABSTRACT

In mammalian cells, Nucleotide Excision Repair (NER) plays a role in removing DNA damage induced by UV radiation. In Global Genome-NER subpathway, DDB2 protein forms a complex with DDB1 (UV-DDB), recognizing photolesions. During DNA repair, DDB2 interacts directly with PCNA through a conserved region in N-terminal tail and this interaction is important for DDB2 degradation. In this work, we sought to investigate the role of DDB2-PCNA association in DNA repair and cell proliferation after UV-induced DNA damage. To this end, stable clones expressing $DDB2^{WT}$ and $DDB2^{PCNA-}$ were used. We have found that cells expressing a mutant DDB2 show inefficient photolesions removal, and a concomitant lack of binding to damaged DNA *in vitro*. Unexpected cellular behaviour after DNA damage, such as UV-resistance, increased cell growth and motility were found in $DDB2^{PCNA-}$ stable cell clones, in which the most significant defects in cell cycle checkpoint were observed, suggesting a role in the new cellular phenotype. Based on these findings, we propose that DDB2-PCNA interaction may contribute to a correct DNA damage response for maintaining genome integrity.

1. Introduction

Genome integrity and its duplication fidelity are of fundamental importance for correct transmission of genetic information. Many factors, both exogenous and endogenous, can endanger the integrity of the genetic material by inducing DNA damage. To remove these lesions, mammalian cells have developed different DNA repair pathways and, among them, Nucleotide Excision Repair (NER) is specialised in removing DNA photoproducts induced by UV radiation [1,2]. In the global genome NER (GG-NER), the sub-pathway responsible for repair of transcriptionally inactive regions of the genome as well as the non-transcribed strands of expressed genes, DDB2 protein carries out a crucial role [3]. This factor forms with DDB1 and Cullin4A (Cul4A) the complex UV-DDB that recognizes both Cyclobutane Pyrimidine Dimers (CPDs) and 6-4 Photoproducts (6-4PPs), the major UV-lesions [4–6]. The complex formation is important not only for the damage recognition associated to the faster XPC recruitment, but also for the chromatin remodelling, thus facilitating the admission and binding of the repair factors [7]. In addition, the UV-DDB complex has a role in ubiquitination of DDB2 and XPC proteins [8,9] and in the same post-translational modification of H2A, H3 and H4 histones [10]. Furthermore, the homology of DDB2 with proteins that allow the reorganization of the chromatin has been demonstrated and the UV-DDB complex interaction with the STAGA complex has been observed [11].

DDB2 is involved in the early stages of damage recognition caused by UV radiation and in the early recruitment of the GG-NER repair proteins [12]. However, a possible role for DDB2 in tumorigenesis is under debate since different DDB2 expression levels in human cancer are reported [13–15]. In addition, experimental data highlight the DDB2 involvement in the epithelial to mesenchymal transition in cancer cells [16], whereas its overexpression limits stem cells abundance in cancer, thereby leading to the repression of tumorigenesis

Abbreviations: DDB2, damaged DNA binding protein 2; $DDB2^{WT}$, DDB2 wild-type protein; $DDB2^{PCNA-}$, DDB2 unable to interact with PCNA protein; CPDs, Cyclobutane Pyrimidine Dimers; Cul4A, Cullin 4A; NER, Nucleotide Excision Repair; PCNA, Proliferating Cellular Nuclear Antigen; PIP, PCNA Interacting Protein; 6-4PPs, 6-4 Photoproducts; UDS, Unscheduled DNA Synthesis; XPC, Xeroderma Pigmentosum group C

* Corresponding authors.
E-mail addresses: prosperi@igm.cnr.it (E. Prosperi), luciaanna.stivala@unipv.it (L.A. Stivala), ornella.cazzalini@unipv.it (O. Cazzalini).

[1] Perucca P. and Mocchi R. contributed equally to this work.
[2] Present address: UB-CARE S.r.l., Spin-off University of Pavia, Pavia.

https://doi.org/10.1016/j.bbamcr.2018.03.012
Received 30 August 2017; Received in revised form 21 March 2018; Accepted 26 March 2018
Available online 28 March 2018
0167-4889/

[17].

Recently, we have demonstrated that DDB2 interacts with PCNA [18], and that the expression of a mutant form abolishing this interaction ($DDB2^{PCNA-}$), promoted cell proliferation [19].

In this work, we sought to study the effect of $DDB2^{PCNA-}$ protein expression on DNA repair efficiency and on cell proliferation and migration after DNA damage. For this reason, $DDB2^{PCNA-}$ transiently or stably transfected epithelial cells were irradiated with UV-C and DNA repair efficiency was evaluated both by CPDs removal and Unscheduled DNA Synthesis (UDS). In addition, $DDB2^{PCNA-}$ binding capability to DNA damaged sites was explored in *in vitro* assay. Finally, cell damage response to UV irradiation was investigated in terms of cell clonogenic efficiency, proliferation and motility.

We demonstrate that the loss of the interaction between DDB2 and PCNA influences different aspects of the DNA damage response: i) delaying the removal of UV-induced DNA damage; ii) determining an increase in UV-resistance; and iii) conferring a proliferation advantage, as determined by changes in cell growth and motility. These results suggest that the interaction between PCNA and DDB2 contributes to preserve genome stability by promoting DNA repair and by controlling cell cycle checkpoints.

2. Materials and methods

2.1. Cell lines and transfection

HeLa S3 cell line was cultured in Dulbecco's modified Eagle's medium (DMEM, Sigma) supplemented with 10% foetal bovine serum (Life Technologies-Gibco), 2 mM L-glutamine (Life Technologies-Gibco), 100 U/ml penicillin, 100 μg/ml streptomycin in a 5% CO_2 atmosphere.

HeLa S3 cells seeded on coverslips or Petri dishes (70% confluent) were transiently transfected with the $DDB2^{WT}$ kindly provided by Q. Wang [13], or the mutated DDB2 form ($DDB2^{PCNA-}$) using Effectene transfection reagent (Qiagen). DDB2 mutated in the PIP-box sequence was produced as previously described [18].

The irradiation was usually performed 24 h after transfection. Cell exposure to UV-C was performed with a lamp (Philips TUV-9) emitting mainly at 254 nm, at doses of 10, 30 or 100 J/m^2, as measured with a DCRX radiometer (Spectronics). Localized irradiation was performed by laying Isopore polycarbonate filters (Millipore) with 3 μm pores on top of the cells.

HEK293 (Human Embryonic Kidney) cell line was grown as above described. Cells (50% confluent) were stably transfected with the same constructs ($DDB2^{WT}$ and $DDB2^{PCNA-}$) [19].

2.2. Analysis of global genome repair (GG-NER)

HEK293 control cells or stably transfected with $DDB2^{WT}$ and $DDB2^{PCNA-}$ were seeded on coverslips or Petri dishes and 24 h later were washed in PBS, exposed to 30 J/m^2 of UV-C radiation, and harvested at 0 min, 0.5, 4, 8, 24 h.

The DNeasy tissue kit (Qiagen) was used to extract the DNA. The GG-NER efficiency was performed by an immunoblot assay of CPDs removal from DNA [20]. Briefly, DNA was denatured using PCR and blotted in triplicate on nitrocellulose using a Schleicher & Schuell apparatus that allows the DNA binding through a vacuum system. Membranes were fixed by heating at 70 °C for 90 min, blocked with 5% dry milk and incubated with the antibodies mouse monoclonal anti-CPDs (Kamiya Biomedical Company; RRID: AB_1233355), mouse anti Ig-G biotinylated (1:2000, Sigma) and streptavidinHRP (1:2000, Amersham Biosciences).

Reactive bands were visualized with the ECL system (Pierce) using a Li-Cor C-DiGit blot scanner and a densitometric analysis was performed with Li-Cor Image Studio Lite software.

2.3. Analysis of DNA repair by UDS determination

In control and transfected HEK293 cells, UDS was determined after irradiation (20 J/m^2), by incubating cells for 2 h in medium containing 1 ml [^{3}H]-thymidine (NEN, 10 Ci/ml specific activity), then chased for 1 h in medium containing 10 mM each cold thymidine and cytidine. Cells were then fixed in 4% formaldehyde and post-fixed in 70% ethanol. Samples were processed for autoradiography using an Ilford K2 emulsion, exposed for 4 days at 4 °C, and then developed and fixed before mounting on microscope slides. Autoradiographic granules were counted in 50 non-S phase cells showing DDB2 staining, in duplicate experiments [21].

2.4. Gel electrophoretic mobility shift assay

For the DNA binding assay, plasmid DNA (pEGFP-N1, Clontech) was irradiated at 800 J/m^2 and then mixed with each recombinant DDB2 (Wt or mutant form) and recombinant DDB1 human protein (Abnova). The reactions were conducted in 28 mM sodium phosphate (pH 7.5), containing 150 mM NaCl, 3.4 mM $MgCl_2$, 1.4 mM EDTA, 2% glycerol and 0.1 mg/ml BSA, at 30 °C for 30 min and 1 h. Gel electrophoresis was performed in TBE 1× buffer and DNA was run on 1% agarose gel at 40 V for 3 h. The gel was photographed by transilluminator UST-20M-8E on Darkhood DH-30/32 (Biostep).

2.5. Immunofluorescence and confocal microscopy

HeLa cells seeded on coverslips and transiently transfected as described above, were locally irradiated (100 J/m^2) and re-incubated in whole medium for the indicated period of time (5, 10, 30, 60 and 240 min). The cells on coverslips were then washed twice in cold PBS, fixed, and lysed in buffer containing freshly made 2% paraformaldehyde, 0.5% Triton X-100 in PBS, 0.2 mM phenylmethylsulfonyl fluoride (PMSF), and 0.2 mM Na_3VO_4 for 30 min at 4 °C. Then, the samples were washed twice with cold PBS and treated with 2 M HCl at 37 °C for 10 min to denature the DNA, followed by a PBS rinse to remove HCl [22]. After re-hydration, the samples were blocked in PBST buffer (PBS, 0.2% Tween 20) containing 1% bovine serum albumin (BSA), and then incubated for 1 h with specific antibodies: goat polyclonal anti-DDB2 (1:100, Santa Cruz; RRID: AB_2088827), mouse monoclonal anti-CPDs (1:1000, Kamiya Biomedical Company; RRID: AB_1233355) and rabbit polyclonal anti-XPC (1:400, Sigma; RRID: AB_796183), all diluted in PBST buffer/BSA. After washing, each reaction was followed by incubation for 30 min with anti-mouse (Molecular Probes; RRID: AB_141607) or anti-rabbit (Molecular Probes; RRID: AB_141708) antibody conjugated with Alexa 488, anti-goat Alexa Fluor 594 (Molecular Probes; RRID: AB_ 14240). After immunoreactions, the cells were incubated with Hoechst 33258 dye (0.5 μg/ml) for 2 min at RT and washed in PBS. The slides were mounted in Mowiol (Calbiochem) containing 0.25% 1,4-diazabicyclo-octane (Aldrich) as antifading agent. Images of fixed cells were taken with a Nikon Eclipse E400 fluorescence microscope equipped with a Canon Power Shot A590 IS digital camera. Fluorescence signals were acquired with a TCS SP5 II Leica confocal microscope, at 0.3 μm intervals. Image analysis was performed using the LAS AF software.

2.6. Western blot and pull down

HeLa S3 and HEK293 cells were seeded at the density of 1×10^6 into 100 mm cell culture dishes. The day after, cells were washed with PBS and irradiated with a lamp at a dose of 10 or 30 J/m^2 UV-C. The medium was added to the cells, incubated at 37 °C to allow repair and harvested at the indicate post-UV irradiation times.

For blot analysis, the cells were directly lysed in SDS sample buffer (65 mM Tris-HCl pH 7.5, 1% SDS, 30 mM dithiothreitol (DTT), 10% glycerol, 0.02% Bromophenol Blue), or fractionated in soluble and

chromatin-bound fractions, as previously described [23] with minor modifications. The cells were lysed in hypotonic buffer containing 10 mM Tris-HCl (pH 7.4), 2.5 mM $MgCl_2$, 1 mM PMSF, 0.5% Nonidet NP-40, 0.2 mM Na_3VO_4, and a mixture of protease and phosphatase inhibitor cocktails (Sigma). After 10 min on ice, the cells were pelleted by low-speed centrifugation (200 g, 1 min), and the detergent-soluble fraction was recovered. Lysed cells were washed once in hypotonic buffer, followed by a second wash in 10 mM Tris-HCl buffer (pH 7.4), containing 150 mM NaCl, and protease/phosphatase inhibitor cocktails. The cell pellets were then incubated with DNaseI (20U/10^6 cells) in 10 mM Tris-HCl (pH 7.4), 5 mM $MgCl_2$, and 10 mM NaCl for 15 min at 4 °C. After a brief sonication on ice, the samples were centrifuged again (13,000g, 1 min), and the supernatant containing the chromatin-bound fraction was collected. For immunoprecipitation, about 10^7 cells were re-suspended in 1 ml lysis buffer and fractionated as above. Equal amounts of each extract were incubated with anti-DDB2 rabbit polyclonal antibody (Santa Cruz; RRID: AB_2276986), pre-bound to protein G Dynabeads (Invitrogen). Half the amount of each antibody was used for chromatin-bound fractions. The reactions were performed for 3 h at 4 °C under constant agitation. The samples were then centrifuged at 14000g (30 min, 4 °C), and immunocomplexes were washed with ice-cold 50 mM Tris-HCl (pH 7.4) containing 150 mM NaCl, 0.5% Nonidet NP-40. Immunoprecipitated peptides were eluted in SDS sample buffer and resolved by SDS-PAGE (SDS-PAGE). Proteins were electro-transferred to nitrocellulose, then membranes were blocked for 30 min in 5% non-fat milk in PBST buffer and probed with the following primary antibodies: anti-DDB1 (1:1000, Genetex; RRID: AB_1950102), anti-DDB2 (1:500, Santa Cruz; RRID: AB_2088827), anti-PCNA (1:1000, Dako; RRID: AB_2160651), anti-CUL4A (1:500, Sigma; RRID: AB_1847339), anti-XPC (1:1000, Sigma; RRID: AB_796183), anti-p21 (1:500, Santa Cruz; RRID: AB_632121) and anti-actin (1:1000, Sigma; RRID: AB_476730), anti-P-Ser139-H2AX (Biolegend, San Diego, CA; RRID: AB_315794), anti-P-Ser-317-Chk-1 (Cell Signalling; RRID: AB_331488), anti-P-Ser-345-Chk-1 (Cell Signalling RRID: AB_330023) diluted 1:1000, anti-panH2AX (Santa Cruz) diluted 1:1000 and anti-panChk (Santa Cruz, RRID: AB_1121554) diluted 1:500. The membranes were then washed in PBST, incubated for 30 min with appropriate HRP-conjugated secondary antibodies: anti-mouse (DAKO), anti-goat and anti-rabbit (KPL) and revealed using enhanced chemiluminescence. All the pull-down experiments were performed at least 3 times. The densitometric analysis was performed using the public software ImageJ (http://rbs.info.nih.gov/nih-image).

2.7. Clonogenic efficiency

Control and stable transfected HEK293 cells were seeded (1×10^6) in 100 mm cell culture dishes. After two days, cells were exposed to 10 J/m^2 UV-C radiation and immediately trypsinized and harvested and re-seeded (5×10^2) in 60 mm cell culture dishes. The clonogenic efficiency was also assessed with cells that were not exposed to UV-C radiations [19]. After a period of 7–10 days, to prevent the cell confluence, the colonies were stained with Gentian Violet to count their number and to analyze their shape for each cell line. Cells were washes twice in PBS and the Petri dishes were covered with the dye for 20 min under constant stirring. Then, the dye was washed several times with distilled water and the colonies were air dried and counted.

To evaluate morphological features of colonies, control and stable transfected HEK293 cells were seeded (5×10^5) in 35 mm cell culture dishes containing a coverslip. After two days, cells were exposed to 10 J/m^2 UV-C radiation, immediately trypsinized, harvested and re-seeded (2×10^5) on coverslips. After 3 days, the samples were stained with May-Grünwald Giemsa using a standard protocol (May-Grünwald, Merck and Giemsa, Carlo Erba). Number of total cells per colony, dead cells and mitosis were counted and photographed under a digital microscope Nikon Eclipse 80i with a camera Nikon Digital Sight DS-Fi1.

2.8. Wound-healing assay

For cell motility assays, wound healing was performed using the Ibidi Culture-Insert (Madison, WI) according to the manufacturer's instructions. Control and stable transfected HEK293 cells were seeded (1×10^6) in 100 mm cell culture dishes. After two days, cells were exposed to 10 J/m^2 UV-C radiation and immediately trypsinized. 70 μl of cell suspension (7×10^4 cells) were applied to each culture-insert, allowing the cells to grow in the designated areas until a confluent layer was formed at 37 °C. Thereafter, the culture-insert was removed, creating a cell-free gap. Wound closure was monitored daily and photographed starting from 0 to 10 d with an inverted light microscope equipped with a Canon A590 IS camera (Tokyo, JP). The analysis was performed using the public software ImageJ (http://rbs.info.nih.gov/nih-image).

2.9. Statistical analysis

Results are expressed as mean ± standard deviation. Statistical significance was calculated using the Student *t*-test.

3. Results

3.1. Expression of $DDB2^{PCNA-}$ impairs UV-lesion removal

In order to verify the capability of $DDB2^{PCNA-}$ protein in removing the UV-induced DNA damage, untransfected control HEK293 and $DDB2^{WT}$ or $DDB2^{PCNA-}$ stable clones were irradiated and collected at different recovery times, as indicated in the Fig. 1A. Total DNA was extracted, quantified, spotted into nitrocellulose membrane and incubated with CPDs antibody (for detail see Material and Methods). Cells expressing $DDB2^{WT}$ showed an efficient DNA repair, with > 40% of CPD removal at 24 h after UV radiation (Fig. 1A), even higher than that of control cells (about 30%). On the contrary, the mutant clone appeared very slow in repairing these DNA lesions. To exclude any effect of lesion dilution by DNA replication, we performed BrdU assays that show comparable results regarding the proliferation of the two stable clones (Fig. S1 in Supplementary Appendix).

Similarly, in UDS experiments (Fig. 1B and C), unscheduled DNA repair synthesis is strongly reduced in human cells expressing DDB2 mutant protein, whereas no significant modifications were observed in cells expressing $DDB2^{WT}$ protein compared to control cells. These two different approaches demonstrated that the mutated form of DDB2 modifies the cellular response against UV-C induced lesions.

In order to evaluate whether $DDB2^{PCNA-}$ affects directly damaged DNA binding, we performed gel electrophoretic motility shift assay. To this end, damaged plasmid DNA was incubated with each recombinant DDB2 proteins, in the presence of DDB1. $DDB2^{WT}$ bound damaged DNA both 0.5 and 1 h after incubation, as demonstrated by the shift in migration of linearized DNA, which was not revealed in the presence of the mutant protein.

3.2. Impairment of $DDB2^{PCNA-}$ recruitment at DNA damaged sites

To verify the DNA damage site recruitment of DDB2 exogenous proteins, we performed immunofluorescence time course experiments. To this end, we used Hela cells since HEK293 cells do not adhere firmly on the glass surface. Hela cells were transiently transfected with $DDB2^{WT}$ or $DDB2^{PCNA-}$ constructs, locally irradiated, lysed at different time points: 0.5, 1 and 4 h after UV damage and immunostained for DDB2. Fig. 2A shows that the highest percentage of DDB2 positive cells was detected at 1 h after damage in cells expressing DDB2 mutated; instead, the highest recruitment for $DDB2^{WT}$ was observed at 0.5 h, as also evidenced by representative images obtained with confocal microscopy. To confirm this different behaviour, we performed co-localization studies using specific antibodies against DDB2 and CPDs. The

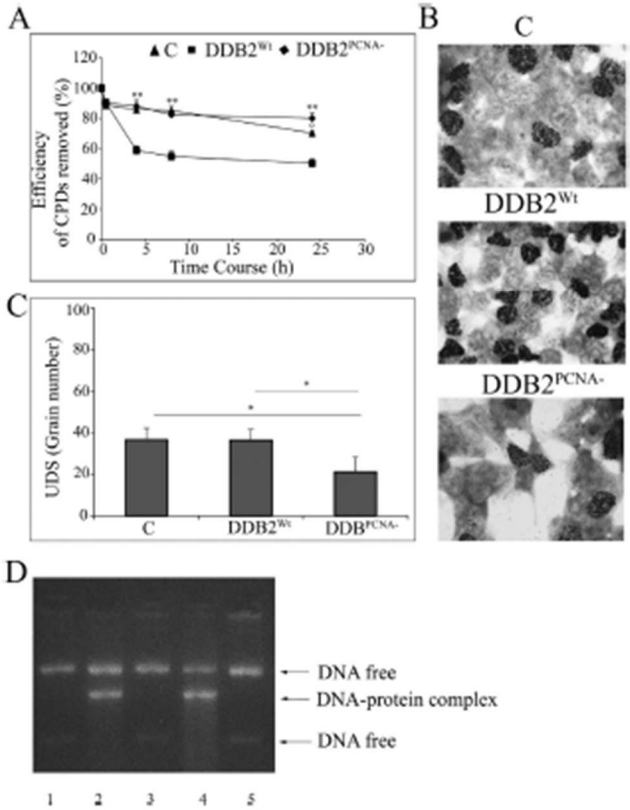

Fig. 1. Effect of the DDB2 mutation on the cells' efficiency to repair the DNA damage after UV-C irradiation. (A) HEK293 control cells, DDB2^{Wt} and DDB2^{PCNA-} stable clones were irradiated (20 J/m^2), collected at the indicated recovery times to detect CPDs removal from DNA. Data are mean ± S.D. from at least three independent experiments; values are expressed in percentage. Asterisks indicate *$p < 0.05$ or **$p < 0.01$ compared to DDB2^{Wt} transfected cells. °$p < 0.05$ compared to HEK293 control cells. (B) HEK293 control cells, DDB2^{Wt} and DDB2^{PCNA-} clones were UV-C irradiated (20 J/m^2), incubated for 2 h in [^{3}H] thymidine and then fixed. UDS is denoted by the presence of nuclear autoradiographic granules. (C) Quantification of UDS grains in nuclei of cells from HEK293 stable clones and control cells treated as above. Mean values of grain number (± S.D.) in triplicate samples are reported. (D) Gel electrophoretic motility shift assay. Damaged plasmid DNA (lane 1), damaged DNA incubated for 30 min (lines 2–3) or 1 h (lanes 4–5) with DDB1 recombinant protein and DDB2^{Wt} (lanes 2–4) or DDB2^{PCNA-} proteins (lanes 3–5).

co-localization images (Figs. 2B and S2) showed that DDB2 mutated protein presents a delayed recruitment at DNA damage sites. In fact, a weak focalized co-localization begins to be detectable only 1 h after UV damage while a diffuse DDB2 staining in all the nuclear area is visible at earlier times. On the contrary, DDB2^{Wt} is distinctly and significantly recruited at foci already 0.5 h after irradiation.

Time-course experiments to analyze the recruitment of DDB2 and XPC proteins (Fig. 2C) showed a very early chromatin association of XPC protein and DDB2^{Wt}, indicating 5 min after DNA damage as the best time for co-localization between these two NER proteins. Whereas, the recruitment of the two proteins occurred significantly only 1 h after UV-damage induction in the presence of the mutated form of DDB2 (Figs. 2C and S3 in Supplementary Appendix).

Altogether, the collected data show that the mutated DDB2^{PCNA-} modifies the kinetic of co-localization with CPDs and/or XPC protein, thus suggesting a delay in the initiation of the repair process.

3.3. DDB2 mutation delays initiation of the NER process

In order to understand the mechanism underlying the different recruitment of DDB2 mutant protein, the interaction of DDB2 with crucial NER proteins was investigated. To this end, immunoprecipitation of proteins recruited at DNA was performed in HeLa cells expressing DDB2^{Wt} or DDB2^{PCNA-}. In Fig. 3, soluble and chromatin bound fractions derived from irradiated cells, harvested at 0.5 and 1 h after UV damage, showed three important differences: i) the persistence of the DDB2^{PCNA-} protein bound to the DNA until 1 h from the irradiation. As expected, no bands of PCNA were detectable in the specific lane, indicating that the protein is not able to immunoprecipitate with DDB2, and confirming that the mutation introduced in the PIP-box is actually able to prevent the interaction between the two proteins (Fig. 3D). (ii) The association between DDB2^{PCNA-} and DDB1 was already detectable in the chromatin fraction immediately after the irradiation, and it increased with the recovery time after DNA damage. A similar trend was observed for XPC protein, whose interaction with DDB2^{PCNA-} increased with time, reaching the highest value at 1 h. The latter result is markedly different from that obtained with the Wt protein, where the XPC level was maximum at 0.5 h (Fig. 3B). (iii) The last aspect, regarding DDB2^{PCNA-}/Cul4A interaction, showed again a shifted forward of their association, compared to the results obtained with DDB2^{Wt}, where already at 0.5 h the Cul4A protein level was of lower intensity (Fig. 3B). This early interaction between DDB2^{Wt} and NER proteins has already been demonstrated [18]. Taken together, these results confirm a delay in NER machinery initiation when DDB2 presents a mutation in the PIP-box.

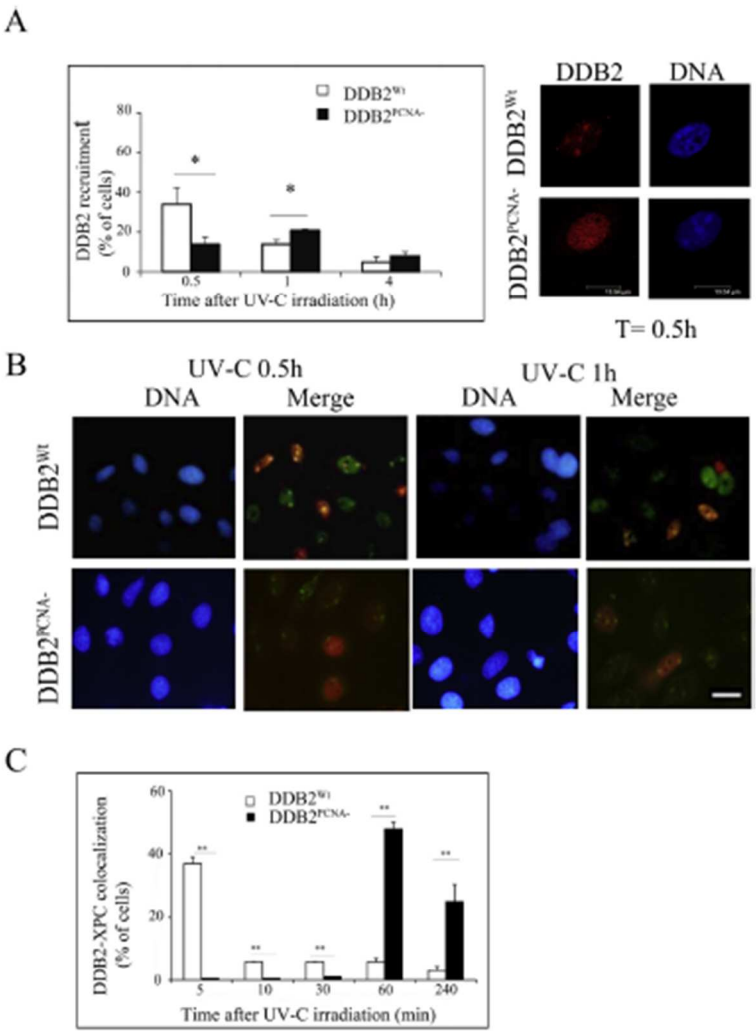

Fig. 2. Recruitment of DDB2 and NER proteins to DNA repair sites. (A) HeLa cells expressing $DDB2^{Wt}$ or $DDB2^{PCNA-}$ were exposed to local UV-C radiation (100 J/m²) through filters with 3 μm pores. After 0.5, 1 and 4 h, irradiated cells were extracted *in situ* and fixed for immunofluorescence staining with anti-DDB2 antibody. Results from $DDB2^{Wt}$ (empty bars) and $DDB2^{PCNA-}$ (black bars) clones were shown. Besides, representative confocal images of the DDB2 recruitment (0.5 h after UV-C) on DNA damage site in $DDB2^{Wt}$ and $DDB2^{PCNA-}$ cells were presented. Scale bar = 13.54 μm. (B) HeLa cells were transfected with pcDNA3.1-$DDB2^{Wt}$ or pcDNA3.1-$DDB2^{PCNA-}$ expression vectors and 24 h later exposed to local UV-C radiation (100 J/m²). Half and 1 h later, samples were extracted *in situ* and fixed for immunofluorescence determination CPDs (green) and DDB2 (red), respectively. In the merged images, spots of colocalization (yellow) are clearly visible. DNA (blue fluorescence) was stained with Hoechst 33258. Scale bar = 20 μm. (C) HeLa cells expressing DDB2 wild type or mutated form were locally irradiated (UV-C 100 J/m²). DDB2-XPC co-localization was analyzed at 5, 10, 30, 60, 240 min after UV-C damage and the percentages of positive cells were reported. * $p < 0.05$ and ** $p < 0.01$. (For interpretation of the references to color in this figure legend, the reader is referred to the web version of this article.)

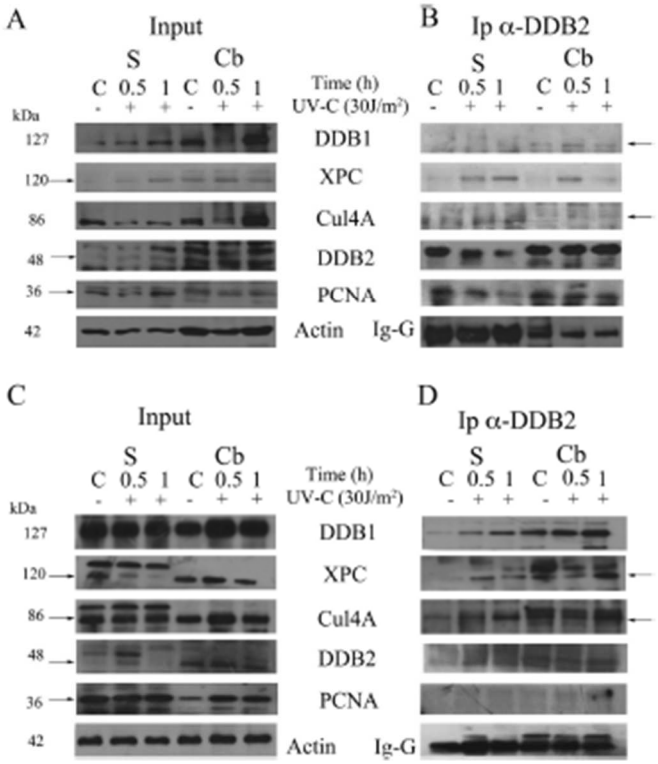

Fig. 3. DDB2 interaction with NER proteins. HeLa cells transfected with pcDNA3.1-DDB2^{WT} and pcDNA3.1-DDB2^{PCNA-} plasmids were grown for 24 h and collected 0.5 and 1 h after UV-C irradiation (30 J/m^2), as described in "Materials and Methods". Cells were fractionated in soluble (S) and chromatin-bound (Cb) samples for immunoprecipitation and analyzed by Western blot. (A–C) Input load: 1/30 of cell extract. (B–D) Immunoprecipitation (Ip) with anti-DDB2 antibody on fractionated cell extracts, as indicated above. Arrows indicate the specific protein bands.

3.4. DDB2^{PCNA-} influences cell growth and motility after UV-C irradiation

We have previously shown that the expression of DDB2^{PCNA-} protein resulted in an increased cell proliferation [19]. To evaluate the effect of DDB2^{PCNA-} protein on cellular growth following DNA damage, we performed a clonogenic assay using HEK293 stable clones irradiated, seeded in 60 mm Petri dishes and incubated for 10 days to allow colony formation.

The results showed that stable DDB2^{PCNA-} clone produces more colonies, characterized also by a larger size, than those observed in cells expressing DDB2^{WT}. As expected, control cells did not grow after UV irradiation and only very few and faded colonies were present (Fig. 4A). All data are summarized in Fig. 4B in which is pointed out that the presence of exogenous DDB2, both wild-type and even more, the mutated form, unexpectedly determined an increase in cell survival after UV irradiation. Similarly, visual scoring of 3 days growing colonies stained with May-Grünwald Giemsa after UV-C irradiation confirmed that the number of cells per colony is higher in both wild-type and, even more, in the mutated clone respect to control cells. In contrast, dead cells are more numerous in the last one, and rare in DDB2^{PCNA-} stable clone. Finally, although the number of mitosis appeared comparable in the both clones, atypical forms are significantly increased in the DDB2 mutated cells (Fig. 4C and D).

Next, we investigated whether DDB2 stable expression could also influence cell motility. HEK293 stable clones exposed to UV-C radiation were seeded and wound healing assay was carried out. Fig. 4C shows representative images obtained by time-course experiments, starting from the cell wall (cell front) formation at time 0 until 10 days later. Cell motility, and consequently the ability to reconstitute the cell monolayer, started to be evident 7 days after UV irradiation, mainly in cells expressing exogenous DDB2 proteins. At this time, a higher cell motility and growth was observable in the presence of DDB2^{PCNA-}; in fact, cells were able to form dense multilayer of growing cells, evident in both cellular walls. The same feature was detectable two days later (9 d) in cells producing DDB2^{WT} when, in the presence of DDB2^{PCNA-}, the wound healing was entirely filled up.

In addition, the disordered and persistent growth in cells expressing DDB2 mutant protein suggests a major UV-C resistance acquired by this clone.

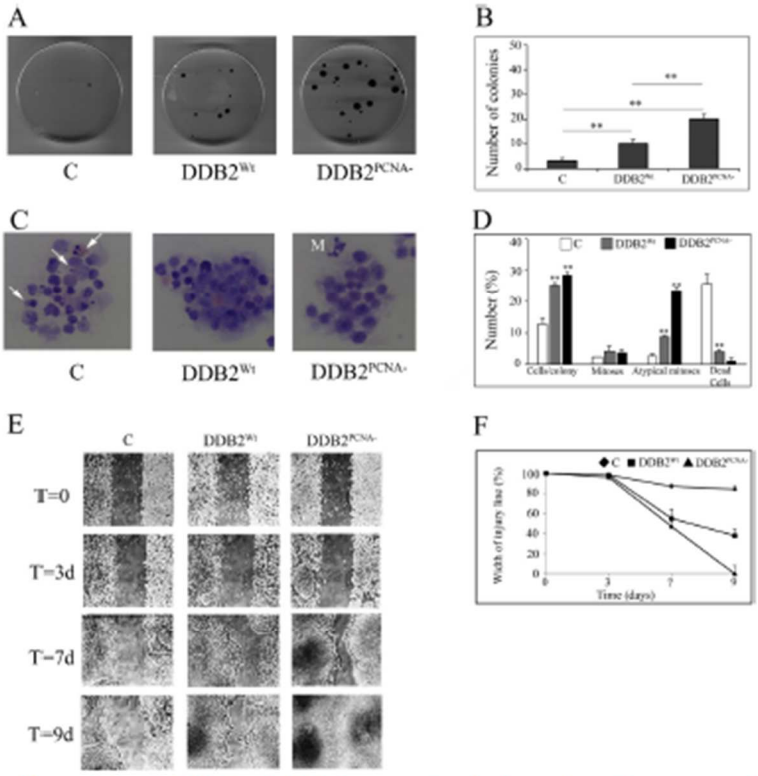

Fig. 4. Clonogenic efficiency and cell motility of DDB2^{Wt} and DDB2^{PCNA-} clones after UV-induced DNA damage. HEK293 cells were seeded at the density of 1×10^6 into 100 mm cell culture dishes, irradiated (10 J/m^2 UV-C) and immediately harvested and re-seeded (5×10^5) both in 60 mm cell culture dishes for colony growth and (7×10^4) in culture-insert for wound-healing assay. (A) Representative images of colonies formed by control HEK293 cells, DDB2^{Wt} and DDB2^{PCNA-} stable clones. After 10 days, the colonies were fixed, stained with crystal violet and then counted. Mean values (± S.D.) are reported from 3 independent experiments. (B) Number of colonies grown of DDB2^{Wt} and DDB2^{PCNA-} clones vs. control cells. * $p < 0.05$ and ** $p < 0.01$. (C and D) Morphological features of May-Grünwald Giemsa-stained growing colonies of control, DDB2^{Wt} and DDB2^{PCNA-} stable clones. Most of the cells in control colonies are dead (arrows) compared to the stable clones. Representative atypical mitosis (M) in DDB2^{PCNA-} stable clone. (E) Representative processed images of cell motility (× 10 magnification objective) of control HEK293 cells, DDB2^{Wt} and mutated clones. (F) Migration rate quantification of HEK293 control and stable clones; data are the mean ± S.D. from at least three independent experiments, normalized to 100% wound closure for untreated cells.

3.5. Reduction on p21 protein level in the presence of DDB2^{PCNA-}

To further understand whether the above results could be dependent on cell cycle regulator factors, p21 protein level were investigated. Our previous data have demonstrated that lower level of this cell cycle inhibitor was related to high cell proliferation rate, in the presence of DDB2^{Wt} and even more with the mutated form [19]. To perform a kinetic analysis of p21 protein level, cells were collected and its amount evaluated by Western blot analysis at 1, 3, 6 and 24 h after UV damage (Fig. 5A). The results reported in Fig. 5B show a rapid decrease in p21 levels, both in control and in DDB2^{Wt} samples; the presence of DDB2^{PCNA-} appears to further reduce this protein. At longer times after UV-damage, p21 protein level remains low and similar in the control and DDB2 stable clones (Supplemental Fig. S4).

3.6. DDB2^{PCNA-} causes defective cell cycle checkpoints activation

To go further insight into the molecular pathway responsible for the loss of cell proliferation control after UV-C exposure, the expression of some key proteins involved in the checkpoints activation was investigated. In particular, the phosphorylated form of the histone H2AX (γ-H2AX), playing a key role in the signalling pathway of genomic damage, was the first protein analysed by Western blot (Fig 6A and B). For this purpose, HEK293 control cells and stable clones DDB2^{Wt} and DDB2^{PCNA-} were irradiated with UV-C (10 J/m^2) and then recovered for 0.5 and 1 h. Cells of each non-irradiated line were kept as negative control. The results showed that the ectopic expression of DDB2^{Wt} did not influence the activation kinetics of the histone H2AX, as compared with control cells in which a statistically significant increase was observed after the induction of DNA damage. High basal levels of γ-H2AX

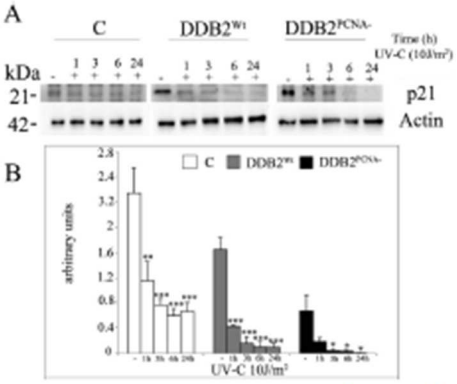

Fig. 5. p21 protein levels in control HEK293 cells, DDB2^{W1} and DDB2^{PCNA-} stable clones at the indicated time point after UV-C irradiation. HEK293 control cells and DDB2 cell clones were plated (1×10^6) in 100 mm cell culture dishes, irradiated (10 J/m^2 UV-C) and harvested at different times. (A) Representative image from Western blot analysis of samples from control and DDB2 cell clones, in which the level of p21 and actin are shown. (B) p21 protein levels normalized to actin values through densitometric analysis. Mean values (± S.D.) are from 3 independent experiments. *$p < 0.05$ and **$p < 0.01$.

was found in cells expressing the mutant form of DDB2 in which no further increase was found one hour after UV irradiation. These data suggest that loss of interaction between DDB2 and PCNA negatively affects the cell response that should be activated immediately after the damage.

Considering both mitotic activity and defective signalling of DNA damage in cells expressing DDB2^{PCNA-}, levels of the phosphorylated forms of Chk1 protein, that plays an important role in blocking cell cycle progression, were considered (Fig. 6A e B). Specifically, this protein is part of the G2/M phase checkpoint that monitors and regulates cellular mitosis. Fig. 6 shows the results of the analysis of the phosphorylated forms of Chk1 (Chk1-P) on both serine 317 (S317) and serine 345 (S345). The increase in the phosphorylation levels of this protein is comparable between the control and the stable DDB2^{WT} clone, indicating that the checkpoint is correctly activated after the DNA damage. In the presence of DDB2^{PCNA-}, however, no activation is detected. In addition, the Chk1-P (S317), as well Chk1-P (S345) levels are low, opening to the hypothesis that the loss of control of this checkpoint could drive cells to mitosis, without repairing DNA damage.

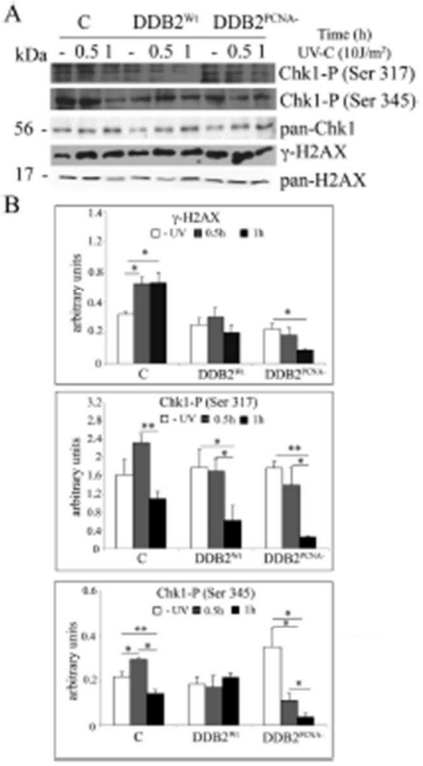

Fig. 6. Checkpoint activation in control HEK293 cells, DDB2^{W1} and DDB2^{PCNA-} stable clones after UV-induced cell damage. HEK293 control cells and DDB2 cell clones were plated (1×10^6) in 100 mm cell culture dishes, irradiated (10 J/m^2 UV-C) and harvested at different times as indicated in the figure. In (A) representative images of γ-H2AX (Ser139), Chk1-P (Ser317), Chk1-P (Ser345) obtained by Western blot. (B) Protein levels normalized to pan-H2AX and pan-Chk1 values through densitometric analysis. Mean values (± S.D.), obtained from 3 independent experiments, were reported. *$p < 0.05$ and **$p < 0.01$.

4. Discussion

The UV rays are responsible for the induction of pyrimidine dimers which, if not removed, can cause genetic instability, mutations and the onset of skin cancer. In fact, some diseases with a defect of the NER machinery (e.g. *Xeroderma pigmentosum*) are characterized by high photosensitivity and high incidence of skin cancers [24].

The DDB2 role in tumorigenesis is still debated since different DDB2 expression levels in human cancer have been reported [13–15]. In addition, the DDB2 involvement in the epithelial to mesenchymal transition in cancer cells has been described [16] whereas its overexpression inhibits tumorigenesis [17].

We have previously demonstrated that mutations in DDB2 PIP-box, a conserved sequence useful to direct interaction with PCNA, promote cell cycle progression [19]. In the present study, we sought to investigate the role of DDB2-PCNA association in the cell response to UV-induced DNA damage. Our results have shown that expression of the mutant DDB2 form unable to interact with PCNA impaired DNA repair, that may be explained by inefficient binding to damaged DNA *in vitro*. Remarkably, the DDB2^{PCNA-} cells acquired uncontrolled cell growth, as indicated by an increased resistance to UV irradiation and also a more aggressive phenotype, as suggested by wound healing experiments. Explanation of such proliferative behaviour appears to be related to a defect in cell cycle checkpoint signalling, since DDB2^{PCNA-} cells show aberrant phosphorylation of H2AX and Chk1 both before and after UV-induced DNA damage. Interestingly, it has been previously reported that DDB2 influences checkpoint activation after UV-damage and, in particular, regulate H2AX and Chk1 phosphorylation [25]. In addition, it has been reported that DDB2 protein level can regulate Chk1 phosphorylation influencing ATR recruitment on chromatin, as well as in signalling checkpoint termination [26,27]. Therefore, our results are in agreement with these findings, and suggest that failure to correctly activate the cell cycle checkpoint could have provided the DDB2^{PCNA-}

cells with an enhanced proliferation and motility, two characteristic hallmarks of tumours. Accordingly, in DDB2^{PCNA-} irradiated cells a higher number of atypical mitosis has been detected in respect to the Wt stable clone or, even more, to control cells. Furthermore, UV-resistance phenotype of both clones is highlighted by the rare events of cell death. These results are also in agreement with the tumour-prone phenotype shown by DDB2-deficient mice, in which the inefficient DNA repair function has been related with the properties of increased cell proliferation and adhesion typical of the cancer phenotype [28,29].

Many papers have demonstrated that p21 has a role in modulating DNA repair process [30–34]. In particular, it has been reported a co-operation between DDB2 and p21 proteins in the cellular response to UV radiation [14,35], besides the DDB2 role in modulating p21 levels after DNA damage [12]. In our experimental model we have found that DDB2-PCNA interaction may have a role to prevent uncontrolled cell proliferation. In fact, in the presence of the DDB2 mutant protein, very low level of p21 was detected, associated to an increased cellular growth and motility.

Based on our results, we speculate that the DDB2-PCNA interaction may have a role in regulating cell cycle progression; in DDB2^{PCNA-} stable clone, the defective checkpoint activation, together with a delayed DNA repair process, could license the cells to enter mitosis even in the presence of unrepaired DNA. The results from clonogenic assay support this hypothesis, driving cells to acquire new capabilities such as uncontrolled cell growth and increased resistance to UV irradiation.

Taken together, the binding between DDB2 and PCNA could play a fundamental role in the correct removing of the UV-C induced DNA damage and its impairment may determine the acquisition of a phenotype characterized by proliferation advantage.

Supplementary data for this article can be accessed on the publisher's website. Supplementary data associated with this article can be found in the online version, at doi: https://doi.org/10.1016/j.bbamcr.2018.03.012

Transparency document

The http://dx.doi.org/10.1016/j.bbamcr.2018.03.012 associated with this article can be found in online version.

Acknowledgments

We thank P. Vaghi (Centro Grandi Strumenti, Università di Pavia) for help in confocal microscopy analysis and C. Scalera for technical help.

References

[1] A.F. Fagbemi, B. Orelli, O.D. Schærer, Regulation of endonuclease activity in human nucleotide excision repair, DNA Repair 10 (2011) 722–729, http://dx.doi.org/10.1016/j.dnarep.2011.04.022.

[2] R.D. Wood, Mammalian nucleotide excision repair proteins and interstrand crosslink repair, Environ. Mol. Mutagen. 51 (2010) 520–526, http://dx.doi.org/10.1002/em.20569.

[3] E.C. Friedberg, How nucleotide excision repair protects against cancer, Nat. Rev. Cancer 1 (2001) 22–33, http://dx.doi.org/10.1038/35094000.

[4] M.E. Fitch, S. Nakajima, A. Yasui, J.M. Ford, In vivo recruitment of XPC to UV-induced cyclobutane pyrimidine dimers by the DDB2 gene product, J. Biol. Chem. 278 (2003) 46906–46910, http://dx.doi.org/10.1074/jbc.M308725200.

[5] J. Moser, M. Volker, H. Kool, S. Alekseev, H. Vrieling, A. Yasui, A.A. van Zeeland, L.H. Mullenders, The UV-damaged DNA binding protein mediates efficient targeting of the nucleotide excision repair complex to UV-induced photo lesions, DNA Repair 4 (2005) 571–582, http://dx.doi.org/10.1016/j.dnarep.2005.01.001.

[6] P. Shiyanov, A. Nag, P. Raychaudhuri, Cullin 4A associates with the UV damaged DNA-binding protein DDB, J. Biol. Chem. 274 (1999) 35309–35312.

[7] A. Datta, S. Bagchi, A. Nag, P. Shiyanov, G.R. Adami, T. Yoon, P. Raychaudhuri, The p48 subunit of the damaged-DNA binding protein DDB associates with the CBP/p300 family of histone acetyltransferase, Mutat. Res. 486 (2001) 89–97.

[8] K. Sugasawa, Y. Okuda, M. Saijo, R. Nishi, N. Matsuda, G. Chu, T. Mori, S. Iwai, K. Tanaka, K. Tanaka, F. Hanaoka, UV-induced ubiquitylation of XPC protein mediated by UV-DDB-ubiquitin ligase complex, Cell 121 (2005) 387–400, http://dx.doi.org/10.1016/j.cell.2005.02.035.

[9] J. Li, Q.E. Wang, Q. Zhu, M.A. El-Mahdy, G. Wani, M. Praetorius-Ibba, A.A. Wani, DNA damage binding protein component DDB1 participates in nucleotide excision repair through DDB2 DNA-binding and cullin 4A ubiquitin ligase activity, Cancer Res. 66 (2006) 8590–8597, http://dx.doi.org/10.1158/0008-5472.CAN-06-1115.

[10] M.G. Kapetanaki, J. Guerrero-Santoro, D.C. Bisi, C.L. Hsieh, V. Rapić-Otrin, A.S. Levine, The DDB1-CUL4ADDB2 ubiquitin ligase is deficient in xeroderma pigmentosum group E and targets histone H2A at UV-damaged DNA sites, Proc. Natl. Acad. Sci. USA 103 (2006) 2588–2593, http://dx.doi.org/10.1073/pnas.0511160103.

[11] E. Martinez, V.B. Palhan, A. Tjernberg, E.S. Lymar, A.M. Gamper, T.K. Kundu, B.T. Chait, R.G. Roeder, Human STAGA complex is a chromatin-acetylating transcription coactivator that interacts with pre-mRNA splicing and DNA damage-binding factors in vivo, Mol. Cell. Biol. 21 (2001) 6782–6795, http://dx.doi.org/10.1128/MCB.21.20.6782-6795.2001.

[12] T. Stoyanova, T. Yoon, D. Kopanja, M.B. Mokyr, P. Raychaudhuri, The xeroderma pigmentosum group E gene product DDB2 activates nucleotide excision repair by regulating the level of p21Waf1/Cip1, Mol. Cell. Biol. 28 (2008) 177–187, http://dx.doi.org/10.1128/MCB.00880-07.

[13] B.M. Bankole, Q.E. Wang, C. Han, K. Miliam, D.T. Yin, Q. Zhao, G. Wani, el-SA Arafa, M.A. El-Mahdy, A.A. Wani, Overexpression of DDB2 enhances the sensitivity of human ovarian cancer cells to cisplatin by augmenting cellular apoptosis, Int. J. Cancer 127 (2010) 977–988, http://dx.doi.org/10.1002/ijc.25112.

[14] T. Stoyanova, N. Roy, S. Bhattacharjee, D. Kopanja, T. Valli, S. Bagchi, P. Raychaudhuri, p21 cooperates with DDB2 protein in suppression of ultraviolet ray-induced skin malignancies, J. Biol. Chem. 287 (2012) 3019–3028, http://dx.doi.org/10.1074/jbc.M111.295816.

[15] M. Brown, R. Klotz, N. Touche, S. Pinel, C. Barbieux, V. Beuzenoen, E. Brunner, D. Thiebaut, A.C. Jung, S. Ledeppipier, L. Domenjoud, J. Abecassis, F. Pflimlin, S. Grandemange, P. Becuwe, DDB2: a novel regulator of NF-κB and breast tumor invasion, Cancer Res. 73 (2013) 5040–5052, http://dx.doi.org/10.1158/0008-5472.CAN-12-3605.

[16] N. Roy, P.V. Bommi, U.G. Bhat, S. Bhattacharjee, I. Elangovan, J. Li, K.C. Patra, D. Kopanja, A. Hunter, R. Benya, S. Bagchi, P. Raychaudhuri, DDB2 suppresses epithelial-to-mesenchymal transition in colon cancer, Cancer Res. 73 (2013) 3771–3782, http://dx.doi.org/10.1158/0008-5472.CAN-12-4069.

[17] C. Han, R. Zhan, X. Liu, A. Srivastava, L. Gong, H. Mao, M. Qu, W. Zhao, J. Yu, Q.E. Wang, DDB2 suppresses tumorigenicity by limiting the cancer stem cell population in ovarian cancer, Mol. Cancer Res. 12 (2014) 784–794, http://dx.doi.org/10.1158/1541-7786.MCR-13-0638.

[18] G. Cazzalini, P. Perucca, R. Macchi, S. Sommariva, E. Prospert, L.A. Stivala, DDB2 association with PCNA is required for its degradation after UV-induced DNA damage, Cell Cycle 13 (2014) 240–248, http://dx.doi.org/10.4161/cc.26987.

[19] P. Perucca, S. Sommariva, R. Macchi, E. Prospert, L.A. Stivala, G. Cazzalini, A DDB2 mutant protein unable to interact with PCNA promotes cell cycle progression of human transformed embryonic kidney cells, Cell Cycle 14 (2015) 3920–3928, http://dx.doi.org/10.1080/15384101.2015.1120921.

[20] L.A. Stivala, F. Riva, G. Cazzalini, M. Savio, E. Prospert, p21(waf1/cip1)-null human fibroblasts are deficient in nucleotide excision repair downstream the recruitment of PCNA to DNA repair sites, Oncogene 20 (2001) 563–570, http://dx.doi.org/10.1038/sj.onc.1204132.

[21] G. Cazzalini, S. Sommariva, M. Villhon, I. Dutto, A. Bachi, A. Rapp, T. Nardo, A.I. Scovassi, D. Necchi, M.C. Cardoso, L.A. Stivala, E. Prospert, CBP and p300 acetylate PCNA to link its degradation with nucleotide excision repair synthesis, Nucleic Acids Res. 42 (2014) 8433–8448, http://dx.doi.org/10.1093/nar/gku533.

[22] Q. Wei, J.Z. Lee, J.E. Gershenwald, M.I. Ross, P.F. Mansfield, S.S. Strom, L.E. Wang, Z. Guo, Y. Qiao, G.I. Amos, M.R. Spitz, M. Duvic, Repair of UV light-induced DNA damage and risk of cutaneous malignant melanoma, J. Natl. Cancer Inst. 95 (2003) 308–315.

[23] F. Riva, M. Savio, O. Cazzalini, L.A. Stivala, I.A. Scovassi, L.S. Cox, R. Ducommun, E. Prospert, Distinct pools of proliferating cell nuclear antigen associated to DNA replication sites interact with the p125 subunit of DNA polymerase delta or DNA ligase I, Exp. Cell Res. 293 (2004) 357–367.

[24] J. Tang, G. Chu, Xeroderma pigmentosum complementation group E and UV-damaged DNA-binding protein, DNA Repair 1 (2002) 601–616.

[25] A. Ray, K. Milum, A. Battu, G. Wani, A.A. Wani, NER initiation factors, DDB2 and XPC, regulate UV radiation response by recruiting ATR and ATM kinases to DNA damage sites, DNA Repair 12 (2013) 273–283, http://dx.doi.org/10.1016/j.dnarep.2013.01.003.

[26] N. Zou, G. Xie, T. Cui, A.K. Srivastava, M. Qu, L. Yang, S. Wei, Y. Zheng, Q.E. Wang, DDB2 increases radioresistance of NSCLC cells by enhancing DNA damage response, Tumour Biol. 37 (2016) 14183–14191, http://dx.doi.org/10.1007/s13277-016-5203-y.

[27] Q. Zhu, S. Wei, N. Sharma, G. Wani, J. He, A.A. Wani, A.A. Human, CUL4DDB2 ubiquitin ligase preferentially regulates post-repair chromatin restoration of H3K56Ac through recruitment of histone chaperon CAF-1, Oncotarget 8 (2017) 10452–10464.

[28] S.Y. Zhang, S.C. Liu, L.F. Al-Saleem, D. Holllstein, J. Ballrb, X. Guo, A.J. Klein-Szanto, E2F-1: a proliferative marker of breast neoplasia, Cancer Epidemiol. Biomark. Prev. 9 (2000) 395–401.

[29] T. Yoon, A. Chakraborty, R. Franko, T. Valli, H. Kiyokawa, P. Raychaudhuri, Tumor-prone phenotype of the DDB2-deficient mice, Oncogene 24 (2005) 469–478, http://dx.doi.org/10.1038/sj.onc.1208211.

[30] P. Perucca, G. Cazzalini, O. Mortusewicz, D. Necchi, M. Savio, T. Nardo, L.A. Stivala, H. Leonhardt, M.C. Cardoso, E. Prospert, Spatiotemporal dynamics of p21CDKN1A protein recruitment to DNA-damage sites and interaction with proliferating cell nuclear antigen, J. Cell Sci. 119 (2006) 1517–1527, http://dx.doi.

org/10.1242/jcs.021808.
[31] O. Cazzalini, A.I. Scovassi, M. Savio, L.A. Stivala, E. Prosperi, Multiple roles of the cell cycle inhibitor p21 (CDKN1A) in the DNA damage response, Mutat. Res. 704 (2010) 12–20, http://dx.doi.org/10.1016/j.mrrev.2010.01.009.
[32] G. Sorda, V. Gottifredi, PCNA-coupled p21 degradation after DNA damage: the exception that confirms the rule? DNA Repair 9 (2010) 358–364, http://dx.doi.org/10.1016/j.dnarep.2009.12.003.
[33] A. Karimian, Y. Ahmadi, B. Yousefi, Multiple functions of p21 in cell cycle, apoptosis and transcriptional regulation after DNA damage, DNA Repair 42 (2016) 63–71, http://dx.doi.org/10.1016/j.dnarep.2016.04.008.
[34] A.G. Georgakilas, O.A. Martin, W.M. Bonner, p21: a two-faced genome guardian, Trends Mol. Med. 23 (2017) 310–319, http://dx.doi.org/10.1016/j.molmed.2017.02.001.
[35] H. Li, X.P. Zhang, F. Liu, Coordination between p21 and DDB2 in the cellular response to UV radiation, PLoS One 8 (2013) e80111, , http://dx.doi.org/10.1371/journal.pone.0080111.

Bassi et al. BMC Cancer (2019) 19:1013
https://doi.org/10.1186/s12885-019-6258-0

BMC Cancer

RESEARCH ARTICLE Open Access

Exploring new potential role of DDB2 by host cell reactivation assay in human tumorigenic cells

Elisabetta Bassi[1], Paola Perucca[1], Isabella Guardamagna[1], Ennio Prosperi[2*], Lucia A. Stivala[1*] and Ornella Cazzalini[1*]

Abstract

Background: The Host Cell Reactivation assay (HCR) allows studying the DNA repair capability in different types of human cells. This assay was carried out to assess the ability in removing UV-lesions from DNA, thus verifying NER efficiency. Previously we have shown that DDB2, a protein involved in the Global Genome Repair, interacts directly with PCNA and, in human cells, the loss of this interaction affects DNA repair machinery. In addition, a mutant form unable to interact with PCNA ($DDB2^{PCNA-}$), has shown a reduced ability to interact with a UV-damaged DNA plasmid in vitro.

Methods: In this work, we have investigated whether DDB2 protein may influence the repair of a UV-damaged DNA plasmid into the cellular environment by applying the HCR method. To this end, human kidney 293 stable clones, expressing $DDB2^{Wt}$ or $DDB2^{PCNA-}$, were co-transfected with pmRFP-N2 and UV-irradiated pEGFP-reported plasmids. Moreover, the co-localization between DDB2 proteins and different NER factors recruited at DNA damaged sites was analysed by immunofluorescence and confocal microscopy.

Results: The results have shown that $DDB2^{Wt}$ recognize and repair the UV-induced lesions in plasmidic DNA transfected in the cells, whereas a delay in these processes were observed in the presence of $DDB2^{PCNA-}$, as also confirmed by the different extent of co-localization of $DDB2^{Wt}$ and some NER proteins (such as XPG), vs the DDB2 mutant form.

Conclusion: The HCR confirms itself as a very helpful approach to assess in the cellular context the effect of expressing mutant vs Wt NER proteins on the DNA damage response. Loss of interaction of DDB2 and PCNA affects negatively DNA repair efficiency.

Keywords: DNA damage response, DNA damaged binding protein 2, Global genome nucleotide excision repair, *Xeroderma Pigmentosum* group G, RNA polymerase II

Background

DNA damaged binding protein 2 (DDB2) plays a crucial role in DNA Damage Response (DDR) activated by UV radiation [1]. This protein is known to act as an important sensor in the Global Genome Nucleotide Excision Repair (GG-NER) by recognizing sites of UV-induced DNA lesions [2]. This function is shared with DDB1, which associates to DDB2 to form the heterodimeric UV-damaged DNA-binding protein complex (UV-DDB); this complex initiates GG-NER by recognizing photodimers (CPDs) and 6–4 photoproducts (PPs), the primary type of lesions induced by UV irradiation. The distortion of the double helix caused by the CPDs is smaller than that of 6-4PPs, and their recognition is performed by the synchronized work of UV-DDB complex and XPC protein [3]. Mutations in NER genes are linked to human genetic diseases (e.g. Xeroderma pigmentosum) as well as cancer predisposition [4–6].

The mutagenic effect of UV is efficiently neutralized by DNA repair processes involving not only GG-NER but also the transcription-coupled nucleotide excision repair (TC-NER), a sub-pathway that preferentially removes DNA lesions generated in highly transcribed DNA regions

* Correspondence: prosperi@igm.cnr.it; luciaanna.stivala@unipv.it; ornella.cazzalini@unipv.it
[2]Istituto di Genetica Molecolare (IGM) del CNR, Pavia, Italy
[1]Dipartimento di Medicina Molecolare, Unità di Immunologia e Patologia generale, Università degli Studi di Pavia, Pavia, Italy

[7]. At the molecular level, both these processes are promoted and regulated by various post-translational modifications of NER factors and chromatin substrate. While GG-NER employs UV-DDB heterodimer and XPC complex to initiate the DNA repair process, TC-NER utilizes elongating RNA polymerase II (Pol II) and Cockayne syndrome B (CSB) proteins as damage sensors [8].

We have previously demonstrated that the interaction between DDB2 and PCNA is important to remove DNA lesions by NER. In fact, a mutated form of DDB2, unable to interact with PCNA ($DDB2^{PCNA-}$), causes a delay in UV-induced NER process activation and confers proliferative and migratory advantages in HEK293 stable clone expressing $DDB2^{PCNA-}$ [9, 10].

In addition, using gel electrophoretic motility shift assay, we showed that $DDB2^{Wt}$ recombinant protein retains the ability to bind directly plasmidic UV-damaged DNA, but not the DDB2 mutated form [10]. Nevertheless, this finding does not prove that $DDB2^{PCNA-}$ since the mutant form at the cellular level localized to DNA damage sites and interact with DDB1 [10]. To clarify this issue, we decided to apply a transfection-based assay, named Host Cell Reactivation (HCR), to investigate DNA lesions removal efficacy in the presence of $DDB2^{Wt}$ protein or DDB2 mutated one. This method allows studying the DNA repair capability in different types of human cells [11] and may be employed as a marker for genetic instability and cancer risk [12, 13]. A subsequent adaptation to FACS technology further improved its sensitivity, compared to the previous luminometer method [14]. The HCR assay assesses repair of a transcriptionally active genes and, once applied to UV lesions, it measures the capacity of the host cells to perform NER [15].

In order to investigate whether DDB2 protein interacts with nude plasmidic UV-damaged DNA in cellular environment and whether the mutation in DDB2 interferes with DNA repair kinetic, we used two stable clones of HEK293 expressing $DDB2^{Wt}$ or $DDB2^{PCNA-}$. HCR assay was performed co-transfecting these cells with UV-C irradiated pEGFP-N1 and not irradiated pmRFP-N2 plasmids. To further elucidate the ability of $DDB2^{Wt}$ and mutant form to interact with transcription machinery, co-localization to the UV-damaged sites between RNA polymerase II (Pol II), a protein sensor of DNA lesions in transcribed genes, was also considered. Finally, DDB2 recruitment and co-localization with XPG was detected to assess potential modifications in the DNA excision step kinetic.

Methods

Cell lines and transfection

HEK293 (Human Embryonic Kidney) cell line was purchased from the European Tissue culture Collection (ECACC) (catalogue code: 85120602). Cells were cultured in Dulbecco's modified Eagle's medium (DMEM, Sigma) supplemented with 10% foetal bovine serum (Life Technologies-Gibco), 2 mM l-glutamine (Life Technologies-Gibco), 100 U/ml penicillin, 100 μg/ml streptomycin in a 5% CO_2 atmosphere.

Cell lines (50% confluent) were stably transfected with $DDB2^{Wt}$ construct kindly provided by dr. Q. Wang [16] or the mutated form $DDB2^{PCNA-}$ using Effectene transfection reagent (Qiagen). $DDB2^{PCNA-}$ mutated in PIP-BOX region was produced in our laboratory, as previously described [9].

HeLa S3 cell line was purchased from European Tissue Culture Collection (ECACC, catalogue code: 87110901). HeLa cells were cultured as above, seeded on coverslips (70% confluent) and transiently transfected with DDB2 wild-type or mutated form constructs as previously described [9]. Both cell lines were periodically tested for mycoplasma contamination.

UV plasmid preparation

pEGFP-N1 (Clontech) was irradiated in 10.5 μl of TE buffer (10 mM Tris–HCl, 1 mM EDTA, pH 8.0) at a DNA concentration of 2.85 μg/μl with 800 J/m^2 UV-C lamp (Philips TUV-9) emitting mainly at 254 nm, as measured with a DCRX radiometer (Spectronics). Ethanol (70%) was added to DNA for the precipitation. After 15 min in freezer, DNA was centrifuged at 15500 g for 15 min at 4 °C (Allegra 21R, Beckman Coulter). The pellet was left to air dry overnight, whereas the supernatant was stored at − 20 °C. Pellet was re-suspended in 15 μl of TE buffer and the DNA was quantified by spectrophotometer (POLARstar Omega, BMG LABTECH). The supernatant was pelleted by centrifugation (Allegra 21R, Beckman Coulter) and quantified.

Host cell reactivation assay and cytofluorimetric analysis

HEK293, stably transfected with $DDB2^{Wt}$ or $DDB2^{PCNA-}$ construct, were co-transfected with pmRFP-N2 (as a positive control), kindly provided by Professor Cardoso, and pEGFP-N1 or UV-pEGFP-N1 (as previously described) employing Effectene transfection reagent (Qiagen).

After 16 and 48 h, the cells were harvested from Petri dishes and centrifuged at 200 g for 3 min (Centrifuge 4236, Alc), the pellets were gently re-suspended on phosphate-buffered saline (PBS) for in vivo flow cytofluorimetry measurements (CyFlow® SL, Sysmex Partec GmbH). Only RFP positive cells were considered for the subsequent analysis in which the ratio between the mean fluorescence intensity (MFI) for the RFP and GFP protein were calculated. After normalization (MFI GFP/MFI RFP), relative expression of GFP protein was computed by comparing the normalized MFI of the UV-irradiated

to the normalized MFI of unirradiated plasmid, thereby detecting the restored plasmidic DNA [14, 15].

Immunofluorescence and confocal microscopy

HeLa cells, seeded on coverslips and transiently transfected as reported above, were locally irradiated at 100 J/m^2 by laying on top of cells an Isopore polycarbonate filters (Millipore) with 3 μm pores. At the end of 5, 10, 30 and 60 min (recovery time for XPG) or 30 and 60 min (recovery time for Pol II), the cells were washed twice in cold PBS, lysed with 0.5% Triton X-100 (Sigma-Aldrich) in cold PBS for 30 min at 4 °C in agitation, fixed with freshly made 2% paraformaldehyde and preserved in Ethanol (70%) at −20 °C for permeabilization.

Next, the samples were washed twice with cold PBS and blocked in PBST buffer (PBS, 0.2% Tween 20) containing 1% bovine serum albumin (BSA) with gentle shaking, and then incubated for 1 h with specific antibodies: mouse monoclonal anti-RNA polymerase II (anti-Pol II, 1:100, Covance, RRID:AB_10013665), rabbit polyclonal anti-XPE/DDB2 (1:100, Novus Biologicals; NBP2–38854) and rabbit polyclonal anti-XPG (1:200, RRID: AB_1080609), all diluted in PBST buffer/BSA. After three washing, each reaction was followed by incubation for 30 min with anti-mouse Alexa Fluor 594 (1:200, RRID: AB_141607) or anti-rabbit Alexa Fluor 488 (1:200, Molecular Probes, RRID: AB_141708). After immunoreactions and washing, the samples were incubated with Hoechst 33258 dye (0.5 μg/ml) for 10 min at room temperature with mild agitation and then washed in PBS. Slides were mounted in Mowiol (Calbiochem) containing 0.25% 1, 4-diazabicyclo-octane (Aldrich) as antifading agent. Images of fixed cells were taken with a Nikon Eclipse E400 fluorescence microscope equipped with a Canon Power Shot A590 IS digital camera. Fluorescence signals were acquired with a TCS SP5 II Leica confocal

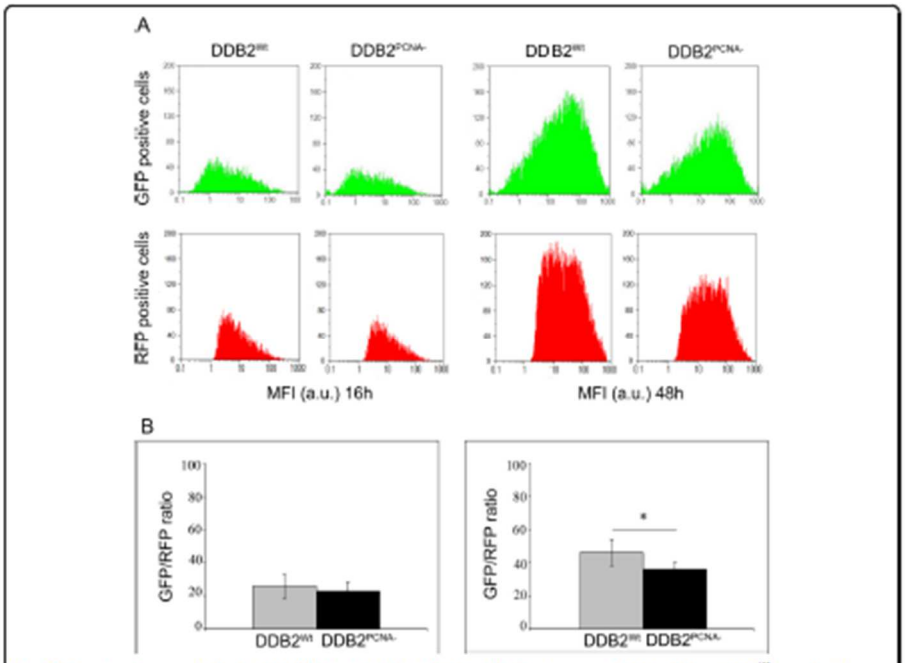

Fig. 1 NER process is impaired when DDB2-PCNA interaction is lost. HEK293 stable clones expressing DDB2 wild-type (DDB2^{WT}) or mutated protein (DDB2^{PCNA-}) were transiently transfected with pEGFP-N1 UV-irradiated plasmid and pmRFP-N2 control plasmid. At 16 and 48 h after transfection, the cells were collected and analysed using in vivo cytofluorimetric protocol (see Materials and Methods section). In **a** GFP and RFP positive cells are reported and the M.F.I. is shown. **b** Statistical analysis of GFP/RFP ratio from three independent experiments is reported. * $p < 0.05$

microscope, at 0.3 μm intervals. Image analysis was performed using the LAS AF software.

Results

DNA damage response is delayed in the presence of DDB2 mutated protein

To evaluate the UV-induced DNA damage response, we performed experiments using irradiated or not irradiated pEGFP-N1 plasmid co-transfected with pmRFP-N2 construct in HEK293 stable clones expressing $DDB2^{Wt}$ or $DDB2^{PCNA-}$ protein. Flow cytometry analysis of GFP and RFP expression, performed at 16 and 48 h after plasmidic DNA-damaged transfection, highlights the production of the green fluorescent protein, indicating the ability of these cells to repair DNA lesions in irradiated pEGFP-N1 plasmid (Fig. 1). In the panel A, monoparametric analysis of the green (GFP positive cells) and red (RFP positive cells) shows no significant differences in the two cell clones at 16 h after transfection. At this time, the presence of DDB2 mutated protein does not influence the repair ability since it produced similar results as wild-type protein. In contrast, the analysis performed 48 h after transfection highlights a significant reduction of DNA damage repair capability in the presence of the mutated protein (Fig. 1b). Considering the ratio of GFP/RFP fluorescence, the GFP protein synthesis is more efficient in the presence of $DDB2^{Wt}$; instead, the loss of DDB2-PCNA interaction determines a reduction of reported gene reactivation after UV irradiation.

DDB2 and RNA polymerase II co-localization is prevented without PCNA involvement

HeLa cells transiently transfected with pc-DNA3.1-$DDB2^{Wt}$ or pc-DNA3.1-$DDB2^{PCNA-}$ constructs were incubated with anti-DDB2 and anti-RNA Pol II antibodies for 30 min and 1 h after UV-C local irradiation. The immunofluorescence analysis shows that $DDB2^{Wt}$ and Pol II were already recruited at DNA damaged sites at 30 min after DNA damage, and their co-localization were still detectable at 1 h after UV irradiation, even if the signal appears to be reduced (Fig. 2a). In the presence of DDB2 mutated protein, the cells did not show well-defined spots of co-localization at both 30 and 60 min (Fig. 2b).

To better evaluate the recruitment kinetics at DNA damaged sites of the above proteins, confocal analysis was performed as shown in Fig. 3. The co-localization between $DDB2^{Wt}$ and Pol II occurs mainly at 30 min after UV irradiation (Fig. 3a); at this time, 52% of cells were positive for colocalization. On the contrary, in the presence of $DDB2^{PCNA-}$ protein, only 1 h after damage, the pixel intensity profile showed a not complete co-localization. In fact, the green and red signals were partially overlapped (Fig. 3b). This

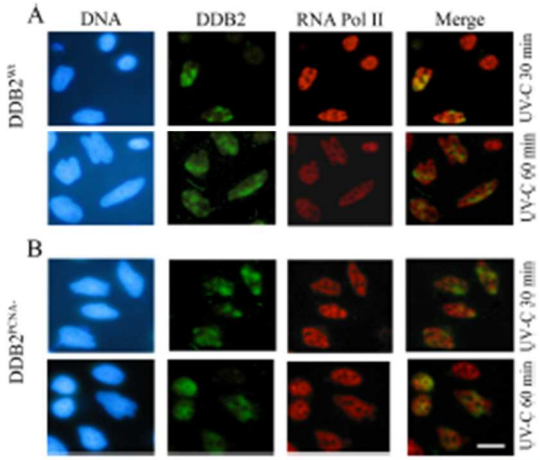

Fig. 2 $DDB2^{PCNA-}$ and Polymerase II proteins partially co-localize in irradiated cells. Immunofluorescence analysis of HeLa cells transiently transfected with constructs expressing $DDB2^{Wt}$ or $DDB2^{PCNA-}$ protein, as indicated. Cells were UVC local irradiated and analysed 30 min and 1 h later. In **a** representative images obtained from cells expressing $DDB2^{Wt}$ protein. In **b** results from HeLa transfected with pc-DNA3.1-$DDB2^{PCNA-}$ construct are shown. Scale bar = 20 μm. Data are at least from three independent experiments

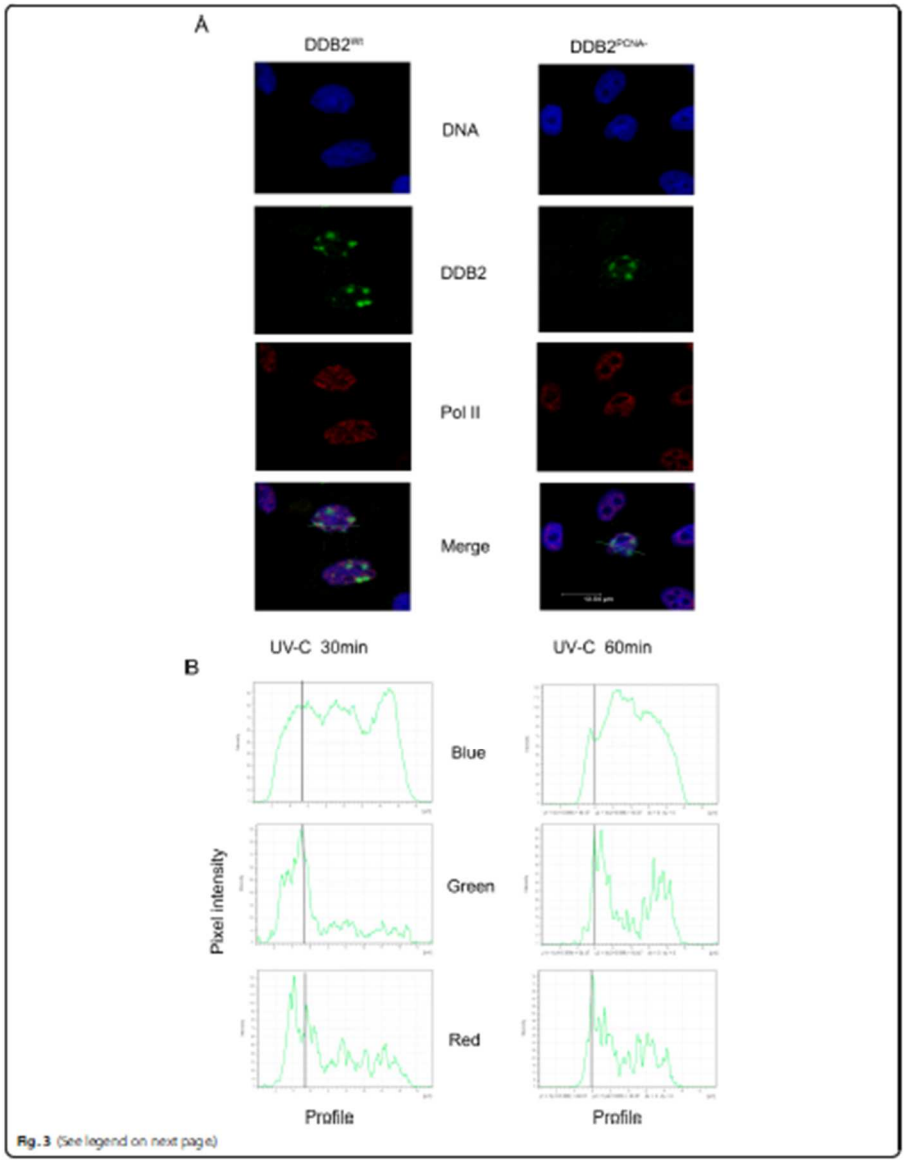

Fig. 3 (See legend on next page)

(See figure on previous page.)
Fig. 3 The loss of DDB2-PCNA interaction determines defects in NER pathway. HeLa cells transiently transfected with pc-DNA3.1-DDB2^{Wt} or pc-DNA3.1-DDB2^{PCNA-} constructs and UV-C local irradiated were analysed 30 min and 1 h after damage. In **a** representative co-localization analysis between DDB2 and Polymerase II proteins after UV-induced damages as obtained by confocal microscopy. The co-localization analyses are reported in panel (**b**). Data are at least from three independent experiments

finding confirms a delay in this co-presence at DNA damage foci.

DDB2-PCNA interaction facilitates the appropriate maintenance of the late NER-phase

To evaluate the potential influence of DDB2-PCNA interaction on the late NER steps, we investigate the interaction between DDB2 and XPG, a protein involved in the incision phase of NER process. HeLa cells transiently expressing DDB2^{Wt} or DDB2^{PCNA-} protein were local irradiated and analysed by fluorescence and confocal microscopies at different recovery times.

Figure 4a shows representative images of the immunofluorescence analysis. The time course after irradiation indicate that DDB2^{Wt} protein is recruited at DNA damaged sites together with the endonuclease XPG. Confocal microscopy confirmed a better co-localization between DDB2^{Wt} and XPG proteins at 10 min after UV irradiation (Fig. 4b), whereas the recruitment at the damage sites appears postponed at 30 min with regards to XPG and DDB2^{PCNA-}. Furthermore, in the last case, the confocal analysis indicated that the two proteins recruited at DNA damaged sites are very closed but not completely overlapped since the profile of the peak intensity reveal that the better fluorescent signals are not superimposable. These data demonstrate that the loss of DDB2-PCNA interaction influences the late phase of NER process.

Discussion

NER process is a highly versatile and complex system removing different types of DNA lesions [17]. UV-induced damages trigger NER process using both sub-pathways TC-NER and GG-NER. The first one is fast and efficient in removing lesions from transcribed regions determining a block of transcription [18].

The role of DDB2 in GG-NER is widely described and this protein is crucial to recognize and remove DNA UV-lesions [19, 20]. We have previously demonstrated that DDB2-PCNA interaction is i) required for DDB2 degradation [9], ii) likely involved in cell cycle progression [21], iii) able to affects DNA repair and iv) implicated in conferring proliferation and migration advantages [10]. In addition, using UV-damaged plasmidic DNA, DDB2^{PCNA-} recombinant protein showed both defective lesion recognition and DNA binding [10].

In this work we applied HRC assay to evaluate plasmidic DNA repair capacity of DDB2 protein and its mutated form. In the past, several approaches based on transfected damaged-DNA have been used to this end. After the initial demonstration on HCR efficiency for studying NER process activation in whole cells [11] or fractionated cell extracts transfected with UV-damaged plasmid DNA [11], different attempts to improve HCR assay have been further developed. Among them, a fluorescent method for detecting cellular ability to incise the damaged strand by NER mechanism [22], as well as a plasmid-type fluorescent probe [23] were proposed.

Based on our results, the re-activated expression of GFP protein in the stable clone producing DDB2^{Wt} demonstrated that DNA lesions are removed from transfected irradiated plasmidic DNA and, therefore, the transcription process is restored. It is known from the literature, that HCR assay, when performed after UV damage, measures the ability of the host cells to complete NER [15]. Our results demonstrated that this capability is influenced by DDB2-PCNA interaction; in fact, the cells expressing DDB2^{PCNA-} protein showed a significant reduction of GFP expression, as shown by the low GFP protein level measured by flow cytometry. By this experimental approach we demonstrated that both DDB2^{Wt} and DDB2^{PCNA-} proteins may intervene on nude UV-damaged plasmidic DNA inserted in human cells. Importantly, the DDB2^{PCNA-} mutant protein causes a delayed repair, confirming our previously published data obtained in an in vitro model [10]. In addition, our data support that the HCR method can be an efficient tool for investigating the role of NER mutant proteins in DNA repair. One advantage of this technical approach is that only the transfected DNA is damaged, while host cells are not irradiated and, therefore, they own intact cellular synthesis machinery and biochemical processes.

Interestingly, the co-localization between DDB2^{Wt} and RNA Pol II protein, as highlighted by confocal analysis at 30 min after UV irradiation, allows us to confirm the co-presence of these proteins at DNA damaged sites. This finding suggests a putative cooperation in DNA repair processes between TC-NER and GG-NER. Cooperation between other repair pathways have already been reported, as well as functional links between apparently separate signalling pathways converging toward a single global DNA damage response [24, 25]. In the presence of DDB2 mutated protein this cooperation is slower and its co-localization with RNA Pol II at DNA damaged sites appears incomplete even one hour after irradiation, thus suggesting a delay in the repair process.

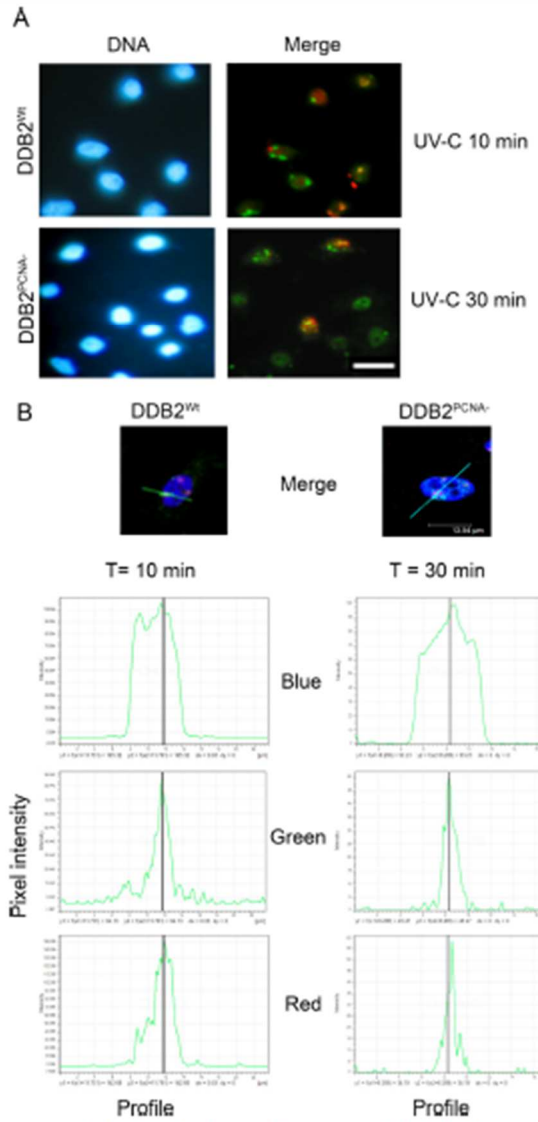

Fig. 4 DDB2-PCNA binding influences the late phase of repair process. Representative analysis obtained from transfected and irradiated HeLa cells using immunofluorescence microscope (**a**). Scale bar = 20 μm. In **b** confocal images and analysis are reported. The peaks exemplify the co-localization studies between DDB2 and XPG proteins. Data are at least from three independent experiments

To verify whether this different DNA damage response occurs also in the next phase of the NER and, in particular, in the excision of DNA lesions, DDB2-XPG co-localization was also considered. Although early report indicated that DDB2 is not required for XPG recruitment [26], this does not mean that co-localization may occur thereafter, as suggested by our results with DDB2^{WT} and further supported by the evidence that loss of DDB2-PCNA interaction determines a delay on the XPG recruitment on DNA lesions. Since XPG-mediated excision of DNA containing the lesions is fundamental for the fast DNA re-synthesis to correct the errors [27], our results suggest that DDB2 may influence not only the recognition, but also the next step of the NER, confirming the results observed in delayed GG-NER process [9, 10].

Conclusions

In conclusion, this work reports two new findings. First, the HCR data allowed highlighting the importance of the DDB2-PCNA interaction to complete correctly NER process. The second result is that HCR approach is useful to study how mutations in NER proteins may influence genome stability.

Abbreviations

DDB2: DNA damaged binding prosin 2; DDR: DNA Damage Response; GG-NER: Global Genome Nucleotide Excision Repair; HCR: Host Cell Reactivation assay; HEK: Human Embryonic Kidney; MFI: Mean Fluorescence Intensity; PCNA: Proliferating Cell Nuclear Antigen; Pol II: RNA Polymerase II; TC-NER: Transcriptional Coupled Nucleotide Excision Repair; XPG: *Xeroderma Pigmentosum* group G

Acknowledgements

The authors wish to thank P. Vaghi, Centro Grandi Strumenti Università di Pavia, for technical assistance to confocal microscopy.

Authors' contributions

EB, PP and IG carried out cell culture and transfection experiments; HCR experiments were performed by EB; immunofluorescence experiments were performed by PP and EB. Flow cytometry analysis was carried out by EP. EP, LAS and OC wrote the manuscript. All the authors contributed to the design of the project. All the authors have read and approved the manuscript.

Funding

This research was supported by a Grant from the Italian Ministry of Education, University and Research (MIUR) to the Department of Molecular Medicine of the University of Pavia under the initiative "Dipartimenti di Eccellenza (2018–2022)". This work was in part supported by AIRC (n° 17041 to EP). No role of the funding body in this study.

Availability of data and materials

The datasets used and/or analysed during the current study are available from the corresponding authors on reasonable request.

Ethics approval and consent to participate

Not applicable.

Consent for publication

Not applicable.

Competing interests

The authors declare that they have no competing interests.

Received: 18 April 2019 Accepted: 14 October 2019
Published online: 29 October 2019

References

1. Wang QE, Zhu Q, Wani G, Chen J, Wani AA. UV radiation-induced XPC translocation within chromatin is mediated by damaged-DNA binding protein, DDB2. Carcinogenesis. 2004;25(6):1033–43.
2. Abousalkhra A, Wood RD. Detection of nucleotide excision repair incisions in human fibroblasts by immunostaining for PCNA. Exp Cell Res. 1995; 221(2):326–32.
3. Wakasugi M, Kawashima A, Morioka H, Linn S, Sancar A, Mori T, Nikaido O, Matsunaga T. DDB accumulates at DNA damage sites immediately after UV irradiation and directly stimulates nucleotide excision repair. J Biol Chem. 2002;277(3):1637–40.
4. Cleaver JE, Lam ET, Revet I. Disorders of nucleotide excision repair: the genetic and molecular basis of heterogeneity. Nat Rev Genet. 2009; 10(11):756–68.
5. Basu AK. DNA Damage, Mutagenesis and Cancer. Int J Mol Sci. 2018;19(4). https://doi.org/10.3390/ijms19040970.
6. Broustas CG, Lieberman HB. DNA damage response genes and the development of cancer metastasis. Radiat Res. 2014;181(2):111–30.
7. Lagerwerf S, Vrouwe MG, Overmeer RM, Fousteri MI, Mullenders LH. DNA damage response and transcription. DNA Repair (Amst). 2011;10(7):743–50.
8. Mullenders LHF. Solar UV damage to cellular DNA: from mechanisms to biological effects. Photochem Photobiol Sci. 2018;17(12):1842–52.
9. Cazzalini O, Perucca P, Mocchi R, Sommatis S, Prosperi E, Stivala LA. DDB2 association with PCNA is required for its degradation after UV-induced DNA damage. Cell Cycle. 2014;13(2):240–8.
10. Perucca P, Mocchi R, Guerdamagna I, Baldi E, Sommatis S, Nardo T, Prosperi E, Stivala LA, Cazzalini O. A damaged DNA binding protein 2 mutation disrupting interaction with proliferating cell nuclear antigen affects DNA repair and confers proliferation advantage. Biochim Biophys Acta Mol Cell Res. 2018;1865(6):898–907.
11. Roguev A, Rusev G. Two-wavelength fluorescence assay for DNA repair. Anal Biochem. 2000;287(2):313–8.
12. Wei Q, Spitz MR. The role of DNA repair capacity in susceptibility to lung cancer: a review. Cancer Metastasis Rev. 1997;16(3–4):295–307.
13. Arikathil R, Jyothish B, Madhavan J, Nair MK. Deficient DNA repair capacity: a predisposing factor and high risk predictive marker in familial colorectal cancer. J Exp Clin Cancer Res. 1999;18(1):33–7.
14. Burger K, Matt K, Keiser N, Gebhard D, Bergemann J. A modified fluorimetric host cell reactivation assay to determine the repair capacity of primary keratinocytes, melanocytes and fibroblasts. BMC Biotechnol. 2010;10:46–57.
15. Johnson JM, Latimer JJ. Analysis of DNA repair using transfection-based host cell reactivation. Methods Mol Biol. 2005;291:321–35.
16. Barakat BM, Wang QE, Han C, Milum K, Yin DT, Zhao Q, Wani G, Arafa E-S, El-Mahdy MA, Wani AA. Overexpression of DDB2 enhances the sensitivity of human ovarian cancer cells to cisplatin by augmenting cellular apoptosis. Int J Cancer. 2010;127(4):977–88.
17. Kusakabe M, Onishi Y, Tada H, Kurihara F, Kusao K, Furukawa M, Iwai S, Yokoi M, Sakai W, Sugasawa K. Mechanism and regulation of DNA damage recognition in nucleotide excision repair. Genes Environ. 2019;41:2.
18. Wang W, Xu J, Chong J, Wang D. Structural basis of DNA lesion recognition for eukaryotic transcription-coupled nucleotide excision repair. DNA Repair. 2018;71:43–55.
19. Stoyanova T, Roy N, Kopanja D, Bagchi S, Raychaudhuri P. DDB2 decides cell fate following DNA damage. Proc Natl Acad Sci U S A. 2009;106(26):10690–5.
20. Stoyanova T, Roy N, Kopanja D, Raychaudhuri P, Bagchi S. DDB2 (damaged-DNA binding protein 2) in nucleotide excision repair and DNA damage response. Cell Cycle. 2009;8(24):4067–71.
21. Perucca P, Sommatis S, Mocchi R, Prosperi E, Stivala LA, Cazzalini O. A DDB2 mutant protein unable to interact with PCNA promotes cell cycle progression of human transformed embryonic kidney cells. Cell Cycle. 2015; 14(24):3920–8.
22. Toga T, Kuraoka I, Watanabe S, Nakano E, Takeuchi S, Nishigori C, Sugasawa K, Iwai S. Fluorescence detection of cellular nucleotide excision repair of damaged DNA. Sci Rep. 2014;4:5578.
23. Tawarahara H, Kuraoka I, Iwai S. Facile preparation of a fluorescent probe to detect the cellular ability of nucleotide excision repair. Anal Biochem. 2017;526:71–4.

24. Simonelli V, Leuzzi G, Basile G, D'Errico M, Fortini P, Franchitto A, Viti V, Brown AR, Parlanti E, Pascucci B, et al. Crosstalk between mismatch repair and base excision repair in human gastric cancer. Oncotarget. 2017;8(49):84827–40.
25. Fortini P, Dogliotti E. Base damage and single-strand break repair: mechanisms and functional significance of short- and long-patch repair subpathways. DNA Repair (Amst). 2007;6(4):398–409.
26. Zotter A, Luijsterburg MS, Warmerdam DO, Ibrahim S, Nigg A, van Cappellen WA, Hoeijmakers JH, van Driel R, Vermeulen W, Houtsmuller AB. Recruitment of the nucleotide excision repair endonuclease XPG to sites of UV-induced dna damage depends on functional TFIIH. Mol Cell Biol. 2006; 26(23):8868–79.
27. Riedl T, Hanaoka F, Egly JM. The comings and goings of nucleotide excision repair factors on damaged DNA. EMBO J. 2003;22(19):5293–303.

Publisher's Note